

Stephen F. Austin State University

**SFA ScholarWorks**

---

Electronic Theses and Dissertations


---

Fall 12-11-2021

## SEASONAL FLAMMABILITY COMPARISONS OF NATIVE AND EXOTIC PLANTS IN THE POST OAK SAVANNAH, BLACKLAND PRAIRIE, AND PINEYWOODS ECOREGIONS OF TEXAS

Michael Tiller  
tillerm@jacks.sfasu.edu

Follow this and additional works at: <https://scholarworks.sfasu.edu/etds>

 Part of the [Forest Biology Commons](#), [Other Forestry and Forest Sciences Commons](#), and the [Physical Chemistry Commons](#)

[Tell us](#) how this article helped you.

---

### Repository Citation

Tiller, Michael, "SEASONAL FLAMMABILITY COMPARISONS OF NATIVE AND EXOTIC PLANTS IN THE POST OAK SAVANNAH, BLACKLAND PRAIRIE, AND PINEYWOODS ECOREGIONS OF TEXAS" (2021). *Electronic Theses and Dissertations*. 417.  
<https://scholarworks.sfasu.edu/etds/417>

This Dissertation is brought to you for free and open access by SFA ScholarWorks. It has been accepted for inclusion in Electronic Theses and Dissertations by an authorized administrator of SFA ScholarWorks. For more information, please contact [cdsscholarworks@sfasu.edu](mailto:cdsscholarworks@sfasu.edu).

---

SEASONAL FLAMMABILITY COMPARISONS OF NATIVE AND EXOTIC PLANTS IN  
THE POST OAK SAVANNAH, BLACKLAND PRAIRIE, AND PINEYWOODS  
ECOREGIONS OF TEXAS

Creative Commons License



This work is licensed under a [Creative Commons Attribution-Noncommercial-No Derivative Works 4.0 License](https://creativecommons.org/licenses/by-nc-nd/4.0/).

SEASONAL FLAMMABILITY COMPARISONS OF NATIVE AND EXOTIC  
PLANTS IN THE POST OAK SAVANNAH, BLACKLAND PRAIRIE, AND  
PINEYWOODS ECOREGIONS OF TEXAS

BY

MICHAEL B. TILLER, Master of Science

Presented to the Faculty of the Graduate School of

Stephen F. Austin State University

In Partial Fulfillment

Of the Requirements

For the Degree of

Doctor of Philosophy

STEPHEN F. AUSTIN STATE UNIVERSITY

December 2021

SEASONAL FLAMMABILITY COMPARISONS OF NATIVE AND EXOTIC  
PLANTS IN THE POST OAK SAVANNAH, BLACKLAND PRAIRIE, AND  
PINEYWOODS ECOREGIONS OF TEXAS

By

MICHAEL B. TILLER, Master of Science

APPROVED:

---

Brian P. Oswald, Ph.D., Dissertation Director

---

Alyx S. Frantzen, Ph.D., Committee Member

---

I-Kuai Hung, Ph.D., Committee Member

---

Yuhui Weng, Ph.D., Committee Member

---

Freddie Avant, Ph.D.  
Interim Dean of Research and Graduate Studies

## ABSTRACT

East Texas' diverse landscape can present year-round wildfire seasons that can be influenced by seasonal and regional differences in climate and physiography. The culmination of these factors can impact wildland fuel flammability, which is of great interest to fire managers in terms of wildfire planning and maintaining ecosystem health and resilience with the effective use of prescribed fire. Greater insight into the fundamental thermal behavior of wildland fuels can aid in fire behavior prediction and development of fire-resistant plant lists that inform burn prescriptions and more fire-resilient ornamental landscaping. This study focused on estimating seasonal and regional flammability characteristics of five evergreen species: yaupon (*Ilex vomitoria*), Chinese privet (*Ligustrum sinense*), greenbrier (*Smilax* spp.), eastern red cedar (*Juniperus virginiana*), and escarpment live oak (*Quercus fusiformis*); and two deciduous species: Chinese tallow (*Triadica sebifera*) and southern red oak (*Quercus falcata*). Live foliar and small diameter branch wood samples were collected in the Pineywoods, Post Oak Savannah, and Blackland Prairie Ecoregions during the dormant (February) and growing (August) season. Oxygen bomb calorimetry (OBC), proximate analyses, and oxidative and pyrolytic

thermogravimetric analyses (TGA) were used to identify any potential variations in species-specific flammability. Proximate analyses yielded volatile matter (VM%), fixed carbon (FC%), and ash percent (ash%), with ash% serving as the correction factor for ash-free net heat contents (NHC-AF; MJ kg<sup>-1</sup>). Oxidative TGA estimated relative spontaneous ignition temperature (RSIT; °C), gas-phase maximum mass loss rate (GP-MMLR; % min<sup>-1</sup>), and gas-phase combustion duration (GP-CD; min.). Pyrolytic TGA measured Friedman and Ozawa-Flynn-Wall model-free activation energies ( $E\alpha(s)$ ) that were used to estimate ignitability and gas-phase and global combustibility based on respective conversion degrees ( $\alpha$ ) ranging from 0.02-0.20 $\alpha$ , 0.02-0.40 $\alpha$ , and 0.02-0.80 $\alpha$ .

Proximate analyses displayed considerable variability, except mean VM%(s), which in greater proportions, was a general indicator of greater mean NHC-AF(s) and GP-MMLR(s). All foliar NHC-AF(s), RSIT(s), and GP-MMLR(s) were significantly different ( $p < 0.05$ ) with respect to species, season, and ecoregion. Mean regional GP-MMLR(s) were consistently greater in the growing season, with the Blackland Prairie yielding the largest number of species with the greatest mean GP-MMLR(s). The Post Oak Savannah and Blackland Prairie consistently yielded species with the greatest mean NHC-AF(s) and oxidative TGA values. Mean global, gas-phase, and ignitability  $E\alpha(s)$  did not present with any

discernable trends relative to season and ecoregion. Differences in species regional flammability may be related to variable soil properties, plant community structure and composition, and large-scale precipitation gradients; whereas, dynamic frontal movements that spawn stochastic convective storms and variable temperatures may have more of a seasonal impact on flammability. Yaupon and eastern red cedar produced some of the greatest mean seasonal NHC-AF(s), RSIT(s), GP-MMLR(s), and GP-CD(s), indicating greater overall flammability, while Chinese tallow foliage produced the lowest NHC-AF, RSIT, and GP-MMLR. The majority of species mean NHC-AF(s) fell below the standard NHC (18.61 MJ kg<sup>-1</sup>) used in common fire models, which may result in over predicted fire behavior. Chinese privet produced the greatest ignitability and combustibility based on low mean  $E\alpha(s)$ , and combined with its intermediate NHC-AF, it may potentially accelerate fire spread in mixed stands and increase fire intensity in dense, monotypic stands. Chinese tallow wood GP-MMLR(s) were significantly greater in the growing season, and may potentially enhance integrated control measures using prescribed fire. Collectively, these bench-scale data serve as an initial survey into the fundamental thermal properties of select wildland fuels, and require further investigation at larger scales and with similar bench-scale methodologies, such as cone calorimetry to visually confirm autoignition and flaming combustion characteristics.

## ACKNOWLEDGEMENTS

I am especially grateful for my family and dear friend Joy Morgan for their dedicated support throughout graduate school. Further appreciation is extended to Stephen F. Austin State University's (SFASU) Arthur Temple College of Forestry and Agriculture McIntire-Stennis program and the Robert A. Welch Foundation Research Grant (AN-0008) for funding my project. Much gratitude and appreciation is extended to Dr. Brian Oswald, my dissertation director, for his guidance and mentoring in the field of fire ecology. I would also like to thank my committee members, Dr. Alyx Frantzen, Dr. I-Kuai Hung, and Dr. Yuhui Weng for their guidance and contributions toward the successful completion of my dissertation. Special thanks to Dr. Alyx Frantzen for providing access to SFASU's chemistry lab and her dedicated support with the lab technicians and instruments.



## TABLE OF CONTENTS

ABSTRACT.....	i
ACKNOWLEDGEMENTS.....	iv
LIST OF TABLES.....	xii
LIST OF FIGURES.....	xvii
LIST OF ABBREVIATIONS.....	xx
INTRODUCTION.....	1
OBJECTIVES.....	10
LITERATURE REVIEW.....	12
History of Fire in East Texas.....	12
East Texas Ecoregions.....	18
Pineywoods Ecoregion.....	19

Post Oak Savannah Ecoregion.....	21
Blackland Prairie Ecoregion.....	23
Regional Implications of Invasive Species.....	25
Pineywoods Ecoregion.....	27
Post Oak Savannah Ecoregion.....	28
Blackland Prairie Ecoregion.....	29
Alteration of Fire Regimes.....	30
Pineywoods Ecoregion.....	31
Post Oak Savannah and Blackland Prairie Ecoregions.....	32
Predicting Wildland Fire Behavior.....	34
Native and Exotic Species.....	37
Yaupon.....	37
Eastern Red Cedar.....	38
Escarpment Live Oak.....	39

Southern Red Oak.....	40
Greenbrier.....	41
Chinese Privet.....	42
Chinese Tallow.....	43
Assessing Flammability and Thermal-kinetics of Wildland Fuels.....	44
Cone Calorimetry.....	50
Oxygen Bomb Calorimetry.....	51
Thermogravimetric Analysis and Differential Scanning Calorimetry.....	53
Assessing Thermal-kinetic Parameters.....	57
METHODS.....	63
Ecoregion and Species Selection.....	63
Research Site Descriptions.....	64
Stephen F. Austin Experimental Forest.....	64
Pineywoods Native Plant Center.....	66

Texas A&M Equine University Equine Center.....	66
Veterans Park Athletic Complex.....	67
Somerville Lake.....	68
Granger Lake.....	68
Trinity River Audubon Center.....	69
White Rock Lake Park.....	70
Heat Content and Thermogravimetric Analysis.....	71
Oxygen Bomb Calorimetry.....	71
Oxidative Thermogravimetric Analysis.....	73
Pyrolytic Thermogravimetric Analysis.....	74
Data Analysis.....	75
RESULTS.....	94
Proximate Analysis.....	94
Pineywoods Ecoregion.....	94

Post Oak Savannah Ecoregion.....	95
Blackland Prairie Ecoregion.....	96
Ecoregion-wide Comparison.....	96
Oxygen Bomb Calorimetry.....	100
Pineywoods Ecoregion.....	100
Post Oak Savannah Ecoregion.....	100
Blackland Prairie Ecoregion.....	101
Ecoregion-wide Comparison and Statistics.....	102
Oxidative Thermogravimetric Analysis.....	109
Pineywoods Ecoregion.....	109
Post Oak Savannah Ecoregion.....	110
Blackland Prairie Ecoregion.....	112
Ecoregion-wide Comparison and Statistics.....	113
Thermal Kinetic Analysis.....	123

Pineywoods Ecoregion.....	123
Post Oak Savannah Ecoregion.....	124
Blackland Prairie Ecoregion.....	125
Ecoregion-wide Global and Gas-Phase Combustion $E\alpha$ 's.....	126
Species foliage samples.....	126
Chinese tallow wood and foliage samples.....	128
Species Ignitability.....	130
DISCUSSION.....	152
Proximate Analysis.....	152
Oxygen Bomb Calorimetry.....	157
Oxidative Thermogravimetric Analysis.....	164
Thermal Kinetic Analysis.....	172
CONCLUSIONS AND MANAGEMENT IMPLICATIONS.....	186
Oxygen Bomb Calorimetry.....	186

Oxidative Thermogravimetric Analysis.....	188
Thermal Kinetic Analysis.....	193
Management Implications.....	197
LITERATURE CITED.....	202
VITA.....	223

## LIST OF TABLES

Table 1.	Species foliar and wood (w) collection times with Corresponding sites and ecoregions. Site abbreviations are as follows: SFAEF – Stephen F. Austin Experimental Forest; PNPC – Pineywoods Native Plant Center; TAMUEC – Texas A&M Equine Center; SOMLK – Somerville Lake; VPAC – Veterans Park and Athletic Complex; TRAC – Trinity River Audubon Center; GRLK – Granger Lake; WRLK – White Rock Lake.....	83
Table 2.	Soil orders and general soil properties specific to each species, site, and ecoregion where foliar and wood samples were collected. Soil data was accessed through the Soil Survey Geographic Database (SSURGO) hosted by Environmental Systems Research Institute (ESRI). Ecoregions are abbreviated as follows: PW – Pineywoods; POS – Post Oak Savannah; BP – Blackland Prairie.....	84
Table 3.	Ecoregion mean monthly precipitation and maximum temperatures from 2013-2019. Mean monthly seasonal National Oceanic and Atmospheric Administration (NOAA) climate data was averaged through Nov.-Mar. and Apr.-Oct. for the dormant and growing season, respectively. Normal seasonal precipitation and maximum temperatures were averaged according to monthly seasonal periods described above using 1981-2010 NOAA data. Respective climate data was accessed at NOAA weather stations in Angelina County Airport, Lufkin, Texas, Easterwood Airport, College Station, Texas, and Ferris, Texas for the Pineywoods, Post Oak Savannah, and Blackland Prairie Ecoregions.....	85



Table 4.	Seasonal proximate analyses for volatile matter %, fixed carbon %, and ash % according to ecoregion. Standard deviation and wood samples (w) are denoted in parentheses.....	98
Table 5.	Mean seasonal NHC-A for foliar and wood samples according to ecoregion. Standard deviations and wood samples (w) are denoted in parentheses. Underlined values meet or exceed the standard NHC value of 18.61 MJ kg <sup>-1</sup> used in common fire models. All foliar samples were significantly different with respect to species (p<0.05), except Chinese tallow and southern red oak. Significant seasonal and regional differences for foliar and wood samples are described by: A: season; B: ecoregion; C: season and ecoregion.....	104
Table 6.	Mean seasonal NHC-AF for foliar and wood samples according to ecoregion. Standard deviations and wood samples (w) are denoted in parentheses. All species foliar samples were significantly different with respect to species (p<0.05), except Chinese tallow and southern red oak. Significant seasonal and regional differences for foliar and wood samples are described by: A: season; B: ecoregion; C: season and ecoregion.....	105
Table 7.	ANOVA table representing NHC-A and NHC-AF indices for semi/evergreen foliar samples. A Tukey's Studentized Range Test was applied to all significant factors (p<0.05). Post hoc testing revealed the following non-significant pairwise differences: <i>NHC-A</i> : Chinese privet-escarpment live oak; <i>NHC-AF</i> : Chinese privet-greenbrier.....	107

Table 8.	ANOVA table representing NHC-A and NHC-AF indices for Chinese tallow wood. A Tukey's Studentized Range Test was applied to all significant factors ( $p < 0.05$ ). Post hoc testing revealed the following non-significant pairwise differences: <i>NHC-A</i> : Post Oak Savannah-Blackland Prairie; <i>NHC-AF</i> : Post Oak Savannah-Blackland Prairie.....	108
Table 9.	Regional oxidative differential thermogravimetric analysis (DTG) results displaying flammability parameters for relative spontaneous ignition temperature (RSIT), gas-phase maximum mass loss rate (GP-MMLR), and gas-phase combustion duration (GP-CD). Standard deviations and wood samples ( <i>w</i> ) are in parentheses. All species foliage except Chinese tallow and southern red oak were significantly different ( $p < 0.05$ ) based on RSIT, GP-MMLR, and GP-CD. Seasonal and regional significant differences are denoted as: A: season, B: ecoregion, C: season and ecoregion.....	116
Table 10.	ANOVA table representing RSIT, GP-MMLR, and GP-CD indices for semi/evergreen foliar samples. A Tukey's Studentized Range Test was applied to all significant factors ( $p < 0.05$ ). Post hoc testing revealed the following non-significant pairwise differences: <i>RSIT</i> : Post Oak Savannah-Blackland Prairie; <i>GP-MMLR</i> : eastern red cedar-escarpment live oak, Pineywoods-Post Oak Savannah; <i>GP-CD</i> : eastern red cedar-greenbrier, Post Oak Savannah-Blackland Prairie.....	120
Table 11.	ANOVA table representing RSIT, GP-MMLR, and GP-CD indices for Chinese tallow foliage. A Tukey's Studentized Range Test was applied to all significant factors ( $p < 0.05$ ). Post hoc testing revealed the following non-significant pairwise differences: <i>RSIT</i> : Pineywoods-Post Oak Savannah; <i>GP-MMLR</i> : Post Oak Savannah-Blackland Prairie.....	121

Table 12.	ANOVA table representing RSIT, GP-MMLR, and GP-CD indices for Chinese tallow wood. A Tukey's Studentized Range Test was applied to all significant factors ( $p < 0.05$ ). Post hoc testing revealed the following non-significant pairwise differences: <i>RSIT</i> : Post Oak Savannah-Blackland Prairie; <i>GP-MMLR</i> : Pineywoods-Blackland Prairie; <i>GP-CD</i> : Pineywoods-Post Oak Savannah and Post Oak Savannah-Blackland Prairie.....	122
Table 13.	Mean Friedman dormant season foliar global $E\alpha(s)$ based on conversion degrees ( $\alpha$ ) ranging from 0.02-0.80. Underlined $E\alpha$ values indicate rough estimations of species maximum mass loss rates that correlate with peak devolatilization and gas-phase combustion. Note that escarpment live oak was not collected in the Pineywoods.....	133
Table 14.	Mean Ozawa-Flynn-Wall dormant season foliar global $E\alpha(s)$ based on conversion degrees ( $\alpha$ ) ranging from 0.02-0.80. Underlined $E\alpha$ values indicate rough estimations of species maximum mass loss rates that correlate with peak devolatilization and gas-phase combustion. Note that escarpment live oak was not collected in the Pineywoods.....	135
Table 15.	Mean Friedman gas-phase combustion (GPC) $E\alpha$ estimates based on species maximum MMLR(s), $E\alpha(s)$ ranged from 0.02-0.52 $\alpha$ . Wood samples (w) are denoted in parentheses.....	137
Table 16.	Mean Ozawa-Flynn-Wall gas-phase combustion (GPC) $E\alpha$ estimates based on species maximum MMLR(s), $E\alpha(s)$ ranged from 0.02-0.52 $\alpha$ . Wood samples (w) are denoted in parentheses.....	138

Table 17.	Mean Friedman growing season foliar global $E\alpha(s)$ based on conversion degrees ( $\alpha$ ) ranging from 0.02-0.80. Underlined values indicate rough estimations of species maximum mass loss rates that correlate with peak devolatilization and gas-phase combustion.....	139
Table 18.	Mean Ozawa-Flynn-Wall growing season foliar global $E\alpha(s)$ based on conversion degrees ( $\alpha$ ) ranging from 0.02-0.80. Underlined values indicate rough estimates of species maximum mass loss rates that correlate with peak devolatilization and gas-phase combustion.....	141
Table 19.	Mean seasonal Friedman and Ozawa-Flynn-Wall (OFW) global $E\alpha(s)$ (0.02-0.80) for southern red oak wood and foliage. Underlined values indicate rough estimations of species maximum mass loss rates that correlate with peak devolatilization and gas-phase combustion.....	143
Table 20.	Mean Friedman and Ozawa-Flynn-Wall (OFW) global $E\alpha(s)$ (0.02-0.80) for Chinese tallow wood based season and ecoregion. Underlined values indicate rough estimations of species maximum mass loss rates that correlate with peak devolatilization and gas-phase combustion. Ecoregions are abbreviated as: PW: Pineywoods, POS: Post Oak Savannah, and BP: Blackland Prairie .....	144
Table 21.	Mean ignitability estimates based on Friedman global $E\alpha(s)$ ranging from 0.02-0.10 and 0.02-0.20 for foliar and wood samples, respectively. Wood samples (w) are denoted in parentheses.....	150
Table 22.	Mean ignitability estimates based on Ozawa-Flynn-Wall global $E\alpha(s)$ ranging from 0.02-0.10 and 0.02-0.20 for foliar and wood samples, respectively. Wood samples (w) are denoted in parentheses.....	151

## LIST OF FIGURES

Figure 1.	Research sites in the Pineywoods, Post Oak Savannah, and Blackland Prairie Ecoregions of East Texas.....	81
Figure 2.	Texas mean annual precipitation gradient extending from west to east; annual precipitation was averaged based NOAA climate data from 1981-2010.....	82
Figure 3.	Understory thicket of yaupon, Chinese privet, Chinese tallow, and greenbrier under a mixed pine-hardwood stand on the Stephen F. Austin Experimental Forest.....	87
Figure 4.	Hardwood stand in the Pineywoods Native Plant Center with a understory cover consisting of Chinese privet and Carolina laurel cherry.....	87
Figure 5.	Thicket of Chinese privet under a remnant post oak motte adjacent to the Texas A&M Equine Center.....	88
Figure 6.	Riparian cover at Veterans Park and Athletic Complex, College Station, Texas with Chinese tallow mixed in the foreground.....	88
Figure 7.	Mix of escarpment live oak, eastern red cedar, and post oak at the Somerville Lake site.....	89
Figure 8.	Small escarpment live oak motte at the Granger Lake site.....	89
Figure 9.	Thicket of Chinese privet at the Trinity River Audubon Center in Dallas, Texas.....	90
Figure 10.	Thicket of Chinese tallow trees at White Rock Lake Park in Dallas, Texas.....	90

Figure 11.	Oxidative thermogram depicting an estimated RSIT using the Pyris 13.2 onset tool tangential lines based on the first derivative mass loss curve (DTG). Onset tool vertices were placed at the endset of the first DTG peak and the corresponding temperature of the second DTG peak maxima.....	91
Figure 12.	Oxidative thermogram depicting gas-phase maximum mass loss rate (%/min) and combustion duration (min) specific to the RSIT onset and second differential thermogravimetric (DTG) peak maxima and endset values.....	92
Figure 13.	Dormant season devolatilization thermograms depicting first DTG peak endset, third DTG peak maxima, and 550°C end points for linear heating rates of 10°, 25°, and 40°C min <sup>-1</sup> .....	93
Figure 14.	Regional and seasonal NHC-AF trends for semi/evergreen species foliar samples. The error bars represent the standard error of the mean.....	106
Figure 15.	Regional dormant season GP-MMLR and GP-CD trends for semi/evergreen species foliar samples. The error bars represent standard error of the mean.....	118
Figure 16.	Regional growing season GP-MMLR and GP-CD trends for semi-evergreen species foliar samples. The error bars represent standard error of the mean.....	119
Figure 17.	Seasonal DTG devolatilization thermograms displaying gas-phase combustion (GPC) $E\alpha$ , maximum mass loss rate temperature, and percent mass loss for Post Oak Savannah yaupon and Chinese privet.....	145

Figure 18.	Seasonal DTG devolatilization thermograms displaying gas-phase combustion (GPC) $E\alpha$ , maximum mass loss rate temperature, and percent mass loss for Post Oak Savannah greenbrier and eastern red cedar.....	146
Figure 19.	Seasonal and regional DTG devolatilization thermograms displaying gas-phase combustion (GPC) $E\alpha$ , maximum mass loss rate temperature, and percent mass loss for Chinese tallow wood in the Pineywoods, Post Oak Savannah, and Blackland Prairie ecoregions.....	147
Figure 20.	Seasonal DTG devolatilization thermograms displaying gas-phase combustion (GPC) $E\alpha$ , maximum mass loss rate temperature, and percent mass loss for Pineywoods Chinese tallow and southern red oak wood.....	148
Figure 21.	DTG devolatilization thermograms displaying foliar gas-phase combustion (GPC) $E\alpha(s)$ , maximum mass loss rate temperatures, and percent mass loss for Pineywoods Chinese tallow and southern red oak and Post Oak Savannah escarpment live oak.....	149

## LIST OF ABBREVIATIONS

<i>A</i>	Pre-exponential Factor
$\alpha$	Conversion Degree
ACOE	U.S. Army Corps of Engineers
AEHOC	Average Effective Heat of Combustion
AMSL	Above Mean Sea Level
ANOVA	Analysis of Variance
Ash %	Ash Percent
ASTM	American Society for Testing and Materials
$\beta$	Heating Rate (K/min)
BEHAVE	Fire Modeling System
BehavePlus	Fire Modeling System
BTU/lb	British Thermal Unit per Pound
$d\alpha$	Derivative of the Conversion Degree
$dt$	Derivative of Time ( <i>t</i> )
DSC	Differential Scanning Calorimetry
DTA	Differential Thermal Analysis



DTG	Differential Thermogravimetric Analysis
$E\alpha$	Activation Energy based on Conversion Degree ( $\alpha$ )
ENSO	El Niño Southern Oscillation
$f(\alpha)$	Kinetic Reaction Model
FARSITE	GIS – Fire Area Simulator
FC%	Fixed Carbon Percent
FI	Fireline Intensity
FL	Flame Length
FlamMap	GIS – Fire Behavior Mapping and Analysis Program
FRI	Fire Return Interval
FsPro	GIS – Fire Spread Probability Simulator
$G(\alpha)$	Integral form of the Kinetic Reaction Model
GCM	General Circulation Model (oceanic and atmospheric)
GHC	Gross Heat Content
GPC	Gas-phase Combustion
GP-CD	Gas-phase Combustion Duration
GP-MMLR	Gas-phase Maximum Mass Loss Rate

GPC $E\alpha$	$E\alpha(s)$ Ranging from the Second DTG Maxima to the Second DTG Endset
Global $E\alpha$	$E\alpha(s)$ Ranging from the Second DTG Maxima to 550°C
HIZ	Home Ignition Zone
HPUA	Heat Per Unit Area
HRR	Heat Release Rate
K	Kelvin
KAS	Kissenger-Akahira-Sunrose Model-free Kinetic Method
KJ mol <sup>-1</sup>	Kilojoules Per Mol
LANDFIRE	Landscape Fire and Resource Management Planning Tools
$M$	Mass of Sample
$m_0$	Initial Mass of Sample
MJkg <sup>-1</sup>	Megajoules Per Kilogram
MLC	Mass Loss Calorimeter
MMLR	Maximum Mass Loss Rate
n	Reaction Order
NHC	Net Heat Content

NHC-A	Net Heat Content with Ash
NHC-AF	Net Heat Content without Ash
NOAA	National Oceanic and Atmospheric Administration
OBC	Oxygen Bomb Calorimetry
OCC	Oxygen Consumption Calorimetry
OFW	Ozawa-Flynn-Wall Model Free Kinetic Method
$p(x)$	Exponential Integral
PDO	Pacific Decadal Oscillation (oceanic and atmospheric)
PHRR	Peak Heat Release Rate
PNPC	Pineywoods Native Plant Center
$R$	Gas Constant (8.314 J/mol/K)
RI	Reaction Intensity
ROS	Rate of Spread
RSIT	Relative Spontaneous Ignition Temperature
SFAEF	Stephen F. Austin Experimental Forest
SFASU	Stephen F. Austin State University
STA	Simultaneous Thermal Analysis

SSURGO	Soil Survey Geographic Database
T	Temperature (kelvin (K))
<i>t</i>	Time (min)
TAMUEC	Texas A&M University Equine Center
TFS	Texas A&M Forest Service
TGA	Thermogravimetric Analysis
THR	Total Heat Release
TSI	Time to Sustained Ignition
USDA	United States Department of Agriculture
USFS	United States Forest Service
WUI	Wildland Urban Interface

## INTRODUCTION

Wildfire impacts in the wildland-urban interface (WUI) continue to challenge fire managers throughout the United States (NICC 2016). Texas lost a record number of homes, totaling 2,947 structures, in the 2011 fire season (Texas A&M Forest Service 2012). Fire suppression continues to be a funding priority, with considerable funding allocations directed to Federal and State agencies to bolster wildland firefighting resources and fuels reduction objectives (Steelman and Burke 2007, Gorte and Bracmort 2012). However, large loss WUI fires have prompted fire managers to increase efforts toward wildfire mitigation with the release of the National Cohesive Wildland Fire Management Strategy (WFLC 2014). Although Cohesive Strategy goals outline safe fire suppression practices, the main underlying goal calls for restoring fire-resilient landscapes and creating fire-adapted communities. Restoring fire-resilient landscapes and communities often require hazardous fuels mitigation using a combination of mechanical and herbicide treatments, and preferably the reintroduction of prescribed fire in fire-prone ecosystems. Ultimately, the overall goal would allow for the safe reintroduction of cost-effective prescribed fires to reduce hazardous

fuels and restore ecosystem health within or adjacent to WUI areas, greatly reducing the risk of structural ignitions.

Creating fire-adapted communities can significantly reduce structural losses from large wildfires and provide extensive safety zones to facilitate the reintroduction of fire in fire-prone ecosystems. The National Fire Protection Association's 1144 Standard for Reducing Structural Ignition Hazards from Wildland Fire (NFPA 2013), combined with the Firewise Communities/USA program, are widely accepted as core mitigation strategies for creating fire-adapted communities (Mell et al. 2010, Abser and Vaske 2011, Toman et al. 2013). Firewise principles reduce structural ignition probability by promoting fire resistive building materials, maintenance of the home ignition zone (HIZ), and defensible space. Maintaining the HIZ and defensible space are formally outlined in the International Wildland Urban Interface Code (ICC 2015) and often require the removal, reduction, or modification of flammable vegetation extending from 0-30 m around the structure. Public perception in terms of managing the intermix of native and ornamental vegetation in the interface can be tenuous due to conflicting objectives related to aesthetics, privacy, noise reduction, wildlife habitat, and energy conservation near homes and structures. Thus, quantitative and qualitative plant flammability listings could facilitate more informed fuels

management decisions that address multiple management options which can improve ecosystem health and community safety. Most hazardous fuels treatments can be accomplished by modifying horizontal and vertical fuel continuity, mowing or irrigating grasses, and thinning shrubs and trees in conjunction with pruning lower limbs that remove ladder fuels.

Texas's ecosystems historically exhibited diverse fire regimes, delineated by a decreasing fire return interval (FRI) gradient extending from west to east (Stambaugh et al. 2014). Historically, the majority of the state has been characterized as having a frequent mean FRI ranging from 1-12 years prior to Euro-American settlement (Stambaugh et al. 2014). Within the past century, fire suppression, livestock overgrazing, landscape-level fragmentation, and land use changes have significantly altered the historic fire cycle to include much longer FRI's. As a result, East Texas ecosystems have undergone significant spatiotemporal change in plant community structure and composition (Diggs et al. 1999, Heilman et al. 2002, Barron 2006, Marshall et al. 2008, Sinha et al. 2010, Stambaugh et al. 2014). The Post Oak Savannah and Blackland Prairie Ecoregions have seen extensive woody plant encroachment into many remnant native grasslands and abandoned agricultural fields (Diggs et al. 1999, Stambaugh et al. 2014). By contrast, privately owned timber interests in the

Piney Woods Ecoregion are generally overgrown with dense woody understories, often due to cost prohibitive understory treatments (Marshall et al. 2008). However, prescribed fire aimed at managing woody encroachment in rangelands and forest understories has increased throughout East Texas due to more intensive silvicultural practices, endangered species habitat restoration, hazardous fuels reduction, and recent interest in restoring prairies and savannahs comprised of oak woodlands, shortleaf pine (*Pinus echinata*), and longleaf pine (*Pinus palustris*).

Since much of Texas consists of fire-adapted ecosystems with historically low FRI's, use of prescribed fire treatments is a cost-effective treatment in meeting land management and ecological restoration objectives. State and Federal agencies actively use prescribed fire to enhance wildlife habitat, restore ecological function to fire-maintained prairie and forest ecosystems, reduce hazardous fuel loads, and maintain the health of existing and restored ecosystems. For example, the U.S Forest Service (USFS) and Texas A&M Forest Service (TFS) use active fire management programs that utilize and promote prescribed fire as a beneficial land management option to enhance and restore ecosystem health and services, as well as mitigate the threat of high intensity wildfires and associated losses of high-value infrastructure and critical



wildlife habitat. Private lands prescribed burn programs are also active, with ~ 94% of the state being privately owned (Texas A&M Forest Service 2012). The Texas Department of Agriculture administers the state's prescribed burn program, while landowners have access to multiple prescribed burn associations such as the Prescribed Burn Alliance of Texas. Conservation organizations such as the Nature Conservancy are also actively using and promoting prescribed burn use within the state.

Active fire management programs rely heavily on predictive services that include fire danger rating systems, fire weather forecasting, and fire behavior and smoke plume modeling. Fuel models are among the key components for predicting and modeling fire behavior. Contemporary fuel models utilize physical, chemical, and thermal-kinetic properties of wildland fuels to improve accuracy of fire behavior prediction and modeling by accounting for flammability differences among all vegetative species in the fuel continuum (Hanson et al. 2000). Improved fire behavior prediction and modeling gained from incorporating new and updated comprehensive fuel model parameters can be a critical component in effective prescribed burn planning, wildfire risk assessment, and development of safe, effective wildfire strategies and tactics. TFS relies heavily on landscape level (GIS-Based) wildfire mapping programs (Texas Wildfire Risk Assessment

Portal) to identify high risk fuels, and to estimate fire behavior near WUI areas (Texas A&M Forest Service 2012). Improved fire management leads to better resource management, firefighter safety, and protection of private property. Significant numbers of plant species have already undergone chemical and thermal-kinetic evaluation, although research is still lacking in geographic relevancy, and standardized testing methodologies continue to be problematic (White and Zipperer 2010).

Fire behavior research is moving toward more advanced fire modeling methodologies based on chemical and thermal-kinetic properties of wildland fuels that may further fire modeling accuracy. Greater knowledge of thermal-kinetic properties of common native and exotic plant species in more fire-prone East Texas ecoregions could aid in the development of more comprehensive fire-resistant plant listings that include plant flammability metrics, and potentially improve physics-based fire models by updating plant flammability data of plant species that comprise large portions of regionally important fuel models. The potential for more informative fire-resistant plant listings and improved fire behavior prediction could be a decisive tool for improving prescribed burn effectiveness and wildfire risk assessments in the WUI. Improved prescribed burn effectiveness could be especially useful for managing invasive woody

species. Further prescribed burn improvements may arise from a better understanding of fuel moisture and flammability characteristics that can potentially lead to greater combustion efficiency, resulting in reduced emission of pollutants in smoke in regions where air quality is a concern (Liu et al. 2016). Comparative flammability data of exotic and native species may also offer further insight into plant community interactions with respect to fire ecology.

Plants selected for this study are native and exotic plants existing within the Piney Woods, Post Oak Savannah, and Blackland Prairie Ecoregions of Eastern Texas. Two invasive species of primary concern existing within all three ecoregions were Chinese privet (*Ligustrum sinense*) and Chinese tallow (*Triadica sebifera*). Native plants included yaupon (*Ilex vomitoria*), greenbrier (*Smilax* spp.), eastern red cedar (*Juniperus virginiana*), escarpment live oak (*Quercus fusiformis*), and southern red oak (*Quercus falcata*). Chinese privet is a nonnative shrub that forms dense, monotypic stands primarily in mesic, riparian areas, and bottomland hardwood forests with increasing encroachment into xeric, upland sites; dense stands are associated with decreased biodiversity and poor hardwood and pine regeneration (Webster et al. 2006, Ulyshen et al. 2010, Greene and Blossey 2012, Wang et al. 2016). Chinese tallow is an invasive, nonnative tree commonly occurring in mesic, riparian areas and bottomland

hardwood sites with some extension into upland sites; when established, Chinese tallow suppresses native species, reduces biodiversity, and alters wildlife habitat (Grace et al. 2001, Webster et al. 2006, Gan et al. 2009, Pile et al. 2017). Chinese tallow and privet are not typically targeted for hazardous fuels reduction due to their greater occurrence on mesic sites; however, control measures using mechanical, chemical, and prescribed fire treatments have become more common as their range expands. As Chinese privet continues to increase in density and expand its range, subsequent increases in fuel loading could become problematic in a variety of ecosystems. Yaupon is an aggressive native shrub that forms dense, monotypic stands in Texas oak woodlands, prairies, and forest understories, suppressing native herbaceous cover and tree regeneration, leading to reduced biodiversity and greater fuel loads (Hough 1969, Mitchell et al. 2005, Shadow 2011, Andreu et al. 2012). Yaupon has been identified as a highly flammable shrub that is not recommended for fire resistant landscaping (Long et al. 2006, Wimberly et al. 2008). Greenbrier is a fire-adapted, rhizomatous vine that is common in xeric and mesic forest understories, thickets, and margins of disturbed sites, especially fence rows. Eastern red cedar is a common evergreen tree that frequently colonizes disturbed sites and is considered an invader species in Texas oak

woodlands and prairies due to past fire suppression. Conversely, eastern red cedar does not tolerate dense forest cover with canopy closure and is more common along forest margins. Escarpment live oak is a common semi-evergreen hardwood trees found throughout the Texas oak woodlands and prairies and are capable of forming shrubby thickets to taller trees with spreading crowns; fire suppression has also facilitated greater escarpment live oak densities throughout its Texas range. Southern red oaks are generally associated with mixed pine-hardwood and upland pine forests, but their range also extends into the Post Oak Savannah.

## OBJECTIVES

The primary objectives for this research were to obtain net heat content and quantitative thermogravimetric analyses for yaupon, eastern red cedar, escarpment live oak, southern red oak, greenbrier, Chinese privet, and Chinese tallow due to their regional importance in the Pineywoods, Post Oak Savannah, and Blackland Prairie Ecoregions of Texas. The specific objectives were to:

- (1) Quantify and compare regional and seasonal differences in ash and ash-free net heat content ( $\text{MJ kg}^{-1}$ ) of native and exotic invasive species using oxygen bomb calorimetry.
- (2) Estimate and compare regional and seasonal differences with respect to species relative spontaneous ignition temperature (RSIT), gas-phase maximum mass loss rate (GP-MMLR), and combustion duration using thermogravimetric analysis in an oxidative atmosphere.

- (3) Quantify and compare regional and seasonal differences in species kinetic parameters related to conversion degree ( $\alpha$ ) and activation energy ( $E\alpha$ ) using thermogravimetric analysis in an inert atmosphere.

## LITERATURE REVIEW

### History of Fire in East Texas

Texas exhibits a wide range of historic fire regimes from a diverse landscape derived from many different landforms, vegetation types, soils, and climates. Stambaugh et al. (2014) conducted a statewide fire regime study using three spatial datasets and a comprehensive literature review to estimate historic regimes prior to Euro-American settlement. Historic fire regime data were primarily limited to anecdotal written accounts of fire activity and comparable data from fire studies of similar ecosystems in adjacent states. Spatial data included maps based on the Physical Chemistry Fire Frequency Model (Guyette et al. 2012), National LANDFIRE Mean FRI's (Keane et al. 2002), and Frost's (1998) pre-settlement fire frequency estimates. Historical fire frequency data were categorized according to Texas natural regions and subregions. Results suggested much of the state consisted of frequent fire regimes with mean FRI's ranging from 1-12 years, and a decreasing FRI gradient extending from west to east (Stambaugh et al. 2014).

The Post Oak Savannah Ecoregion is characteristic of most fire-dependent grasslands in temperate North America with short FRI's that promote herbaceous species, while limiting woody species encroachment (Smeins et al. 2005). Early fire ignitions were primarily started by lightning strikes and intentional and accidental fire



ignitions by Native Americans and early settlers (Pyne 2011). Written accounts by early Texas explorers and settlers describe the occurrence of frequent and large fires across much of Texas' rangelands (Smeins et al. 2005). Woody species were intermixed in small heterogeneous patches in grassland-dominated ecosystems, while greater woody species densities persisted in riparian areas, canyons, and rocky outcroppings (Short and Hamilton 1993). A dendrochronological fire scar study of old growth post oaks (*Quercus stellata*) located on the western edge of the Post Oak Savannah Ecoregion revealed a 6.9 year mean FRI from 1681-2005, with a 5.9 year mean FRI prior to 1853 (Stambaugh et al. 2011a). During the 1850's the region experienced a fire deficit of 50 years that coincided with the rapid expansion of agriculture and Euro-American settlement (Stambaugh et al. 2011a). Consequently, the continuation of decades of fire suppression has left much of the region overgrown with woody species that include American beautyberry (*Callicarpa americana*), eastern red cedar, yaupon, and greenbrier (Keith 2009). As Texas prairies and savannahs saw increased settlement, fire suppression remained a primary concern to prevent loss of livestock forage, while overgrazing and land fragmentation from road and agricultural development effectively constrained fire by significantly reducing fine fuel loads and disrupting fuel bed continuity (Smeins et al. 2005). In recent years, the role of fire in restoring and maintaining these ecosystems

has gained momentum and prescribed fire use has increased significantly aided by the state's prescribed burn program and regional prescribed burn associations.

Similar to the Post Oak Savannah Ecoregion, the Blackland Prairie is a fire-dependent ecosystem that relies on frequent FRI's. The Blackland Prairie is considered a southern extension of the tall grass prairie; however, it experiences a longer growing season and higher average annual temperatures than comparable tall grass prairie systems, which may potentially decrease FRI's by extending the annual burn window (Smeins 1972). Stambaugh et al. (2017) reported a 10.9 year mean FRI for the 1653-1829 pre-settlement period estimated from dendrochronological fire scars of 50 post oaks. Many of the trees sampled exhibited crown morphologies resembling past open canopy conditions and short 1-3 year FRI's during the regional settlement period of 1885-1940. The study concluded that general fire frequency's increased from the early 1700's to the 1920's and declined thereafter (Stambaugh et al. 2017). Like much of Texas' prairies and savannahs during the settlement period, the Blackland Prairie was heavily cultivated for agriculture and overgrazed by livestock, which led to a significant reduction in fire frequency. Likewise, fire suppression and prevention measures were also used to prevent loss of livestock forage as evidenced by Texas laws established in 1848 and 1884 that made it illegal to set prairies on fire between July 1 and February 15, thus making any ignitions to grasslands a felony (Smeins et al. 2005). In recent years,

increasing human development in both the Blackland Prairie and Post Oak Savannah has resulted in increased wildfire risk and created greater prescribed burn complexity near developed areas.

The Pineywoods Ecoregion lacks quantitative fire history data, but fire frequency data can be reasonably inferred from similar fire studies across southeastern U.S. forests. East Texas and Louisiana longleaf pine savannahs are well-known fire-dependent ecosystems that require frequent, low intensity understory fires every 1-5 years to reduce competition, maintain overstory health, and promote quality herbaceous forage such as bluestem grasses (Varner et al. 2005, Frost 2006, Frost 2007). Stambaugh et al. (2011b) reported a 3.3-year pre-settlement (1650-1793) mean FRI in a southcentral Louisiana longleaf pine savannah. In addition to longleaf pine savannahs, mixed-pine-hardwood forests consisting of longleaf, loblolly (*Pinus taeda*), and shortleaf pine were also prevalent in East Texas. Representative fire regime studies for were conducted in the Ozark Mountains of Arkansas and Oklahoma, where fire frequencies ranged from 3-7 years (Guyette et al. 2006, Stambaugh et al. 2013). Pine-dominated ecosystems occupying more xeric, upland sites tended to be more fire-prone with 1-8 year FRI's, whereas more hardwood-dominated ecosystems occupying more mesic, bottomland sites exhibited a 30-35 year FRI (USDA Forest Service 1981).

Prior to Euro-American settlement, forested ecosystems in the southeastern United States were maintained through natural disturbance regimes influenced by wildfires ignited by lightning and Native Americans, and severe weather events that manifested as tornadoes, straight-line winds, and hurricanes with associated flooding (Komarek 1964, Marshall et al. 2008). Consequently, wildfire events burned unchecked across the landscape and were typically low intensity understory fires, with an occasional moderate to high intensity understory or crown fire influenced by drought and severe fire weather conditions (USDA Forest Service 1981).

East Texas forest communities have endured many changes since Euro-American settlement began in the 1800's, resulting in significant clearing of forested lands for crops, pastures, towns, and roads (USDA Forest Service 1988, Marshall et al. 2008). By 1920, large tracts of forests were either harvested or converted to agricultural use (Glitzenstein 1986). After the surge in timber harvest and agricultural expansion between the 1860's and 1920's, East Texas was severely impacted by the Great Depression, leaving most agricultural crop and pasture lands idle, while previous clearcuts naturally regenerated (USDA Forest Service 1988, Marshall et al. 2008). A resurgence in the timber industry brought new concerns for future timber stocks, which led to the development of new programs addressing fire protection, research, education, and the establishment of managed forests owned by public and private sectors (USDA Forest Service 1988).

Nationally, wildfires were perceived as a destructive force that destroyed pine regeneration in the understory, and led to the passage of the Weeks Act of 1911, which provided Federal matching funds to state agencies to help protect forests from wildfire (USDA Forest Service 1988). The Weeks Act of 1911 was further enhanced by the Clarke-McNary Act in 1924, which authorized increased funding for cooperative Federal-State fire protection programs (USDA Forest Service 1988). The Federal-State wildfire campaign in the South succeeded in abating wildfire damage for many years, and was a key component in reestablishment of southern forest timber resources (USDA Forest Service 1988). However, many researchers advocated prescribed burning to reduce dense understory fuels that suppressed pine growth and promoted major wildfires (Carle 2002). Prescribed burning was also recognized as a good management tool for controlling undesirable species, improving wildlife habitat, promoting livestock forage, and natural regeneration of pine stands (USDA Forest Service 1988). As the fire exclusion and prescribed fire debate continued, research beginning in 1958 at the Tall Timbers Research Station conveyed scientific evidence promoting prescribed fire as a viable management tool in southern forests. Eventually, fire management evolved into a balanced management approach that employs both fire suppression and management through prescribed fire to accomplish sustainable forestry management practices.

Fire suppression continued to drive federal policy, as evidenced by the passage of the Rural Development Act of 1974 that allocated federal funds to help state foresters train and equip volunteer fire departments with wildland firefighting equipment to help protect rural communities (USDA Forest Service 1988). A culture of fire exclusion ideologies was promoted through mass media campaigns which swayed public opinion toward wildfire suppression for decades, and remains in modern culture. Consequently, statewide fire regimes were altered severely, resulting in dense wooded thickets in prairie and savannah ecosystems, decreased biodiversity, and dense forest understories exhibiting heavy fuel loads that increase the likeliness of crown fire initiation and extreme fire behavior. (Smeins et al. 2005, Stephens et al. 2012).

#### East Texas Ecoregions

The East Texas region covers roughly 16.2 million ha and includes the Pineywoods, Post Oak Savannah, and Blackland Prairie Ecoregions (Diggs et al. 2006). Regional boundaries are delineated by the state line to the east and Red River to the north, while the western and southern extend through Austin, San Antonio, and Houston (Diggs et al. 2006). The region has high biological diversity and species richness, with 3,402 floral species and 3,660 taxa (Hatch et al. 1990 Turner et al. 2003) due to its wide range of climatic and geologic variation coupled with extensive biological mixing of flora from the tall grass prairie and eastern

forests. Annual temperatures average roughly 21°C in the south and 18°C in the north, with temperature extremes ranging from -18° to 43°C in the winter and summer (Diggs et al. 2006). Precipitation patterns exhibit a significant increasing west-east gradient that is primarily driven by frontal mixing of colder air from northwestern air masses colliding with warm, moisture-laden air coming off the Gulf of Mexico resulting in intense convective storms (Bomar 1995).

### Pineywoods Ecoregion

The Pineywoods Ecoregion spans approximately 6.3 million ha and occupies the western edge of the southeastern coastal plain (Diggs et al. 2006). The climate is humid subtropical, with 235-270 frost-free days and an annual precipitation ranging from 1,000-1,425 mm; elevation varies from 8-215 m above mean sea level (AMSL) and major soil orders include Ultisols, Alfisols, and Vertisols (Shaw 2011). Floristically, the region is representative of the southeastern mixed and conifer forest cover types with a well-developed understory. Timber production accounts for 2.9 million ha of the region, while pasture and croplands account for 878,740 ha (Shaw 2011).

Current forest communities are mostly fragmented patches of pine plantations adjacent to agricultural fields. Although the region lacks significant topography, distinct forest communities exist within the region due to diverse soil types, hydrology, and terraced topography. Upland forest communities are generally

classified according to degree of soil moisture, ranging from xeric to moderately mesic, dependent on the proportion of sand and loam in the upper soil profile. Dry, sandy upland sites typically support shortleaf and longleaf pine with a mix of oaks (*Quercus* spp.) and hickories (*Carya* spp.). Moderately dry, sandy loam upland sites generally favor loblolly and introduced slash pine (*Pinus elliottii*), with southern red oak, post oak, sweetgum (*Liquidambar styraciflua*), black-gum (*Nyssa sylvatica*), and elms (*Ulmus* spp.). Common upland understory associates include yaupon, American beautyberry, greenbrier, and summer grape (*Viti aestivalis*). More mesic lower slopes favor hardwood-pine forests with a mix of loblolly pine and moderately flood-tolerant hardwoods such as American beech (*Fagus grandifolia*), southern magnolia (*Magnolia grandiflora*), and white oak (*Quercus alba*). Alluvial floodplains (bottomlands) support more flood-tolerant species such as black gum, bald cypress (*Taxodium distichum*), water elm (*Planera aquatica*), and overcup oak (*Quercus lyrata*).

Prior to the 1820's, much of East Texas' forests were mature, uneven-aged stands (Diggs et al. 2006). In the southeast portion of the region near the present Big Thicket National Preserve, longleaf pine savannahs dominated the landscape (Frost 1993, Diggs et al. 2006). Wet longleaf pine savannahs occurred on the southern extent of the poorly drained Big Thicket area, while upland longleaf pine savannahs occurred on the northern extent of the range (Diggs et al. 2006). Upland



sites in the north and western reaches of the region were dominated by uneven-age stands of shortleaf pine-mixed hardwood communities with various oaks and hickories common to dry sites (Diggs et al. 2006). Mixed hardwood-pine forests persisted at the margins of more mesic sites occurring on lower slopes where FRI's were significantly longer, aided by moist soils and low intensity backing fires creeping downhill. Mixed hardwood-pine stands were interspersed with more fire-sensitive loblolly pine and a diverse mixture of hardwoods.

#### Post Oak Savannah Ecoregion

The Post Oak Savannah Ecoregion covers approximately 5.3 million ha of east central Texas, and borders the Blackland Prairie to the west and Pineywoods to the east (Diggs et al. 2006). Annual precipitation ranges from 762-1,143 mm and the climate is subtropical with roughly 235-270 annual frost-free days (Shaw 2011). Topography is primarily rolling hills with elevations ranging from 90-250m AMSL (Diggs et al. 2006). Major soil orders consist of Ultisols, Alfisols, and Vertisols (Shaw 2011). Approximately 85% of the region has been converted to agriculture, with 2.2 million ha of native grasslands used for livestock grazing (Shaw 2011). Improved pasture and row crops of corn, sorghum, cotton, and soybeans account for 2.9 million ha (Shaw 2011).

Floral diversity in the Post Oak Savannah is accentuated by the transition (ecotone) from eastern hardwood forests to a diverse grassland comprised of 434

herbaceous species, making it the most diverse grassland in Texas (Shaw 2011). Much of the region exhibits a post oak or blackjack oak (*Quercus marilandica*) overstory with little bluestem (*Schizachyrium scoparium*), Indian grass (*Sorghastrum nutans*), and switch grass (*Panicum virgatum*) in the understory (Diggs et al. 2006). Areas containing deep, sandy soils give rise to Xeric Sandylands characterized by post oak, sand post oak (*Quercus margaretta*), sandjack oak (*Quercus incana*), and black hickory (*Carya texana*), with common understory associates that include eastern prickly-pear (*Opuntia humifusa*), Texas bull-nettle (*Cnidoscolus texanus*), and small-flower paw-paw (*Asimina parviflora*) (MacRoberts et al. 2002). Southern reaches of the region also exhibit small isolated populations of loblolly pine along the Colorado River, but larger stands are associated with the “Lost Pines” area of Bastrop County (Diggs et al. 2006). Riparian flood plains in the eastern extent of the region are generally dominated by post oak, water oak (*Quercus nigra*), green ash (*Fraxinus pennsylvanica*), elms, and eastern red cedar. Western riparian flood plains are generally dominated by cedar elm (*Ulmus crassifolia*), boxelder (*Acer negundo*), sugarberry (*Celtis laevigata*), western soapberry (*Sapindus saponaria*), and American elm (*Ulmus americana*).

Livestock overgrazing and fire suppression have had profound effects in the region, culminating in widespread brush encroachment, development of dense hardwood stands, and degraded rangeland quality. Overgrazing is very visible where

unpalatable species such as wooly croton (*Croton capitatus*), snow-on-the prairie (*Euphorbia bicolor*), bitterweed (*Helenium amarum*), and silver nightshade (*Solanum elaeagnifolium*) are common (Diggs et al. 2006). Fire suppression has resulted in dense stands of post oak, blackjack oak, and winged elm (*Ulmus alata*), while yaupon, farkleberry (*Vaccinium arboreum*), and American beautyberry have increased in the understory. Fence lines have also facilitated the movement of yaupon, sugarberry, winged elm, and greenbrier into open herbaceous cover by serving as corridors and seed sources (Diggs et al. 2006).

#### Blackland Prairie Ecoregion

The Blackland Prairie Ecoregion spans roughly 4.6 million ha extending nearly 483 km from the Red River south to the San Antonio area, and is bound by the Cross Timbers, Post Oak Savannah, and Gulf Coast Prairie Ecoregions to the west, east, and south (Diggs et al. 2006). Geographically, the region is spatially disjunct, comprised of a main wedge-shaped swath that runs north-south, with two separate prairie patches to the southeast known as the San Antonio and Fayette Prairies. Annual rainfall ranges from 760-1,145 mm and the climate is classified as subtropical to humid subtropical (southeast), with 227-277 frost-free days annually (Shaw 2011). Topography is flat to gently rolling plains, with elevations ranging from 92-244 m (Diggs et al. 1999). Major soil orders consist of Vertisols, Alfisols, and Mollisols (Shaw 2011). The ecoregion is among one of the most imperiled

ecosystems in North America, with less than 1% of the original prairie remaining due to extensive agricultural development (Eidson and Smeins 1999, Sinah et al. 2010). Currently, more than 75% is used for agriculture, split roughly 50% in row crop production and 50% improved pasture (Shaw 2011).

The region is considered a southern extension of the North American tallgrass-prairie, and is comprised of a diverse mosaic of tall grass communities primarily determined by soil (Diamond and Smeins 1993, Diggs et al. 1999). Diamond and Smeins (1993) classified six major tall grass communities within the Blackland Prairie Ecoregion, with various mixtures of dominant grasses that included, little blue stem, Indian grass, eastern gamma grass (*Tripsacum dactyloides*), switch grass, big blue stem (*Andropogon gerardii*), long-spike tridens (*Tridens strictus*), Texas cup grass (*Eriochloa sericea*), and Florida paspalum (*Paspalum floridanum*). Woodlands can be found along riparian corridors, sloped scarps, and protected areas where soils are conducive for woody growth (Diamond and Smeins 1993). Common tree species include, Texas ash (*Fraxinus texensis*), Ashe juniper (*Juniperus ashei*), escarpment live oak (*Quercus fusiformis*), Texas red oak (*Quercus buckleyi*), cedar elm, sugar berry, and eastern red-cedar (Diggs et al. 2006).

Early prairie exploitation occurred with large-scale ranching operations of cattle and horses in the early 1800's, followed by extensive crop cultivation in the

1870's and 1880's, aided by improved rail access and advances in plow designs (Hayward and Yelderman 1991). Cotton crops dominated the region, and by 1920, 25% of the world's annual cotton crop was produced in the Texas Blackland Prairie (Diggs et al. 2006). As a result, much of the Blackland Prairie was lost with the exception of a few marginal slope-lands. Small, isolated pockets of remnant prairie were further degraded by disruption of historic fire regimes and grazing wild ungulates (especially bison (*Bison bison*)), which were essential for the maintenance of the prairie ecosystem (Diamond and Smeins 1993). Fire suppression and relatively high regional precipitation facilitated the invasion and dominance of some endemic shrubs and trees, especially Ashe juniper, cedar elm, and eastern red-cedar. Further prairie degradation from increased use of herbicide and mowing in native pastures rather than rotational grazing and maintenance of historic fire regimes resulted in more grasses at the expense of endemic broadleaf species (Diamond and Smeins 1993). Endemic grass species have also been displaced by the introduction of Bermuda grass (*Cynodon dactylon*), Johnson grass (*Sorghum halepense*), and King Ranch bluestem (*Bothriochloa ischaemum*) from improved pastures.

### Regional Implications of Invasive Species

The effects of terrestrial and aquatic invasive plant species proliferation present a multitude of ecological impacts at local and regional scales (Mack et al.

2000, Webster et al. 2006). Human activities have contributed to the breakdown of natural biogeographic barriers, allowing foreign plant species to extend their ranges at unprecedented rates (D'Antonio and Vitousek 1992). Plant taxa that once evolved in isolation are now introduced to foreign ecosystems, both accidentally and deliberately. Land use changes have also enabled many foreign plant species to successfully invade disturbed sites (Mack et al. 2000, Daehler 2003, Rejmanek et al. 2013). Ecological sites that have been altered by invasive species present a complex cascade of ecological changes that can impact entire ecosystem processes (Mack and D'Antonio 1998). Dominance of a single, non-native plant species can impact nutrient cycling, nutrient uptake, water consumption, light absorption, microclimates, geomorphology, hydrology, and disturbance effects (Brooks et al. 2004). One of the most profound ecological effects is the alteration of disturbance regimes beyond the range of variation which native species are adapted, resulting in community changes and ecosystem-level transformations (Mack and D'Antonio 1998).

Invasive plant species are commonly introduced to new regions through ornamental cultivation, contaminated crop seed, medicinal plantings, and intentional planting for improved crop yields, soil erosion reduction, and windbreaks (Liebhold et al. 1995, Reichard and White 2001). Colonization of invasive woody species is predominately caused by escaped ornamental landscaping. Invasive herbaceous

species tend to be accidentally or intentionally planted for agricultural purposes (Reichard and White 2001). Typical plant species selection involves physiological characteristics enabling the plant to adapt to similar climatic patterns and geography in regions other than its native range (Rejmanek et al. 2013). When introduced, invasive species outcompete native flora through greater resource sequestration, growth and development, injury avoidance from disturbance, and propagule pressure resulting in greater numbers of mobilized propagules available to colonize the community (Lonsdale 1999).

### Pineywoods Ecoregion

The Pineywoods Ecoregion comprises the western terminus of the southeastern forest. Abundant rainfall, relatively consistent moderate temperatures, and an extended growing season make the region favorable for a wide range of terrestrial plant species to persist. Research indicates potential links to increased exotic species abundance in deforested, mesic habitats with frequent disturbances (Brooks 2008, Rajmanek et al. 2013), which are similar to regional hardwood forest ecosystems. Human development and expanding population growth have further contributed to ecosystem disturbance rendering large pine, hardwood, and mixed pine-hardwood communities fragmented throughout the landscape (Heilman et al. 2002, Marshall et al. 2008).

Naturalized exotic invasive species, including Chinese privet and tallow, are extensive throughout the region (Rudis et al. 2006, Wang et al. 2016, Pile et al. 2017). Stands of Chinese privet and tallow can decrease FRI's by reducing herbaceous fuel loads, but increase woody fuel loading potentially increasing fire intensity in dry conditions. Chinaberry (*Melia azedarach*), Japanese privet (*Ligustrum japonicum*), Mimosa (*Albizia julibrissin*), and giant reed (*Arundo donax*) are prevalent in riparian and disturbed sites (Stocker and Hupp 2008). Yaupon is a volatile shrub that is also considered an aggressive native shrub due to its propensity to form dense thickets in forest understories. Invasive vine species like kudzu (*Pueraria montana var. lobata*), Japanese honeysuckle (*Lonicera japonica*), and Japanese climbing fern (*Lygodium japonicum*) have also become problematic, and may increase understory fuel loads and ladder fuels potentially increasing fire intensity and crown fire potential (Stocker and Hupp 2008). Nonnative grasses used for improved pastures include bahia grass (*Paspalum notatum*), rescuegrass (*Bromus catharticus*), and Bermuda grass (Diggs et al. 2006, Stocker and Hupp 2008).

#### Post Oak Savannah Ecoregion

Diverse biological mixing culminating from the convergence of the tall-grass prairie association and eastern deciduous forest make the Post Oak Savannah Ecoregion susceptible to both woody and herbaceous invasive species. Widespread



agricultural development into improved pasture has facilitated introductions of exotic grasses to bolster livestock forage, including wild oats (*Avena fatua*), perennial rye grass (*Lolium perenne*), Bermuda grass, bahia grass, Johnson grass, and rescuegrass (Diggs et al. 2006). Active fire suppression has also facilitated dense yaupon growth and intrusion into grasslands and oak woodlands. Chinaberry, Japanese privet, and Chinese privet and tallow have become established along riparian corridors, disturbed sites, and fencerows. Increased woody encroachment into grassland areas increases fire intensity, which can overwhelm fire suppression resources resulting in more frequent escaped initial attack efforts and greater risk to human infrastructure (Twidwell et al. 2013).

#### Blackland Prairie Ecoregion

Exceptional soil fertility, moderate rainfall, and an extended growing season give rise to a diverse floral community that is characteristic of much of the Blackland Prairie Ecoregion. Like the Post Oak Savannah, livestock ranching operations have introduced exotic grasses for improved pasture, which include Johnson grass, King Ranch bluestem, and Bermuda grass (Diggs et al. 1999). Other important broadleaf invasive species include bastard cabbage (*Rapistrum rugosum*), field bindweed (*Convolvulus arvensis*), and redtip photinia (*Photinia x fraseri*) and pincushions (*Scabiosa atropurpurea*). Exotic invasive woody species include Chinaberry, Chinese privet, and Chinese tallow. Lack of recurrent fire has caused a significant

increase in woody encroachment into open grasslands, which increases risk to infrastructure in developed areas (Twidwell et al. 2013).

### Alteration of Fire Regimes

Fire regimes are influenced by spatial and temporal variations in physiography, physiognomy, and climate. Physiognomic features that define ecosystem fuel complexes are highly correlated with fire regime feedback loops through intrinsic ecosystem properties and plant species composition (Brooks et al. 2004, Brooks 2008). Shifts in plant species composition can result in modified fuel parameters outside the natural range of native plant communities, creating variances in fire behavior and fire regime characteristics. Alteration of fire behavior and fire regimes can adversely influence ecosystem processes that impact native plant species' life cycles, while enhancing invasive plant expansion and dominance (Mack and D'Antonio 1998, Brooks 2008).

The physiognomic properties that define ecosystems are primary factors that determine fire behavior and fire regime effects (Brooks et al. 2004, Brooks 2008). Intrinsic and extrinsic properties of plant assemblages are key data to delineate complex fuel structures (D'Antonio 1999, Brooks et al. 2004, Brooks 2008). Extrinsic fuel properties constitute the arrangement of plants across the landscape which are measured by fuel continuity (vertical and horizontal), fuel load (fuel per unit area), and fuel packing ratio (fuel per unit volume of space). Intrinsic fuel properties are

described as physiological attributes of plant species that involve phenological development, fuel moisture content, chemical volatility, and heat content of plant tissue (DeBano et al. 1998). The cumulative effects of both sets of fuel properties relate to fire type, frequency, intensity, seasonality, and fuel ignitability (Brooks et al. 2004, Brooks 2008).

### Pineywoods Ecoregion

The Pineywoods Ecoregion was historically maintained by frequent FRI's associated with xeric, upland sites dominated by pine, especially longleaf pine ecosystems (Christensen 1981, Marshall et al. 2008, Stambaugh et al. 2011). In the absence of frequent FRI's, midstory hardwoods and understory woody species developed dense, closed canopies that produced an abundance of broad-leaf litter that decomposed rapidly, further reducing understory fuel flammability and suppressing herbaceous growth (Williamson and Black 1981, Mitchell et al. 2006). Greater understory shrub densities, combined with greater amounts of low flammability broadleaf litter, significantly reduces fire frequency and intensity creating a positive feedback cycle favoring fire-intolerant species that produce fewer flammable fuels (Mitchell et al. 2006, Brooks 2008, Rundel et al. 2014). However, greater densities of woody understory fuels, especially yaupon, may increase fire intensity (Long et al. 2006, Wimberly et al. 2008, Stambaugh et al. 2011). In addition to dense understory fuel loading, well-developed midstory tree and shrub strata

combined with a greater abundance of vines may also serve as ladder fuels increasing the potential for crown fires and torching of individual trees (Stocker and Hupp 2008).

### Post Oak Savannah and Blackland Prairie Ecoregions

Frequent warm-season fires, with mean FRI's <10 years (Brown 2000, Wade et al. 2000), likely maintained the grassland-dominated ecoregions of the Post Oak Savannah and Blackland Prairie prior to Euro-American settlement (Brown 2000, Wade et al. 2000). Stambaugh et al. (2011a) and (2017) reported respective pre-settlement mean FRI's of 5.9 and 8.4 years in the Post Oak Savannah and Blackland Prairie. However, Smeins (1972) suggests that fire frequency in Texas grasslands may be quite different compared to similar tall-grass prairies based on relatively higher temperatures and an extended growing season which may potentially lengthen the burn window for fire ignitions. In addition to frequent FRI's, Diggs and Schulze (2003) postulated differences in tree distributions on the Post Oak Savannah compared to the Blackland Prairie were related to soil-dependent fire frequency and intensity, with more productive clay soils exhibiting greater fire intensity that effectively controlled woody growth through more dense, continuous herbaceous fuel beds compared to less dense herbaceous fuel beds occurring on sandy, rocky soils.

Fire suppression and overgrazing have resulted in widespread encroachment of eastern red cedar and Ashe and redberry juniper into the Blackland Prairie, while yaupon encroachment dominates much of the eastern Post Oak Savannah. Overgrazing has greatly reduced herbaceous fuel loads, which diminishes the capacity to carry prescribed fire of sufficient intensity to effectively control invading woody species. Some of the most profound effects of fire exclusion is the potential for increased wildfire intensity due to greater woody fuel loading in Central Texas (Texas A&M Forest Service 2012). Central Texas experienced the Bastrop County Complex Fire in 2011, which burned 13,112 ha, destroying 1,691 homes and was the single most destructive wildfire in Texas history (Texas A&M Forest Service 2012). Future climate change is uncertain; however, statistical general circulation models (GCMs) of large scale oceanic and atmospheric patterns in the Pacific Ocean depicting El Niño Southern Oscillation (ENSO) and Pacific Decadal Oscillation (PDO) suggest quasi-periodic patterns of fire occurrence in western North America when compared to historical fire records (McKenzie et al. 2004). ENSO cycles have been associated with synchronous years of intensifying wildfire seasons in the southwestern United States and southern Rocky Mountain regions (Swetnam and Betancourt 1990, Veblen et al. 2000), which could potentially extend southeast, influencing regional climatic variation.

## Predicting Wildland Fire Behavior

Richard Rothermel designed the first fire spread model based on the conservation of energy of a spreading wildland fire flame front. The model incorporated 11 fuel models, live and dead fuel moisture, fuel loading, surface area-to-volume ratio of fuels, ignition temperature, energy release rate, slope, and wind speed to accurately assess fire spread through Rate of Spread (ROS), Fireline Intensity (FI), Flame Length (FL), Heat per Unit Area (HPUA), and Reaction Intensity (RI) indices (Rothermel 1972). Rothermel tested model accuracy by inventorying surface fuel loading using the method devised by James Brown in 1972, which incorporated estimates of site-specific fuel loads that produced more accurate biomass volumes per unit of area as opposed to using standard fuel loads outlined in the standard fuel models. Frank Albini expanded the utility of fire modeling by increasing the number of fuel models to 13 and developed a series of nomograms (graphs) that calculated ROS, FI, and FL from slope steepness, wind speed, and moisture content data (Wells 2008). Further improvements by Rothermel served as an advanced user's guide for fire command staff using the model as a "decision support system" to devise tactical firefighting strategies on major wildfire incidents (Rothermel 1983). One of the few limitations of the fire model was a lack of predicting crown fire intensity and spread, which were addressed in 1991 with a simple guide to predicting crown fire behavior (Rothermel 1991).

Prescribed fire managers often need precise fire behavior predictions to evaluate fire escape potential and to maintain proper burn prescriptions to accomplish ecological objectives. The release of the BEHAVE program in 1984 greatly improved fire modeling by incorporating a suite of sub models into one program that produces new outputs for crown scorch, crown fire rate of spread, and tree mortality. BEHAVE became BehavePlus in 2002, with significant improvements aided by the increase in computational power of modern computers and GIS technology. BehavePlus was an upgrade from the original BEHAVE program developed in 1977, and was later adopted by the USFS as a nationally supported system in 1984 (Andrews 2007). BEHAVE represented the beginning of technologically advanced fire modeling systems which incorporated a set of five sub-models developed from earlier fire behavior research from Rothermel's surface fire spread model and Burgan's newly described fuel models (Andrews 2007). Original versions of BEHAVE were utilized by most of the leading wildland fire management agencies, furthering the demand for increased fire modeling capabilities that consequently lead to a series of upgrades in BehavePlus versions 1 (2002), 2 (2003), 3 (2005), 4 (2007), and 5 (2010). BehavePlus now consists of 35 models, highlighted by nine core modules that estimate surface fire spread, crown fire spread, safety zone considerations, fire size profiles, containment indices, spot fire potential, crown scorch potential, ignition potential of firebrands, and mortality

associated with bark thickness and crown scorch in pine-dominated systems (Heinsch and Andrews 2010). Further enhancement of BehavePlus can be attributed to the increased availability of standardized fuel models that have increased from the original 13 fuel models to a comprehensive set of 53 fuel models as well as the ability to create customized fuel models. With the addition of greater input parameters and output indices, BehavePlus has continued to be the leading “point-based” fire modeling approach that has provided quality fire simulations for predetermined geographical regions of the landscape. In addition to physical and weather inputs, most fire models use fuel chemistry inputs such as net heat content (NHC) and kinetic data derived from oxygen bomb calorimetry (OBC) and thermogravimetric analysis (TGA). For example, BehavePlus utilizes a suite of fuel models that uses a standardized NHC value of 8,000 BTU/lb for all fuel model types except high load, humid climate grass which uses 9,000 BTU/lb (Scott and Burgan 2005, Rivera et al. 2012). To a lesser extent, some kinetic data has been used in other physical fire models (Tihay and Gillard 2011).

BehavePlus is particularly well suited for prescribed burn managers who are concerned with predefined burn compartments and fuels management projects rather than wildfire containment concerns requiring fire growth modeling features found in spatial modeling systems like FARSITE, FSpro, and FlamMap (Andrews 2007). A number of assumptions and limitations associated with each system remain



problematic, and one system alone cannot effectively produce ideal sets of fire behavior outputs required for every fire management decision. For example, fire researchers today are still challenged with accurate prediction of crown fire spread and initiation, and still rely on older versions of crown fire behavior models (Stratton 2006).

### Native and Exotic Species

#### Yaupon

Yaupon is a native evergreen shrub, adapted to open sites and has a shade tolerance that allows it to persist under tree canopies (Vines 1960, Halls 1977, Scifres 1980), and may form dense thickets ranging from 5-9 m in height (Halls 1977). Foliar biomass accumulations have been reported up to 168 kg ha<sup>-1</sup> underneath conifer stands in East Texas; however, biomass production in open rangeland can yield 5-57 times greater foliar production compared to plants of the same age persisting beneath forest stands (Halls 1977). Dense infestations can inhibit desired seedling establishment and may increase understory flammability (Hough 1969, Long et al. 2006, Shadow 2011).

Effective management regimes for controlling yaupon entail multiple management approaches utilizing prescribed fire and herbicides. Yaupon's capacity to reproduce asexually through root or basal crown sprouting result in low mortality post prescribed fire, indicating the need for follow up herbicide treatments for

effective control. Between 60-100% mortality can be achieved, depending on prescribed burn timing, age structure, and herbicide application regimes (Mitchell et al. 2005).

### Eastern Red Cedar

Eastern red cedar is a common evergreen tree that ranges from 10-20 m tall (NRCS). Reproduction is exclusively by seed and is frequently distributed by avian foraging with subsequent seed deposition along perching sites, especially fence lines and open woodlands. Eastern red cedar is shade intolerant and can persist on a wide range of soils. Distributions of eastern red cedar in the Pineywoods is limited by increased forest stand density, which constrains establishment to forest gap openings, road sides, fence lines, and abandoned fields. Due to its propensity to invade abandoned agricultural fields and disturbed sites, eastern red cedar has greatly expanded its range in the Post Oak Savannah and Blackland Prairie Ecoregions, and is often targeted in grassland restoration efforts (Smeins et al. 2005).

Eastern red cedars' lack of asexual reproduction makes its especially vulnerable to fire, making prescribed burning a very cost-effective treatment option. However, rural population growth in the Post Oak Savannah and Blackland Prairie Ecoregions has complicated prescribed burn campaigns due to mixed public perceptions of prescribed burning. Additionally, mature stands of eastern red cedar

require low fuel moistures and windy, dry conditions to carry prescribed fire through dense contiguous canopies that lack herbaceous fuels, increasing the risk of fire escape. Consequently, mechanical removal of eastern red cedar is generally a preferred treatment option near populated areas, as well as for dense, mature stands with inadequate herbaceous fuel loading and continuity.

### Escarpment Live Oak

Escarpment live oak is a monoecious tree capable of forming shrub-like thickets and can range from 15-25 m in height (Goldman 2017). The leaves have an evergreen appearance, but are considered deciduous due to considerable leaf-drop prior to flowering in early spring. Southern live oaks (*Quercus virginiana*) occupy the south to southeastern regions of the Pineywoods, Post Oak Savannah, and Black Prairie Ecoregions, while escarpment live oaks are generally found in the west to northwestern regions of the Post Oak Savannah and Blackland Prairie Ecoregion. Appearance of both species are similar, but the escarpment live oak is generally smaller and is more drought-tolerant and cold-hardy. Other common names for the escarpment live oak include scrub, plateau, and Texas live oak. Hybridization is common between southern and escarpment live oaks, and has led to significant confusion with respect to differentiating between the two species (Goldman 2017).

Escarpment live oaks are moderately shade tolerant and can persist on a wide range of sites. Fire exclusion and overgrazing in central Texas has led to a

greater live oak densities and intrusion into grassland communities resulting in reduced grazing potential (Rollins and Bryant 1986). Escarpment live oaks are susceptible to top-kill by fire due to relatively thin bark, but can resist fire by vigorous basal sprouting in young trees. Stands with well-developed crowns tend to reduce fire intensity, which facilitates greater soil moisture retention and cooler humid conditions. Since young escarpment live oaks sprout vigorously post disturbance, frequent prescribed fire can control tree densities, but infrequent prescribed fire can cause increases in stem densities limiting the use of fire in some prairie restoration activities (Carey 1992).

#### Southern Red Oak

Southern red oak is common throughout the southeastern U.S., and are generally found in the Pineywoods of Texas, with some extension into the Post Oak Savannah to the Brazos River line (Carey 1992). Trees generally occur on xeric, upland sites with sand, loam, or clay soils in the Alfisol and Ultisol orders. Southern red oaks' thin bark is vulnerable to fire, but fire resistance increases as a function of increasing tree diameter growth. Fire also encourages basal sprouting which can increase stem density under moderate fire frequencies. In general, fire can be used to control regeneration in pine stands, while low intensity fires can facilitate advanced regeneration through faster oak sprouting growth compared to its competitors (Carey 1992).

## Greenbrier

Greenbrier is a rhizomatous, evergreen to semi-evergreen climbing woody vine that can reach lengths of 3-8 m (Carey 1994, Sullivan 1994). Regeneration is by seed and rhizomes, and seeds are widely dispersed by birds and other wildlife (Sullivan 1994). Common greenbrier (*Smilax rotundifolia*) and saw greenbrier (*Smilax bona-nox*) are commonly found throughout the Pineywoods, Post Oak Savannah, Blackland Prairie Ecoregions. Greenbrier is considered a facultative pioneer species and colonization can occur across many sites (Carey 1994). When established, greenbrier can dominate sites and is capable of forming dense, impenetrable thickets.

Fire generally top-kills greenbrier, but rhizomatous sprouting allows greenbrier to persist under varying fire regimes. Stransky and Halls (1979) reported significant height reductions of saw and common greenbrier vines, with slight increases in stem density as well as 11-31% mortality post fire; thus, making greenbrier more accessible to wildlife herbivory while also reducing ladder fuels. Although greenbrier generally increases in abundance post fire, prescribed fire intensity and frequency will dictate the degree of control, while eradication is very unlikely without the aid of herbicides.

## Chinese Privet

Chinese privet (*Ligustrum sinense*) is an evergreen to semi-deciduous shrub that can grow up to 10 m (USDA NRCS). Chinese privet occupies a variety of ecosystems and can tolerate a wide range of conditions; typically preferring mesic soils and abundant sunlight (Thomas 1980). Colonization is prevalent on disturbed sites found along fencerows, streams, bayous, and forest margins (Godfrey 1988). Chinese privet has a prolific reproductive capacity aided by high seed production and adventitious root and bud sprouting (Ulyshen et al. 2010), and grows in dense thickets in and adjacent to mesic sites throughout East Texas (Greene and Blossey 2012). Thickets have been reported covering 100% of the forest floor and completely displacing native species (Merriam and Feil 2002, Ulyshen et al. 2010, Greene and Blossey 2012).

Several studies have evaluated the impact of Chinese privet on ecosystems and potential management strategies including mechanical removal, herbicide application, and prescribed fire (Faulkner et al. 1989, Hanula 2009, Ulyshen et al. 2010, Greene and Blossey 2012). Prescribed fire application had mixed results, with moderate fire behavior and patchy burn patterns resulting in moderate aboveground mortality, likely attributed to Chinese privet's affinity to moist, low-lying sites (Faulkner et al. 1989). The combination of mechanical and herbicide applications

proved more successful in ecological restoration and controlling Chinese privet (Hanula 2009).

### Chinese Tallow

Chinese tallow is a deciduous tree capable of rapid growth, ranging from 7-20 m (Vines 1960, Grace et al. 2001). Chinese tallow has adapted to a wide variety of ecosystems, limited only by frigid and arid conditions (Jubinsky and Anderson 1996), and it has invaded several woodland types in the southeastern U.S., including bottomland hardwood, pine, mixed-pine, and mixed hardwood stands with a propensity for disturbed sites (Nijjer et al. 2002, Ramsey et al. 2005). Shade tolerance is highly variable, although increased sunlight enhances growth rates (Gan et al. 2009). Chinese tallow is highly prolific, exhibiting high seed production, and adventitious root and crown sprouting stimulated by disturbance (Grace et al. 2001, Gan et al. 2009). Seed dispersal is facilitated by a number of avian species foraging on abundant seed yields and floodwaters may exacerbate seed dispersion in riparian systems (Renne et al. 2000).

Chinese tallow proliferation and range expansion has triggered a suite of management approaches, including prescribed fire, prevention measures, mechanical removal, herbicide application, and public education campaigns. Research on Brazoria National Wildlife Refuge suggests that prescribed fire may have significant impacts on Chinese tallow relative to available fuel loading

characteristics, repeated burns, target size structure, and timing of burn during the growing season (Grace 1998, Grace et al. 2001). Experimental prescribed fire regimes suggest gradual susceptibility of Chinese tallow to fire by the continual reduction of size classes of trees from repeated hot burns and the regeneration of flammable native species to carry fire in future burns (Grace 1998, Grace et al. 2001). Prescribed fire treatments post mastication may also benefit from differences in seasonal ignitability and combustibility of cured wood residue (Tiller et al. 2020). Mechanical and herbicide control regimes have been met with similar results, dependent on time of treatment, establishment of tree infestation, and combined herbicide treatment measures.

#### Assessing Flammability and Thermal-kinetics of Wildland Fuels

Determining wildland fuel flammability is a complex process involving evaluation of the physical, chemical, and thermal-kinetic properties of natural fuels relative to the cascading effects of combustion reactions. Flammability is defined as having four elements intrinsic to all wildland fuels: conceptual and quantitative measures of (1) ignitability, (2) combustibility, (3) sustainability, and (4) consumability (Anderson 1970, Martin et al. 1993). All four are influenced by individual plant moisture content, percent carbon composition, presence of volatile compounds, leaf thickness, and overall surface area-to-volume ratio of foliage (Behm et al. 2004). Ignitability is the minimum temperature required for ignition and



has also been reported as ignition delay time (Anderson 1970), time to ignition (Dimitrakopoulos and Panov 2001), and relative spontaneous ignition temperature (Liodakis et al. 2008). Combustibility is the rapidity in which a fuel burns and is measured through heat release rates, peak temperature trends, and visual observations of flame spread or height (White and Zipper 2010). Sustainability is the measure of the fuels' capacity to continue burning with, or without, an external heat source and is commonly correlated to heat of combustion, total heat release, and duration of observed flame emission (White and Zipper 2010). Consumability is the proportion of mass or volume loss of the fuel resulting from combustion and is measured according to mass loss rate and residual mass fraction indices.

Physical factors affecting natural fuel flammability can be attributed to the inherent variability in plant phenology, physiology, chemical composition, geographic location, and physiologic cycles derived from changing environmental cues associated with the transition of seasons (White and Zipperer 2010). Natural plant communities constitute the fuel complex continuum, and can express a multitude of spatial and temporal variations derived from species-specific attributes, as well as combined attributes of the entire plant community (Mack and D'Antonio 1998). Fire propagation across structurally diverse fuel complexes is inherently difficult to describe, given variances in individual plant and ecosystem structure. Species-specific attributes can be described through physical structures according to branch

size, leaf size, crown density, retention of dead material, surface area-to-volume ratio, total aboveground biomass, and branch configurations that contribute to horizontal and vertical fire spread (White and Zipperer 2010). Likewise, structural configuration of the entire plant community fuel complex is dependent on fuel continuity, density, packing ratio, and vertical and horizontal spatial arrangement. Individual plant species' physiologic and chemical compositions add further complexity by expressing differences in fuel moisture, volatile compounds, carbon composition, and mineral and lignin content (White and Zipperer 2010).

Environmental cues associated with seasonal changes and differing geographic regions can also have significant effects on individual plant species physiology, reflecting potential variations in chemical composition both spatially and temporally (Weise et al. 2005). Greater wildland fuel flammability is correlated with fuel moisture and the proportion of volatile compounds present in wildland fuels (Rothermel 1972, Shafizadeh et al. 1977). Fuel moisture consequently formed one of the major input parameters into fire behavior modeling systems. The significance of volatile compound content in wildland fuel was also recognized in early research, but has had limited application in fire behavior modeling systems (Rothermel 1983).

Volatile compounds such as terpenes, fats, oils, and waxes contain secondary chemicals or extractives that have high heats of combustion, low heat capacity, and volatility that increase fuel flammability (Shafizadeh et al. 1977, Susott

1980). The chemical process of combustion involves the pyrolysis of organic substrate releasing combustible gases, resulting in ignition of gas-phase products under sufficient air-fuel ratio parameters. Relative flammability of solid fuels is dependent on effective heat content released by gas-phase products and is measured through proportional calculations of total heat release resulting from combustion relative to the temperature dependence required for gasification of combustible volatiles. These parameters are used to determine the effective heat content and rate of heat release as a function of temperature (gasification profile) compared to loss of substrate mass during combustion analysis (Shafizadeh et al. 1977). Resulting data analysis details the proportion of volatile extractives and correlating temperature profiles to assess green foliage chemical volatility and contribution to both low temperature ignition probability and high temperature fire intensity. Many southeastern Coastal Plain shrub species contain volatile oils and waxes that enhance flammability, including gallberry (*Ilex glabra*), wax myrtle (*Myrica cerifera*), rhododendron (*Rhododendron sp.*), and swamp titi (*Cyrilla racemiflora*) (Burgan and Susott 1991).

Wildland fuel flammability has been studied since the late 1960's, with a primary focus on wildfire research and plant selection for the WUI and biomass energy industry (Weise et al. 2005, Leroy et al. 2010). However, significant challenges exist with standardized testing methodologies and obtaining a consensus

of how to incorporate the chemical and thermal-kinetic properties of natural fuels into existing and modern fire modeling systems (Weise et al. 2005). Early research primarily used thermogravimetric analysis (TGA), differential thermogravimetric analysis (DTG), differential scanning calorimetry (DSC), differential thermal analysis (DTA), and OBC. TGA utilizes small amounts (10-20 mg) of ground sample that are placed in either an oxidative (21% O<sub>2</sub>) or non-oxidative (Inert-N<sub>2</sub>) atmosphere which is subjected to a calibrated, increasing temperature ramp that depicts temperature-mass loss curves relative to thermal degradation of fuel. DTG is the derivative of the temperature-mass loss curve divided by the sample mass (Tihay and Gillard 2011), while DSC also utilizes a calibrated temperature ramp in inert and oxidative atmospheres, but differs from TGA by measuring heat flow curves of the sample as an exothermic or endothermic reaction as a function of temperature. DSC and DTA are essentially the same testing methodology, but differ in data acquisition, with DSC measuring quantitative heat flux values, whereas DTA measures qualitative thermal values (Leoni et al. 2001). OBC is used to obtain gross heat content (GHC) by combusting the sample in a 100% oxidizing atmosphere to obtain complete thermal degradation and subsequent total heat output.

More recent flammability testing methodologies use oxygen consumption calorimetry (OCC) that estimates heat release values according to oxygen depletion measurements. OCC assumes that most materials containing carbon, hydrogen,

oxygen, and nitrogen have an average net heat release of  $13.1 \text{ MJ kg}^{-1}$  of oxygen (Hugget 1980). OCC has been accepted as the worldwide standard testing methodology for evaluating fire code standards in building materials, and has recently seen further application in flammability testing of natural vegetation (White and Zipper 2010). Flammability studies of plants utilizing OCC have increased, primarily from the simplification of heat release measurements derived from exhaust gases that can be channeled into exhaust gas hood systems. OCC testing procedures have also expanded the utility of flammability testing by using an open combustion system that can incorporate small bench-scale (cone calorimeter) experiments to full-scale experiments of entire plant specimens. The four primary flammability parameters can be evaluated through visual estimation of onset and duration times associated with flame emission in an open combustion atmosphere throughout the experiment, as opposed to the closed system of TGA, which measures heat release rates according to temperature and mass loss indices. Both cone calorimetry and TGA methodologies constitute the primary flammability testing procedures used in past and present research, with both methodologies possessing distinct advantages and disadvantages associated with defining significant flammability parameters of wildland fuels for inclusion into fire modeling systems.

## Cone Calorimetry

The cone calorimeter is the most common bench-scale testing method that uses OCC in an exhaust gas hood system, where samples are exposed to a constant heat flux from a conical heating element. It is fitted with a spark igniter for piloted ignition, a sample load cell that measures mass loss, a helium-neon laser that measures smoke obscuration, and a suite of different sample holders developed to address heat release rate variances associated with differing fuel sample configurations. Sample holder configuration continues to be debated due to the large number of possible fuel configurations that include ground samples, whole plant parts, and green or dry samples. Even though the cone calorimeter is gaining international acceptance and greater use, there are limitations associated with its use due to a lack of availability and cost (White and Zipperer 2010).

Research utilizing cone calorimetry relative to the four primary fuel parameters has yielded Time to Sustained Ignition (TSI), Average Effective Heat of Combustion (AEHOC), Total Heat Release (THR), Peak Heat Release Rate (PHRR), and Residual Mass Fraction (RMF) indices (White et al. 2002, Enniful and Torvi 2005, Weise et al. 2005, Blank et al. 2006, Dibble et al. 2007). All five cone calorimetric outputs can address all four fuel flammability properties through TSI (ignitibility), AEHOC (sustainability), THR (sustainability), PHRR (combustibility), and RMF (consumability) indices (Dibble et al. 2007).

Heat Release Rates (HRR) of wildland fuels are one of the most important characteristics for understanding the combustion process, fire characteristics, and fire propagation rates (Shafizadeh et al. 1977, Weise et al. 2005, Dibble et al. 2007, Schemel et al. 2008, Rivera et al. 2012). Continued interest in addressing HRR variances associated with OCC led to the modification of the cone calorimeter to include thermopile sensors in the hood as opposed to the traditional oxygen consumption sensors to quantify HRR more efficiently. The mass loss calorimeter (MLC) and subsequent test results indicated good repeatability, reasonable HRR approximation, and ease of use (Madrigal et al. 2009). However, HRR, relative to TSI and PHRR values, were still variable due to the heterogeneous nature of porosity inherent to fuel beds and varying fuel moistures existing in live and dead fuels of differing species. Overall, cone calorimetric studies have been successful in broadening the knowledge of fuel flammability characteristics relative to AEHOC, but continued variability in TSI and PHRR data compared to AEHOC outputs still exist and testing procedures need to be refined (Dibble et al. 2007).

#### Oxygen Bomb Calorimetry

OBC measures the gross heat content of small, ground samples of natural and processed products by monitoring total heat release values resulting from the complete combustion (100% O<sub>2</sub> atmosphere), compared to the total mass loss of the sample. Studies have utilized OBC to assess GHC and NHC values to evaluate

wildland fuel flammability. NHC is obtained by subtracting the heat of vaporization of water from the GHC value, while the NHC value can be further refined by subtracting the mass of the remaining ash residue to obtain an ash-free NHC. Standard NHC values (with ash residue) formed the first thermal heat content parameter in early fire modeling systems by incorporating a constant low heat of combustion of  $18.61 \text{ MJ kg}^{-1}$  and a mineral ash content value of 5.55% for surface fuels specific to the standard fire models used in the BEHAVE and FARSITE fire behavior models (Burgan and Rothermel 1984, Andrews 1986, Finney 1998).

Van Wagtendok et al. (1998) investigated NHC (ash) of 19 Sierra Nevada conifer species, resulting in an average  $2.50 \text{ MJ kg}^{-1}$  increase in standard NHC values outlined in the standard fuel models, indicating a potential under-prediction of fire line intensity by an average of 16%, but up to 47% for some species. Williams and Agee (2002) reported an average 10% increase in ash-free foliar heat content of three Pacific Northwest conifers over the standard heat content, which could introduce errors in estimating crown fire intensity. Both studies suggest an ash-free correction factor for local species' NHC indices for improved fire behavior prediction. Further limitations of OBC relative to flammability studies is the measurement of heat content in a 100%  $\text{O}_2$  atmosphere as opposed to ambient air (21%  $\text{O}_2$ ). Even with the limitations associated with OBC, current NHC inputs have served as an acceptable estimation of fire behavior prediction for past and present fire models.



However, the incorporation of ash-free NHC's in fuel models may help improve fire behavior predictions.

### Thermogravimetric Analysis and Differential Scanning Calorimetry

The thermal degradation of natural products is a complex process involving a series of temperature dependent, decomposition reactions among four primary fractions of organic compounds existing in plant tissue: extractives (volatiles), cellulose, hemicellulose, and lignin. Wildland fuels are also referred to as lignocellulosic fuels, which describe the lignin-cellulose matrix of plant-based products that differ with respect to thermal properties. TGA, DTG, DSC, and DTA are all well suited to evaluate the four primary chemical components associated with combustion of lignocellulosic fuels and their use has been applied extensively worldwide.

DTA and DSC studies are excellent methods for measuring heat flow versus temperature indices for evaluating global reaction enthalpies (heat release at constant pressure) associated with thermal degradation of lignocellulosic fuels. DTA and DSC curves describe three distinct phases of thermal degradation, which include the distillation of water and volatile compounds followed by the oxidation of cellulosic compounds and carbonaceous char. The first phase represents an endothermic reaction involving a dehydration process consisting of water vapor and low molecular weight volatiles, while the two subsequent exothermic reactions

represent the combined oxidation of cellulose, hemicellulose, and lignin. DSC indices have also been used to determine the conversion degree  $\alpha$  component of the Arrhenius kinetic equation by defining the ratio between the partial enthalpy and the total heat of reaction as Equation (1),

$$\alpha = \frac{\Delta H_{\text{partial}}}{\Delta H_{\text{total}}} \quad (1)$$

where  $\alpha$  can be introduced into Equation (2) (see page 52) (Leoni et al. 2001). Leroy et al. (2009) investigated the enthalpy values associated with the thermal degradation of the four universal biopolymers existing in lignocellulosic fuels by conducting a series of extraction methods to separate cellulose, holocellulose (cellulose + hemicellulose), and lignin from four Mediterranean species. Each extraction was run through DSC using dry air (80% N<sub>2</sub>/20% O<sub>2</sub>) at a rate of 30 mL min<sup>-1</sup> with a temperature range of 400-900 K resulting in mean values of reaction enthalpies ( $\Delta_r H^\circ / J g^{-1}$ ) of -8176, -6892, -15109, and -16329 indicating significant changes in heat energies with respect to extractive, cellulose, hemicellulose, and lignin fractions.

TGA and DTG have been extensively used for thermogravimetric studies, although less commonly in the United States where OCC is of primary interest. TGA relies exclusively on the DTG profile, defined as the derivative of the mass versus the temperature, divided by the initial sample mass (Tihay and Gillard 2011). DTG

curves are evaluated by measuring the mass loss as a function of temperature at the onset, maxima, and end-point of the curves to produce flammability and thermal kinetic parameters. TGA studies using biomass have focused on the devolatilization reaction using non-oxidative (inert-N<sub>2</sub>) atmospheres to calculate the pyrolytic effects of first-order kinetic reactions (Saddawi et al. 2009). Interest in wildfire behavior modeling has led to an increased interest in TGA applications utilizing oxidative (80% N<sub>2</sub>, 20% O<sub>2</sub>) atmospheres to better simulate conditions associated with wildfire environments. Utilizing TGA under inert conditions is reasonably accurate, and repeatable by slowing the thermal degradation process to capture a controlled release of all the pyrolytic products associated with hemicellulose, cellulose, and lignin. However, TGA studies utilizing oxidative atmospheres have presented challenges due to the rapidity of the combustion reaction producing erratic and increased mass loss rates associated with the DTG curves across the temperature range (Munir et al. 2009, Elder et al. 2011). Further complications have been reported with DTG curve convergences associated with the degradation of cellulose and hemicellulose. TGA studies using an inert atmosphere (pyrolysis) will typically graph 3-4 DTG peaks as opposed to 2-3 DTG peaks using an air atmosphere. Many of the issues related to the rapidity of combustion in an oxidative atmosphere were expected and the relevance of TGA studies for wildfire behavior modeling clearly

needed a technique that utilizes the appropriate gas proportions existing in ambient air.

Munir et al. (2009) used TGA to collect the proximate values of percent ash, fixed carbon, and volatile mass on biomass products by using a series of temperature ramps under a N<sub>2</sub> atmosphere and finished the test with an introduction of air to combust the remaining products. This procedure is known as a proximate elemental analysis, which follows American Society for Testing and Materials (ASTM) E1131-08 guidelines (Cantrell et al. 2010), and can serve to measure and compare flammability parameters (Biagini et al. 2006, Maryandyshev et al. 2015). Liodakis et al. (2008) used TGA to evaluate four Mediterranean forest species in an air atmosphere to measure relative spontaneous ignition temperature (RSIT) and gas-phase combustion maximum weight loss rate and duration according to the onset of the first DTG peak and concluding at the end-point of the second DTG peak. Leroy et al. (2010) used TGA analysis utilizing an air environment to evaluate the strawberry tree (*Arbutus unedo*), a species of concern due to its abundance on the Corsican landscape and recent increase in wildfire activity regionally. This study used a series of three heating ramps to evaluate the kinetic parameters associated with activation energy ( $E\alpha$ ) as function of conversion degree ( $\alpha$ ) to develop a model using  $E\alpha$  versus temperature to simulate greater heating ramps. They concluded

that greater heating rates could be used to overcome some of the limitations associated with TGA studies involving oxidative atmospheres.

### Assessing Thermal-kinetic Parameters

All four testing methodologies associated with TGA, DTG, DTA, and DSC may be complemented by measuring endothermic and exothermic heat flow, mass loss, and heat release curves which constitute all of the essential kinetic mechanisms required for assessing the thermal kinetic parameters (kinetic triplet) of activation energy ( $E\alpha$ ), pre-exponential factor ( $A$ ), and reaction order ( $n$ ) where  $E\alpha$  is a function of conversion degree ( $f(\alpha)$ ). All three kinetic parameters and the degree of conversion " $\alpha$ " are widely recognized as decisive inputs for fire models that are based on a comprehensive set of physical mechanisms associated with the fluid dynamic theory. The most widely used kinetic method is based from the Arrhenius law and constant kinetic parameters coupled with the kinetic theory of heterogeneous condensed-phase reactions described by Brown et al. (1980) (Equation 2):

$$\frac{d\alpha}{dt} = \beta \frac{d\alpha}{dT} = f(\alpha)A \exp\left(-\frac{E\alpha}{RT}\right) \quad (2)$$

where  $\alpha$  is the degree of conversion,  $t$  the time,  $T$  the temperature,  $\beta$  the constant heating rate,  $f(\alpha)$  the differential conversion function,  $E\alpha$  the activation energy,  $A$  the pre-exponential factor, and  $R$  the gas constant. The degree of conversion ( $\alpha$ ) is derived from Equation (3) (Tihay and Gillard 2011):

$$\alpha = \frac{m - m_o}{m_{650} - m_o} \quad (3)$$

where  $m$  is the initial sample mass,  $m_o$  is the sample mass at temperature, and  $m_{650}$  the sample mass at 650°C. With the foundation of the universal kinetic method combined with the knowledge of  $E_a$ ,  $A$ , and  $f(\alpha)$  parameters, a global kinetic scheme describing fuel pyrolysis over time can be expressed as a reaction model  $f(\alpha)$  (Equation 4):

$$f(\alpha) = (1-\alpha)^n \quad (4)$$

where  $n$  is the reaction order. Equation (4) is inserted into Equation (2) with the logarithm applied to both sides of the equation (Equation 5):

$$\ln\left(\frac{d\alpha}{dt}\right) - n \ln(1 - \alpha) = \ln A - \frac{E_a}{RT} \quad (5)$$

where  $n$  is determined by fitting its value to obtain a straight line by plotting  $\ln(d\alpha/dt) - n \ln(1 - \alpha)$  vs.  $T^{-1}$ .  $E_a$  and  $A$  can be calculated from the slope intercept. This method can be used for a degree of conversion between 0.1 and 0.9 for three heating rates that are averaged to obtain global kinetic parameters (Tihay and Gillard 2011). Mathematical derivations can be further separated into two classes of kinetic evaluations utilizing a model-fitting or model-free isoconversional approach (Tihay and Gillard 2011). The model-fitting method calculates kinetic data according to assumptions derived from the reaction model  $f(\alpha)$ , where only one thermogravimetric heating rate is conducted per sample, leading to unreliable and

useless kinetic parameters (Vyazovkin and Wight 1999, Ortega 2000). Model-free kinetic methods serve as the best approach by utilizing several thermogravimetric heating rates which are evaluated according to the kinetic parameters as a function of the degree of conversion rather than one thermogravimetric heating rate based on an assumed reaction model  $f(\alpha)$  (Friedman 1964, Flynn and Wall 1966, Akahira and Sunrose 1971, Sbirrazzuoli et al. 2000, Starink 2003).

The isoconversion method (model-free method) is the preferred approach for accurately describing kinetic parameters as a function of time (Han et al. 2011, Tihay and Gillard 2011). Isoconversional methods are based on the idea that the reaction rate given a constant degree of conversion depends only on temperature (Tihay and Gillard 2011); therefore, each degree of conversion can be derived by the following the expression (Equation 6):

$$\frac{df(\alpha)}{dT} = \frac{dA}{dT} = 0 \quad (6)$$

Isoconversional methods involve two approaches; differential methods based on Equation (2), or integral methods that separate the expressions and are dependent on the  $\alpha$  and  $T$  for integration into Equation (2). There are three well-accepted isoconversion methods that utilize both of the approaches stated above: Friedman (differential), Ozawa- Flynn-Wall (integral), and Kissinger-Akahira-Sunrose (integral) (Friedman 1964, Flynn and Wall 1966, Akahira and Sunrose 1971). All three methods were tested by Tihay and Gillard (2011) using TGA/DTG on three

Mediterranean forest fuels, with the Friedman method demonstrating good results for the degree of conversion parameters between 0.1 and 0.9, while the three heating rates produced mean coefficient of determinations ( $R^2$ ) of 97.8, 98.8, and 98.8% for all three species tested (Tihay and Gillard 2011). Positive results were attributed to the differential method of Friedman that does not use approximations of the temperature integral as opposed to the integral method of Ozawa-Flynn-Wall (OFW) and Kissinger-Akahira-Sunrose (KAS) (Tihay and Gillard 2011). Integral methods have been thoroughly investigated with a significant number of proposed functions for the reaction model  $f(\alpha)$  that are dependent on the type of approximation and the ratio of the  $E_a/RT$  function (Starink 2003, Tihay and Gillard 2011). Friedman's differential method takes the logarithm of equation (2) to obtain Equation (7):

$$\ln\left(\frac{d\alpha}{dt}\right) = \ln(f(\alpha)) + \ln(A(\alpha)) - \frac{E_a(\alpha)}{RT} = \ln(A'(\alpha)) - \frac{E_a(\alpha)}{RT} \quad (7)$$

where  $A'(\alpha) = f(\alpha)A(\alpha)$ .  $E_a(\alpha)$  and  $A'(\alpha)$  were derived from plotting  $\ln(\beta d\alpha/dT)$  vs.  $1/T$  with a constant  $\alpha$  (0.1 to 0.9) for three heating rates (Tihay and Gillard 2011).

Model-free isoconversion methods developed by OFW and KAS continue to be well-accepted methodologies. The OFW method (Flynn and Wall 1966) integrates Equation (2) leading to Equation (8):



$$G(\alpha) = \int_{\alpha_0}^{\alpha} \frac{d\alpha}{f(\alpha)} = \frac{A}{\beta} \int_{T_0}^T \exp\left(-\frac{E_a(\alpha)}{RT}\right) dT = \frac{AE_a(\alpha)}{R\beta} p(x) \quad (8)$$

Where, Equation (9) completes Equation (8)

$$p(x) = \frac{\exp(-x)}{x} - \int_{-x}^{\infty} \frac{\exp(x)}{x} dx \quad \text{with } x = \frac{E_a(\alpha)}{RT} \quad (9)$$

and further transformation is achieved by using an approximation developed by Doyle (1962) (Equation 10):

$$\ln(p(x)) = 5.3308 - 1.0516x \quad (10)$$

combined with final logarithmic transformation of Equation (7) in to Equation (11):

$$\ln \beta = \ln\left(\frac{A \cdot E_a(\alpha)}{R}\right) - \ln(G(x)) + 5.3308 - 1.0516 \frac{E_a(\alpha)}{RT} \quad (11)$$

where  $E_a(\alpha)$  can be determined by plotting  $\ln \beta v. T^{-1}$  at a constant  $\alpha$  (0.1-0.9) for three heating rates. The KAS approach (Akihira and Sunrose 1971) uses the same concept as OFW with the exception of substituting Doyle's approximation of Equation (10) in to Equation (12):

$$p(x) = \frac{\exp(-x)}{x^2} \quad (12)$$

with the logarithmic transformation of Equation (7) in to Equation (13):

$$\ln \frac{\beta}{T^2} = \ln\left(\frac{AR}{E_a(\alpha)}\right) - \ln(G(\alpha)) - \frac{E_a(\alpha)}{RT} \quad (13)$$

where  $E_a(\alpha)$  can be determined by plotting  $\ln \frac{\beta}{T^2} v. T^{-1}$  at a constant  $\alpha$  (0.1-0.9) for three heating rates.

There have been many attempts at refining the global, kinetic parameters of lignocellulosic fuels according to isoconversional methodologies based on both the integral and differential approach. Tihay and Gillard (2011) reported the benefits of the Friedman differential approach that does not approximate the temperature integral by making no assumptions related to the reaction model  $f(\alpha)$ . However, there has been no consensus whether kinetics should be determined globally or segregated into multiple conversion degree fractions (Saddawi et al. 2009). Likewise, development of suitable kinetic calculations for testing wildland fuels at higher heating rates more representative of flaming combustion and wildfire conditions are needed (Saddawi et al. 2009, Leroy et al. 2010)

## METHODS

### Ecoregion and Species Selection

Site selection was based on the presence of native and nonnative focal species occurring within the ecoregions. The Post Oak Savannah and Blackland Prairie were selected due to connectivity to the Pineywoods where Tiller et al. (2020) conducted work on yaupon, Chinese privet and Chinese tallow. These ecoregions are comprised of fire-adapted ecosystems that historically exhibit frequent FRI's ranging from 1-12 years (Stambaugh et al. 2014). Invasive plant species selection was based on Tiller et al. (2020), while eastern red cedar and greenbrier were selected due to their common occurrence across all three ecoregions. Escarpment live oak was selected for the Post Oak Savannah and Blackland Prairie due to its semi-evergreen foliage, which could potentially be impacted by both dormant and growing season fires. Southern red oak was selected for the Pineywoods based on its common occurrence in upland, fire-prone forest communities.

As shown in figure 1, sampling in the Pineywoods occurred at the USDA Forest Service, Stephen F. Austin Experimental Forest (SFAEF) and the Stephen F. Austin State University (SFASU), Pineywoods Native Plant Center (PNPC). Post Oak Savannah sites were located at the Texas A&M University Equine Center (TAMUEC), Veterans Park and Athletic Complex in College Station, Texas, and the

U.S. Army Corps of Engineers (ACOE) property at Somerville Lake. Blackland Prairie sites included ACOE property at Granger Lake, and the Trinity River Audubon Center and White Rock Lake Park in Dallas, Texas.

All sites were visited during the dormant (February) and growing (August) seasons to collect foliage and wood samples of five separate plants in the 0-2 m height class. All samples were live foliage borne on separate plants, and were consistently collected at chest height. The 0-2 m height class was chosen as it represents the generally accepted height for effective control of woody plants using prescribed fire. Since Chinese tallow and southern red oak exhibit fall leaf abscission, their seasonal foliage comparisons were limited to the growing season. To account for this limitation, small diameter ( $\leq 0.635$  cm) stem wood samples were collected during both seasons in order to maintain consistency with potential seasonal variances related to chemical composition. Regionally diverse and seasonal collection periods were used to account for potential species-specific physiological differences that may influence flammability.

#### Research Site Descriptions

##### Stephen F. Austin Experimental Forest

The SFAEF is a designated research subunit of the Angelina National Forest that consists of 1041 ha of mixed pine-hardwood forest. The 54.3 ha sample collection site was located on the WNW forest boundary where the terrain was flat to

gently sloped (3-10%), with aspects ranging from SSE-SSW. The climate is humid subtropical, with annual precipitation ranging from 1016-1422 mm (Shaw 2011; Figure 2). Common overstory species consisted of loblolly pine, longleaf pine, shortleaf pine, sweetgum, southern red oak, cherrybark oak (*Quercus pagoda*), white oak, American hophornbeam (*Ostrya virginiana*), and red maple (*Acer rubrum*). Common understory cover included yaupon, Chinese privet, American beautyberry, wax myrtle, greenbrier, muscadine grape (*Vitis rotundifolia*), and peppervine (*Ampelopsis arborea*). Much of the understory is a dense thicket from years of little forest management, most notably a lack of prescribed burning (Figure 3).

Species foliar and wood samples were collected from 2013-2019 (Table 1). All species were collected on well-drained Alfisol soils with a fine, sandy, loam texture (Table 2). Soil data was accessed through the Soil Survey Geographic Database (SSURGO) hosted by Environmental Systems Research Institute (ESRI). Average monthly precipitation was estimated for each year according to dormant (Nov.-Mar.) and growing (Apr.-Oct.) season time periods using National Oceanic and Atmospheric Administration (NOAA) climate data (NOAA 2020) from the Angelina County Airport weather station (Table 3). Mean monthly normal precipitation and maximum temperatures were also calculated using 1981-2010 NOAA climate data (NOAA 2020). Mean monthly normal dormant and growing season precipitation and

maximum temperatures were 108.20 mm and 100.33 mm, and 18.4°C and 30.6°C, respectively (Table 3). Mean monthly seasonal precipitation was below normal in the 2013 and 2017 dormant season, while mean monthly seasonal maximum temperatures were all above normal with the exception of the 2019 dormant season.

#### Pineywoods Native Plant Center

The PNPC is a native hardwood forest located on the SFASU campus. Sample collections occurred within a 21.0 ha block of relatively flat terrain with little to no slope and aspect features. The climate is humid subtropical, with annual precipitation ranging from 1016-1422 mm (Shaw 2011; Figure 2). The forest type is mixed hardwood-pine with common overstory associates consisting of American elm, cherrybark oak, Florida maple (*Acer floridanum*), red maple, green ash, American hophornbeam, loblolly pine, mockernut hickory (*Carya tomentosa*), southern red oak, sweetgum, sugarberry, and water oak. Common understory species include Chinese privet, Carolina laurel cherry (*Prunus caroliniana*), wax myrtle, muscadine grape, and greenbrier (Figure 4). Chinese privet collection occurred in 2013 (Table 1) on a well-drained Alfisol soil of fine loamy texture (Table 2). Mean monthly dormant and growing season precipitation was below normal, while maximum temperatures remained above normal (Table 3).

### Texas A&M University Equine Center

Yaupon, Chinese privet, and greenbrier foliage were collected in 2016 (Table 1) on a 36.0 ha block of undeveloped land at the TAMUEC. Property management had not occurred for many years, and the site developed into a thicket of woody species with an intermix of mature post oaks. Terrain was flat, with the exception of a relatively deep creek running through the southern boundary of the property. The climate is humid subtropical with annual precipitation ranging from 762-1143 mm (Shaw 2012). Overstory composition consisted primarily of post oaks, eastern red cedar, sugarberry, and cedar elm. Dominant understory cover consisted of Chinese privet, yaupon, and greenbrier (Figure 5). All species were collected on a moderately well-drained Alfisol soil of fine, sandy, loam texture (Table 2). Mean monthly precipitation and maximum temperatures were all above normal for all seasons (Table 3).

### Veterans Park and Athletic Complex

The Veterans Park and Athletic Complex is located within the City of College Station, Texas, just east of State Highway 6 between East University Drive and Harvey Road. Topography was flat, with a few small depressions interspersed throughout. The climate is humid subtropical with annual precipitation ranging from 762-1143 mm (Shaw 2012). Overstory cover included winged elm, American elm, sugarberry, water oak, cedar elm, and Chinese tallow (Figure 6). Chinese tallow

samples were collected from 2016-2017 (Table 1) on a 2.0 ha site along the western boundary of the park, which lies within the flood plain of Hudson Creek. The soil was a moderately well-drained Inceptisol of fine, loam texture. Mean monthly precipitation and maximum temperature were above normal for all seasons, with the exception of the 2017 dormant season, which had below normal precipitation (Table 3).

### Somerville Lake

The Somerville Lake site is a 7.2 ha tract located just east of Apache Hills boat ramp on the NNE arm of the lake. Terrain was relatively flat with low rolling hills of ~ 1-4% slope. In wet years, lake levels are capable of flooding some of the site. The climate is humid subtropical with annual precipitation ranging from 762-1143 mm (Shaw 2012). Dominant overstory composition was comprised of eastern red cedar, escarpment live oak, honey mesquite (*Prosopis glandulosa*), and post oak (Figure 7). Dominant herbaceous cover included Indiangrass, little bluestem, and switchgrass (*Panicum virgatum*). Eastern red cedar and escarpment live oak foliage were collected in 2017 (Table 1). The soil was a well-drained Alfisol of fine, sandy, loam texture. Mean monthly precipitation and maximum temperatures were above normal in all seasons, with the exception of the 2017 dormant season, which had below normal precipitation (Table 3).



### Granger Lake

Granger Lake is a 1,645 ha lake owned by the ACOE located ~ 9 miles NNE of Taylor, Texas. Escarpment live oak samples were collected in 2017 (Table 1) on a 14.1 ha site located on the SSW side of the dam. Terrain was flat with rolling hills of roughly 1-3% slopes. The climate is subtropical with annual rainfall ranging from 762-1143 mm (Shaw 2012). Common tree species on the site included escarpment live oak, sugarberry, and honey mesquite (Figure 8). Dominant herbaceous cover consists of side-oats grama (*Bouteloua curtipendula*), big bluestem, eastern gamagrass, and Indiangrass. The soil was a well-drained Inceptisol of silty, clay, loam texture. Mean monthly precipitation was above normal in the growing season and below normal in the dormant season, whereas, mean monthly maximum temperatures were above normal in the dormant season and below normal in the growing season.

### Trinity River Audubon Center

The Trinity River Audubon Center is a 48.5 ha property established by the City of Dallas-Trinity River Corridor Project. Sample collection occurred on a 6.57 ha section of the Audubon Center that was upslope from the adjacent Trinity River bottomland forest. Terrain was relatively flat with rolling hills of ~1-4% slope. The climate is subtropical with annual rainfall ranging from 762-1143 mm (Shaw 2012). Common overstory associates included pecan (*Carya illinoensis*), sugarberry,

American elm, cedar elm, and green ash. Dominant understory species consisted of Chinese privet, yaupon, honey locust (*Gleditsia triacanthos*), possumhaw (*Ilex decidua*), and greenbrier (Figure 9). Species foliar samples were collected in 2016-2017 (Table 1). The soil was a well-drained Alfisol of loamy, fine, sand texture. Mean monthly precipitation was above normal in all seasons, with the exception of the 2017 dormant season, which exhibited below normal rainfall. Mean monthly maximum temperatures were above normal in all seasons, with the exception of the 2017 growing season, which exhibited a below normal average temperature.

#### White Rock Lake Park

White Rock Lake Park is a 411 ha municipal lake owned by the City of Dallas, located ~8.0 km NE of downtown Dallas. The 4.2 ha site was located near the dam in the southwest corner of the lake. Terrain was relatively flat within the floodplain while some 5-15% slopes lead to higher terraces extending out of the bottomland. The climate is subtropical with annual rainfall ranging from 762-1143 mm (Shaw 2012). Common overstory associates consisted of green ash, cedar elm, sugarberry, black willow (*Salix nigra*), American elm, slippery elm (*Ulmus rubra*), and eastern cottonwood (*Populus deltoides*) (Figure 10). Common understory species included swamp privet (*Forestiera acuminata*), possumhaw, and boxelder. Chinese tallow samples were collected in 2016-2017 (Table 1) in a bottomland hardwood flood plain immediately behind the dam. The soil was a well-drained Mollisol of fine texture.

Mean monthly precipitation and maximum temperatures for the 2016 growing seasons were above normal. Whereas, mean monthly precipitation in the 2017 dormant season was below normal, while the mean monthly maximum temperature was above normal.

### Heat Content and Thermogravimetric Analyses

Heat content and thermogravimetric analyses were evaluated at the SFASU Chemistry Lab. OBC and thermogravimetric and differential thermogravimetric analyses (TGA/DTG) were used to investigate each species' flammability properties. Undried green foliar samples were treated with liquid nitrogen to increase the rigidity of leaf tissue to facilitate grinding in a standard coffee grinder. Stem wood samples were ground in a Thomas Model 4 Wiley mill utilizing a 2-mm sieve to maintain consistent sample texture. Ground samples were dried for 48 hours at 40° C in an air-convection oven to avoid loss of volatiles from high heat exposure. Both foliage and wood samples were processed to a uniform texture by using a series of 10-, 20-, 35-, 42-, 100-, and 150-mesh U.S. Standard sieves. Each mesh fraction underwent preliminary testing using OBC and TGA to ascertain the fraction with the most reproducible test results. Post testing, the 35-mesh fraction yielded the best results for both testing procedures and was subsequently used throughout the study.

## Oxygen Bomb Calorimetry

OBC testing was performed with a model 1301 Parr calorimeter that was standardized with benzoic acid per manufacturer specifications (Parr 2008). Preliminary testing using standard pelletized samples resulted in numerous misfires and incomplete combustion, so an alternative method using hard, double ought (OO) gelatin capsules was used as a sample holder. The gelatin capsules were standardized with water-corrected (13%) heat of combustion spike corrections every time the OBC was re-standardized with benzoic acid. Gelatin capsules were stored in a desiccator, so the lower range of the gelatin capsule water content (13-16%; Chang et al. 1998) was used as a correction. Since the initial mass loss associated with the first oxidative TGA peak (35-150°C) mainly represents water vaporization (Munir et al. 2009, Tihay and Gillard 2011, Amini et al. 2019), heat of combustion corrections for water vapor were determined by dividing the mass loss at the first oxidative TGA peak of each species by the initial mass of the sample, which adjusts GHC to NHC.

After net heat content with ash (NHC-A) was obtained, a proximate analysis procedure was performed using TGA to evaluate percent ash (ash%) content (Munir et al. 2009). Subsequent ash% values were used to adjust NHC-A to obtain ash-free net heat content (NHC-AF) indices. Ash% values served as potential indicators of seasonal changes specific to each species, while allowing for an NHC-A correction

value that may lead to improved fire line intensity calculations and fire behavior predictions (Williamson and Agee 2002). TGA proximate analysis values for percent volatiles (VM%), percent fixed carbon (FC%), and ash% were performed following Munir et al. (2009), utilizing a heating regime of 35-910°C with a linear heating rate of 25°C min<sup>-1</sup> in a nitrogen atmosphere and held for 10 min. at 910 °C; after the 10 min. hold, a gas switch to air was performed to ignite all combustible products, reducing the sample to noncombustible, inorganic ash residue. Proximate analysis metrics served as contrasting data for species-specific flammability estimates, with > VM%(s) generally indicating greater potential for increased flammability, while > ash%(s) are general indicators of reduced ignitability and gas-phase combustibility.

#### Oxidative Thermogravimetric Analysis

Oxidative TGA/DTG data were evaluated with a PerkinElmer Simultaneous Thermal Analyzer (STA) 6000 calibrated to manufacturer specifications (PerkinElmer 2010). Ground, 20-mg dried samples were placed in a porcelain crucible and analyzed with a 10°C min<sup>-1</sup> linear heating ramp ranging from 35-650°C in an air atmosphere (21% O<sub>2</sub> by volume); air purge gas was set at 20 ml min<sup>-1</sup>. DTG curves produced in air atmospheres were evaluated by measuring mass loss as a function of temperature at the onset, maxima, and endset of the DTG peaks to yield estimated flammability parameters. Flammability parameters were based on relative spontaneous ignition temperature (RSIT), gas-phase maximum mass loss rate (GP-

MMLR), and gas-phase combustion duration (GP-CD) (Liodakis et al. 2008).

Ignitability parameters were derived from RSIT estimates using the onset tool in Pyris 13.2, where tangential vertices were placed at the endset of the first DTG peak and the temperature correlating with the second peak maxima located on the second derivative TGA curve (Figure 11). Combustibility parameters for gas-phase combustion (GPC) were estimated by subtracting the second DTG peak maximum mass loss % ( $\% \text{ min}^{-1}$ ) by the corresponding mass loss % ( $\% \text{ min}^{-1}$ ) at the estimated RSIT (Figure 12). Gas-phase combustibility and sustainability parameters were also estimated with GP-CD values, which were calculated by subtracting the second major DTG peak maxima time (min) with the onset time at the RSIT (Figure 12). Greater ignitability was reported as a function of increasing RSIT values according to previous studies (Liodakis et al. 2005, Liodakis et al. 2008). GP-CD values can serve as either an estimate of combustibility based on the rapidity of combustion, or sustainability based on greater gas-phase combustion times.

### Pyrolytic Thermogravimetric Analysis

Pyrolytic thermokinetics were assessed using a PerkinElmer STA 6000 using three linear heating ramps of  $10^\circ$ ,  $25^\circ$ , and  $40^\circ \text{ C min}^{-1}$  ranging from  $35\text{-}650^\circ \text{ C}$  in a nitrogen atmosphere; nitrogen purge gas was set at  $20 \text{ ml min}^{-1}$ . Seasonal and regional thermokinetics were evaluated by Friedman and Ozawa-Flynn-Wall (OFW) model-free isoconversional methods. Each species underwent foliar and wood

testing from five separate plants to evaluate mean composite  $E\alpha(s)$  ranging from 0.02-0.80  $\alpha$  and 0.02-0.52  $\alpha$  for global and GPC  $E\alpha$  combustibility estimates, respectively. Mean composite global  $E\alpha(s)$  were limited to 0.80  $\alpha$  to reduce data noise associated with high degrees of  $E\alpha$  (Sbirrazzuoli et al. 2009). Global  $E\alpha$  estimates were further modified by starting kinetic analyses for the prescribed linear heating rates at the endset of the first DTG peak (130-160°C) to exclude any variation in sample dehydration (Amini et al. 2019), while concluding at 550°C where mass loss was minimal due to the higher energy required to break lignin bonds (Collard and Blin 2014, Papari and Hawboldt 2015). Mean GPC  $E\alpha$  estimates were derived from the endset of the first DTG peak extending to the third DTG peak maxima, which represents the maximum mass loss rate (MMLR) associated with the rapid devolatilization of low molecular weight volatiles, hemicellulose, and lignin at the 10°, 25°, 40°C linear heating rates (Figure 13). Ignitability estimates for foliar samples were derived from  $E\alpha(s)$  ranging from 0.02-0.10  $\alpha$ , while wood samples were calculated from  $E\alpha(s)$  ranging from 0.02-0.20  $\alpha$ . All estimated flammability metrics were based on low mean  $E\alpha$  values that indicate lower energy inputs required to break chemical bonds that initiate the pyrolysis of low molecular weight volatiles, hemicellulose, cellulose, and lignin; in theory, the corresponding TG-DTG profiles with lower  $E\alpha$  values would constitute greater degrees of combustibility and

ignitability based on lower amounts of energy required for the evolution of combustible pyrolytic gases.

### Data Analysis

All statistical analyses were evaluated at the  $p < 0.05$  significance level. OBC data was evaluated for differences in NHC-A and NHC-AF values with respect to species, season, and ecoregion. Five foliage and wood samples were collected from five separate plants per species and underwent five replicate OBC analyses per sample. TGA proximate analysis yielded ash% indices which were used to determine NHC-AF values by adjusting ash% from original NHC-A values. NHC-A and NHC-AF indices derived from foliar samples were analyzed using two three-way ANOVA's, with species, season, and ecoregion serving as three independent factors, while NHC-A and NHC-AF values served as dependent variables. Chinese tallow stem NHC(s) were analyzed with a two-way ANOVA, with season and ecoregion serving as two independent factors. Chinese tallow foliage NHC(s) were tested using a one-way ANOVA with ecoregion serving as the independent factor. A post hoc Tukey's Studentized Range Test was applied to all ANOVA results to identify any pairwise differences between species, season, and ecoregion. Southern red oak stem was tested using a Two-sample T-test to identify any significant differences in NHC-A and NHC-AF with respect to season. Southern red oak foliage



data was excluded from these analyses due to the lack of foliage available for collection in the dormant season.

TGA oxidative flammability metrics classifying RSIT, GP-MMLR, and GP-CD were estimated by graphing the DTG curve based on a  $10^{\circ}\text{C min}^{-1}$  linear heating rate ranging from  $35\text{-}650^{\circ}\text{C}$  using percent mass loss as a function of temperature ( $^{\circ}\text{C}$ ) (Liodakis et al. 2008). Each species underwent one TGA oxidative test per five separate samples collected. Subsequent RSIT and combustion indices were averaged to approximate overall RSIT, combustion, and sustainability indices. Further statistical analysis was accomplished by evaluating semi/evergreen foliar samples with a three-way ANOVA, with species, season, and ecoregion serving as the three independent factors, and RSIT, GP-MMLR, and GP-CD serving as dependent variables. Chinese tallow foliage and wood were analyzed using a one-way (ecoregion) and two-way (season and ecoregion) ANOVA, respectively. A post hoc Tukey's Studentized Range Test was applied to all ANOVA results in order to identify any pairwise differences associated with species, season, and ecoregion. Southern red oak stem was analyzed using a two-sample T-test to identify any significant seasonal differences in oxidative flammability parameters within the Pineywoods.

Thermal-kinetic data was evaluated by Friedman and OFW model-free isoconversional methods. The Friedman method used the following equation:

$$\alpha = \frac{m - m_o}{m_{650} - m_o}$$

where  $\alpha$  equals mass,  $m$  is sample mass,  $m_o$  is initial sample mass at 35°C, and  $m_{650}$  is sample mass at 650°C; the logarithm form of the kinetics of heterogeneous condensed-phase reaction equation:

$$\ln\left(\frac{d\alpha}{dt}\right) = \ln(f(\alpha)) + \ln(A(\alpha)) - \frac{E_a(\alpha)}{RT} = \ln(A'(\alpha)) - \frac{E_a(\alpha)}{RT}$$

where d = derivative,  $\alpha$  = conversion degree, t = time,  $T$  = temperature, f = function,  $A$  = pre-exponential factor,  $R$  = gas constant,  $E_a$  = activation energy, and  $A'(\alpha) = f(\alpha)A(\alpha)$ .  $E_a(\alpha)$  and  $A'(\alpha)$  were derived by plotting ( $\beta$  = heating rate)  $\ln(\beta d\alpha/dt)$  vs.  $1/T$  at a constant  $\alpha$  (0.02 to 0.80) for three heating rates ( $\beta$ ) (Tihay and Gillard 2011). The kinetics equation was rewritten in slope intercept ( $y = -mx + B$ ) format as Equation 14:

$$\ln\left(\beta \frac{d\alpha}{dT}\right) = -\left(\frac{1}{T}\right)\left(\frac{E_a(\alpha)}{R}\right) + \ln(A'(\alpha)) \quad (14)$$

where  $y = \ln\left(\beta \frac{d\alpha}{dT}\right)$ ,  $mx = -\frac{1}{T} \frac{E_a(\alpha)}{R}$ , and  $b = \ln(A'(\alpha))$  with  $R$  serving as the gas constant of 8.314 J K<sup>-1</sup> mol<sup>-1</sup>. Thus, plotting  $\ln(\beta d\alpha/dT)$  vs.  $1/T$  will produce  $\ln(A'(\alpha))$  as the y-intercept and  $E_a(\alpha)$  the slope.

The OFW method (Flynn and Wall 1966) integrates ( $G(\alpha)$ ) the standard kinetic equation:

$$\frac{d\alpha}{dt} = \beta \frac{d\alpha}{dT} = f(\alpha)A \exp\left(-\frac{E_a}{RT}\right)$$

leading to equation:

$$G(\alpha) = \int_{\alpha_0}^{\alpha} \frac{d\alpha}{f(\alpha)} = \frac{A}{\beta} \int_{T_0}^T \exp\left(-\frac{E_a(\alpha)}{RT}\right) dT = \frac{AE_a(\alpha)}{R\beta} p(x)$$

where equation (9),  $\int_{\alpha_0}^{\alpha}$  = conversion degree ( $\alpha$ ) from 0-0.9%,  $\int_{T_0}^T$  = heating range,

and  $p(x)$  = temperature integral (no analytical solution):

$$p(x) = \frac{\exp(-x)}{x} - \int_{-x}^{\infty} \frac{\exp(x)}{x} dx \quad \text{with } x = \frac{E_a(\alpha)}{RT}$$

Further transformation is achieved by using an approximation developed by Doyle (1962) in equation:

$$\ln(p(x)) = 5.3308 - 1.0516x$$

combined with the final logarithmic transformation of Equation (7) in to equation:

$$\ln \beta = \ln\left(\frac{A \cdot E_a(\alpha)}{R}\right) - \ln(G(x)) + 5.3308 - 1.0516 \frac{E_a(\alpha)}{RT}$$

where  $E_a(\alpha)$  can be determined by plotting  $\ln \beta$  v.  $T^{-1}$  at a constant  $\alpha$  (0.1-0.9) for three heating rates ( $\beta$ ).

$E_a$  calculations were conducted using Netzsch software and displayed  $E_a$  as a function conversion degree ( $\alpha$ ) for both Friedman and OFW model-free isoconversional methods. Each species  $E_a(s)$  were averaged based on five separate foliar and wood samples. Global kinetic parameters of composite  $E_a(s)$  were calculated from the endset of the first DTG peak to 550 °C (Figure 13). Similarly, gas-phase kinetic parameters were evaluated from the endset of the first DTG peak

extending to the maxima of the third DTG peak (Figure 13). Ignitability kinetic parameters were estimated from the endset of the first DTG peak and concluded at  $0.10 \alpha$  for foliar samples and  $0.20 \alpha$  for wood samples. Kinetic parameters associated with global, GPC, and ignitability were estimated by averaging the specified range of composite  $E\alpha$  values specific to each sample and kinetic parameter. Each species range of respective  $E\alpha$  values were tested for outliers by using a modified Z-score according to Iglewicz and Hoaglin (1993). Subsequent mean composite  $E\alpha$  values were categorized according to low values, which in theory, represent species with greater flammability.

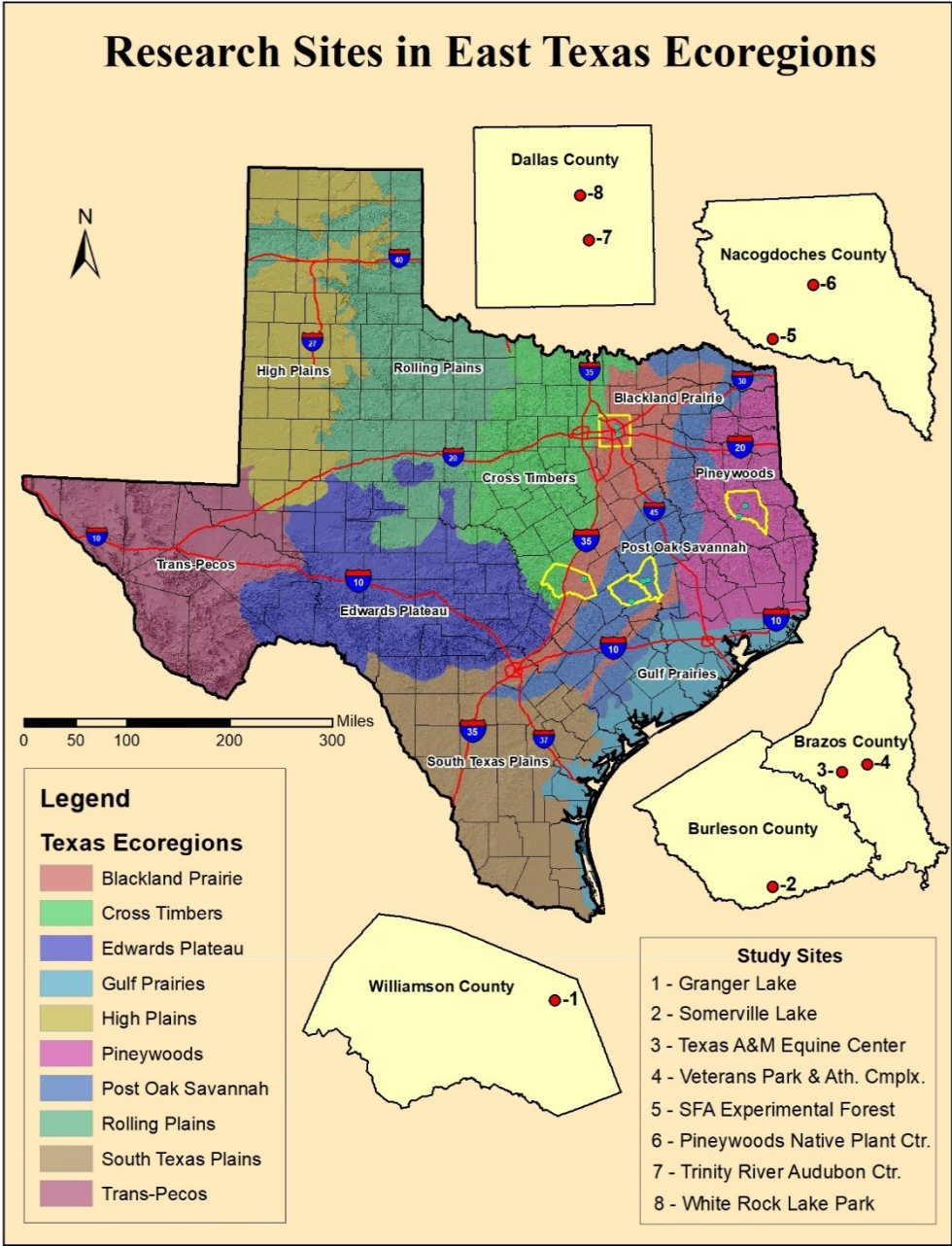


**Figure 1.** Research sites in the Pineywoods, Post Oak Savannah, and Blackland Prairie Ecoregions of East Texas.

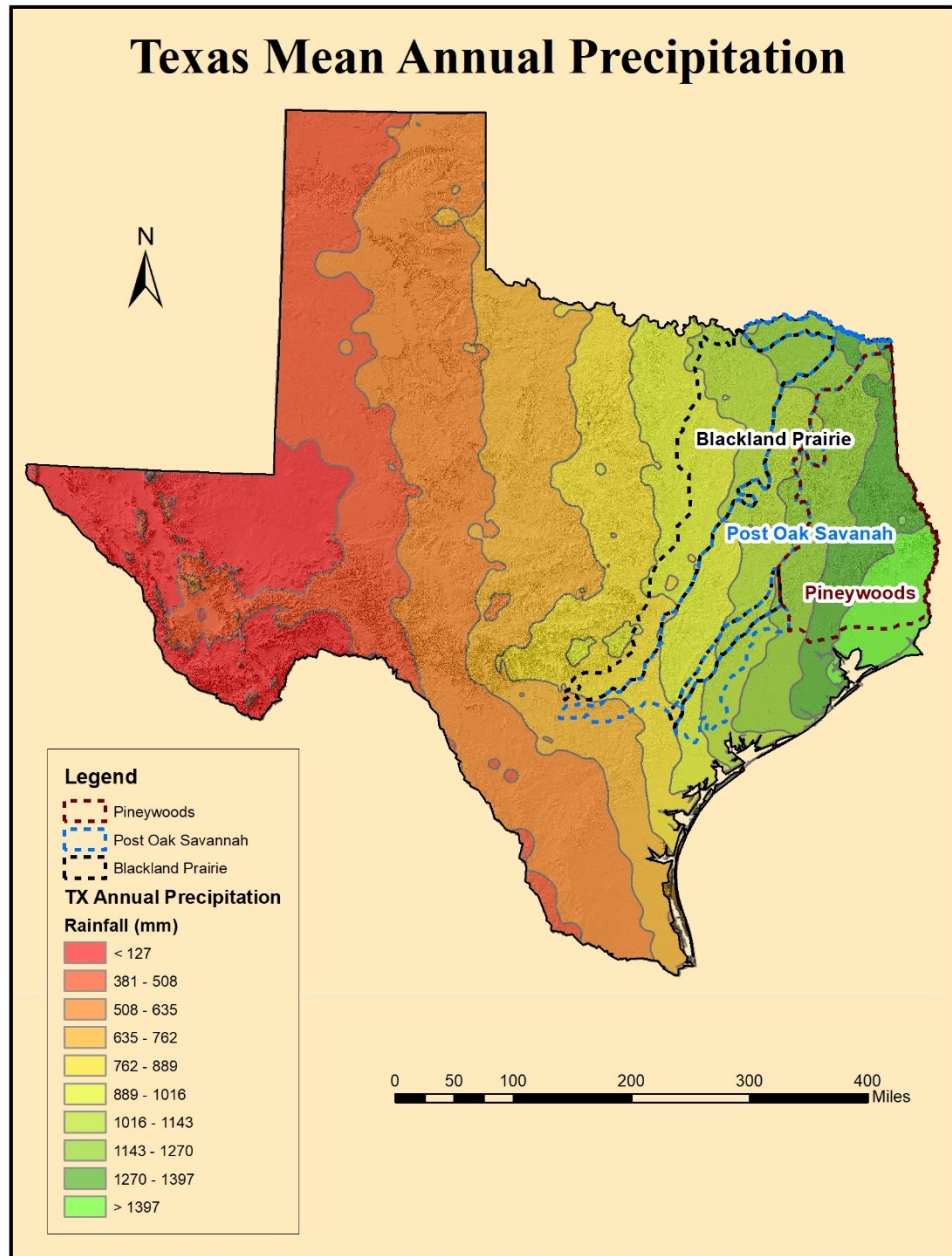


**Figure 2.** Texas mean annual precipitation gradient extending from west to east; annual precipitation was averaged based on NOAA climate data from 1981-2010.

**Table 1.** Species foliar and wood (w) sample collection times with corresponding sites and ecoregion. Site abbreviations are as follows: SFAEF – Stephen F. Austin Experimental Forest; PNPC – Pineywoods Native Plant Center; TAMUEC – Texas A&M Equine Center; SOMLK – Somerville Lake; VPAC – Veterans Park and Athletic Complex; TRAC – Trinity River Audubon Center; GRLK – Granger Lake; WRLK – White Rock Lake.

<i>Ecoregion/Site/ Yr.</i>	Pineywoods	Post Oak Savannah	Blackland Prairie
<i>Season/Species</i>			
<i>Dormant (Feb)</i>			
Yaupon	SFAEF - 2013	TAMUEC - 2016	TRAC - 2016
Chinese Privet	PNPC - 2013	TAMUEC - 2016	TRAC - 2016
Greenbrier	SFAEF - 2013	TAMUEC - 2016	TRAC - 2016
Eastern Red Cedar	SFAEF - 2017	SOMLK - 2017	TRAC - 2017
Escarpment Live Oak	-	SOMLK - 2017	GRLK - 2017
Chinese Tallow (w)	SFAEF - 2013	VPAC - 2017	WRLK - 2017
Southern Red Oak (w)	SFAEF - 2019		-
<i>Growing (Aug)</i>			
Yaupon	SFAEF - 2013	TAMUEC - 2016	TRAC - 2016
Chinese Privet	PNPC - 2013	TAMUEC - 2016	TRAC - 2016
Greenbrier	SFAEF - 2016	TAMUEC - 2016	TRAC - 2016
Eastern Red Cedar	SFAEF - 2016	SOMLK - 2017	TRAC - 2017
Escarpment Live Oak	-	SOMLK - 2017	GRLK - 2017
Chinese Tallow	SFAEF - 2013	VPAC - 2017	WRLK - 2016
Chinese Tallow (w)	SFAEF - 2013	VPAC - 2016	WRLK - 2016
Southern Red Oak	SFAEF - 2018	-	-
Southern Red Oak (w)	SFAEF - 2018	-	-

**Table 2.** Soil orders and general soil properties specific to each species, site, and ecoregion where foliar and wood samples were collected. Soil data was accessed through the Soil Survey Geographic Database (SSURGO) hosted by Environmental Systems Research Institute (ESRI). Ecoregions are abbreviated as follows: PW – Pineywoods; POS – Post Oak Savannah; BP – Blackland Prairie.

<i>Soil Properties Species/Ecoregion</i>	Soil Order	Soil Texture	Drainage
Yaupon-PW	Alfisols	Fine, Sandy, Loam	Well Drained
Yaupon-POS	Alfisols	Fine, Sandy, Loam	Mod. Well Drained
Yaupon-BP	Alfisols	Loamy, Fine, Sand	Well Drained
Chinese Privet-PW	Inceptisols	Fine, Loamy	Well Drained
Chinese Privet-POS	Alfisols	Fine, Sandy, Loam	Mod. Well Drained
Chinese Privet-BP	Alfisols	Loamy, Fine, Sand	Well Drained
Greenbrier-PW	Alfisols	Loamy, Fine, Sand	Well Drained
Greenbrier-POS	Alfisols	Fine, Sandy, Loam	Mod. Well Drained
Greenbrier-BP	Alfisols	Loamy, Fine, Sand	Well Drained
E. Red Cedar-PW	Alfisols	Fine, Sandy, Loam	Well Drained
E. Red Cedar-POS	Alfisols	Fine, Sandy, Loam	Well Drained
E. Red Cedar-BP	Alfisols	Loamy, Fine, Sand	Well Drained
E. Live Oak-POS	Alfisols	Fine, Sandy, Loam	Well Drained
E. Live Oak-BP	Inceptisols	Silty, Clay, Loam	Well Drained
Chinese Tallow-PW	Alfisols	Fine, Sandy, Loam	Well Drained
Chinese Tallow-POS	Inceptisols	Fine, Loam	Mod. Well Drained
Chinese Tallow-BP	Mollisols	Fine	Well Drained
S. Red Oak-PW	Alfisols	Fine, Sandy, Loam	Well Drained



**Table 3.** Ecoregion mean monthly precipitation and maximum temperatures from 2013-2019. Mean monthly seasonal National Oceanic and Atmospheric Administration (NOAA) climate data was averaged through Nov.-Mar. and Apr.-Oct. for the dormant and growing season, respectively. Normal seasonal precipitation and maximum temperatures were averaged according to monthly seasonal periods described above using 1981-2010 NOAA data. Respective climate data was accessed at NOAA weather stations in Angelina County Airport, Lufkin, Texas, Easterwood Airport, College Station, Texas, and Ferris, Texas for the Pineywoods, Post Oak Savannah, and Blackland Prairie Ecoregions.

<i>Precipitation-Temp.</i>	Precipitation (mm)	Max. Temp. (°C)
<i>Season-Normal-Year</i>		
<i>Dormant</i>		<i>Pineywoods</i>
<i>Normal</i>	108.2	18.4
2013	72.6	20.4
2016	122.7	20.1
2017	92.2	21.2
2019	120.1	16.5
<i>Growing</i>		<i>Pineywoods</i>
<i>Normal</i>	100.3	30.6
2013	98.6	31.4
2016	111.5	30.9
2018	131.2	30.8
<i>Dormant</i>		<i>Post Oak Savannah</i>
<i>Normal</i>	79.8	19.0
2016	102.6	20.7
2017	72.6	22.1
<i>Growing</i>		<i>Post Oak Savannah</i>
<i>Normal</i>	88.4	31.4
2016	124.2	31.5
2017	142.8	31.4

**Table 3.** Continued

<i>Dormant</i>		<i>Blackland Prairie</i>	
<i>Normal</i>	82.3		17.0
2016	125.5		17.9
2017	60.7		19.3
<i>Growing</i>		<i>Blackland Prairie</i>	
<i>Normal</i>	84.8		30.7
2016	111.3		31.0
2017	96.3		29.8

---



**Figure 3.** Understory thicket of yaupon, Chinese privet, Chinese tallow, and greenbrier under a mixed pine-hardwood stand on the Stephen F. Austin Experimental Forest.



**Figure 4.** Hardwood stand in the Pinewoods Native Plant Center with a understory cover consisting of Chinese privet and Carolina laurel cherry.





**Figure 5.** Thicket of Chinese privet under a remnant post oak motte adjacent to the Texas A&M Equine Center.



**Figure 6.** Riparian cover at Veterans Park and Athletic Complex, College Station, Texas with Chinese tallow mixed in the foreground.



**Figure 7.** Mix of escarpment live oak, eastern red cedar, and post oak at the Somerville Lake site.



**Figure 8.** Small escarpment live oak motte at the Granger Lake site.





**Figure 9.** Thicket of Chinese privet at the Trinity River Audubon Center in Dallas, Texas.



**Figure 10.** Thicket of Chinese tallow trees at White Rock Lake Park in Dallas, Texas.

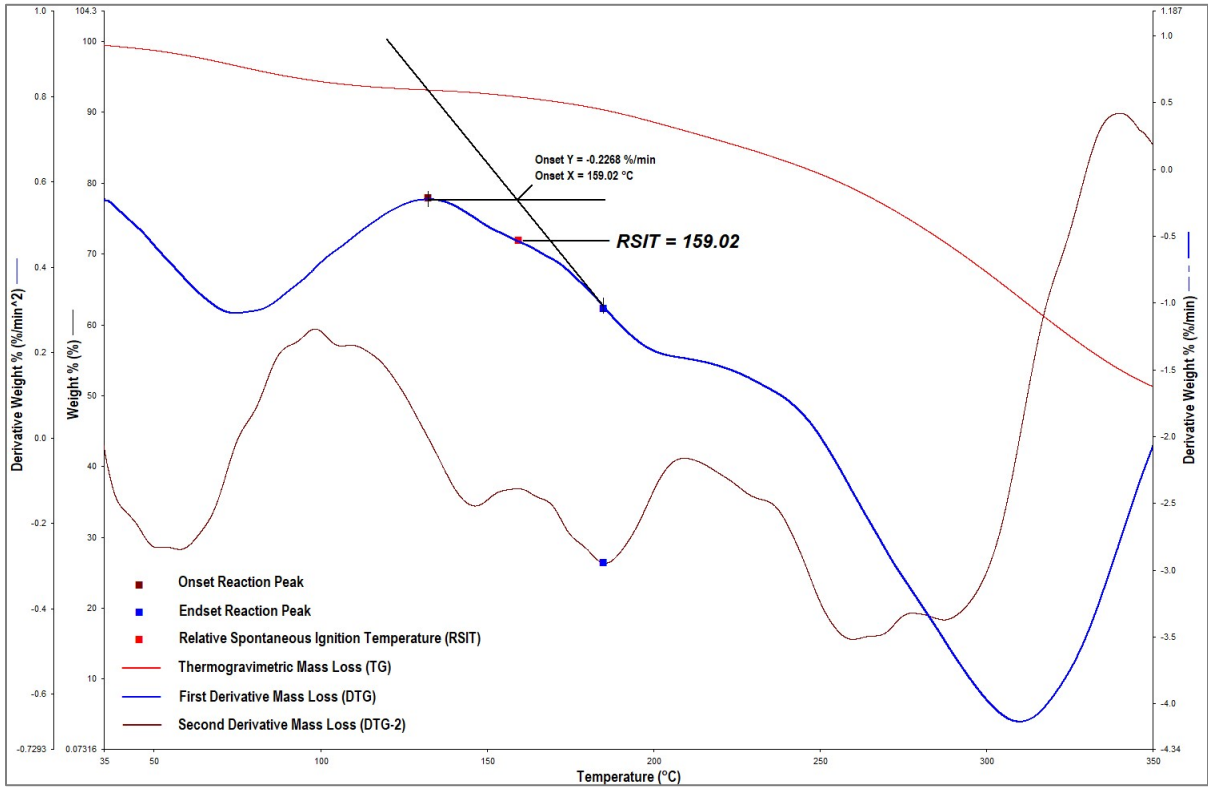


**Figure 11.** Oxidative thermogram depicting an estimated RSIT using the Pyris 13.2 onset tool tangential lines based on the first derivative mass loss curve (DTG). Onset tool vertices were placed at the endset of the first DTG peak and the corresponding temperature of the second derivative DTG peak maxima.

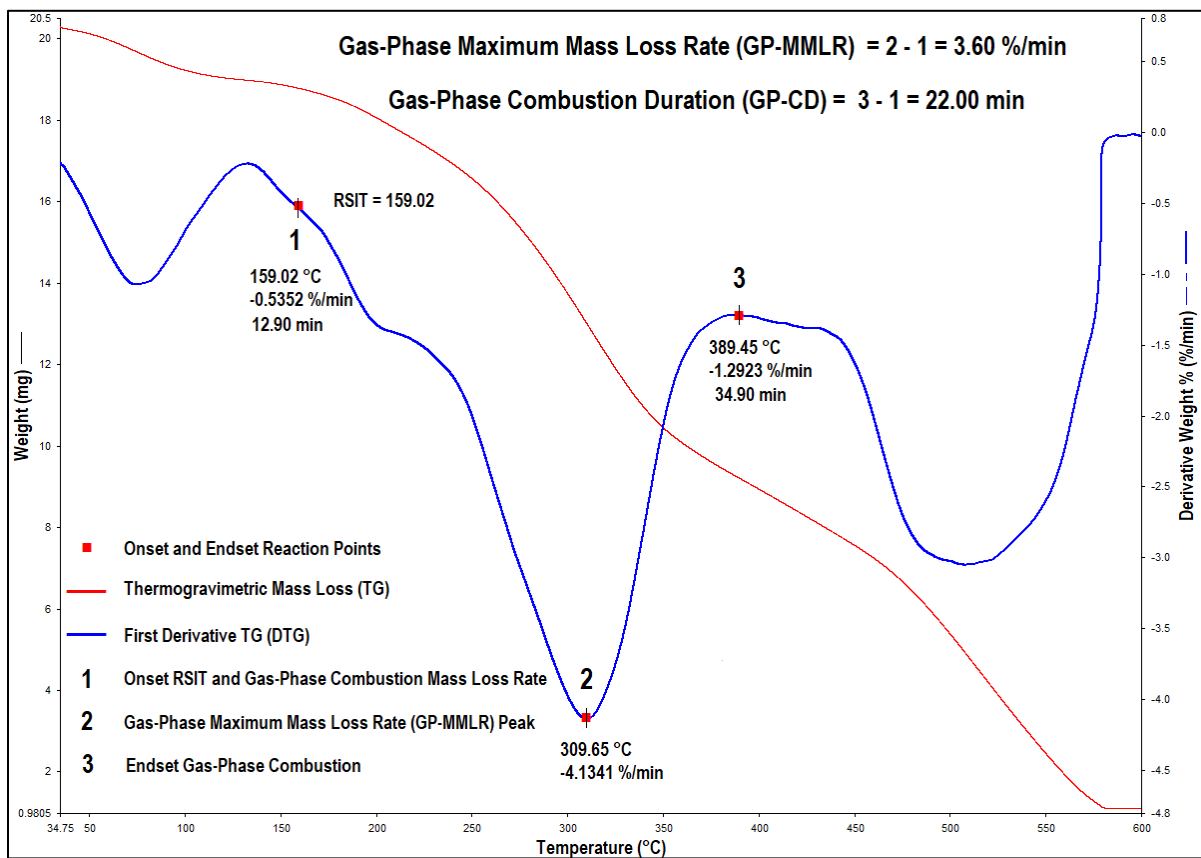


**Figure 12.** Oxidative thermogram depicting gas-phase maximum mass loss rate (%/min) and combustion duration (min) specific to the RSIT onset and second differential thermogravimetric (DTG) peak maxima and endset values.



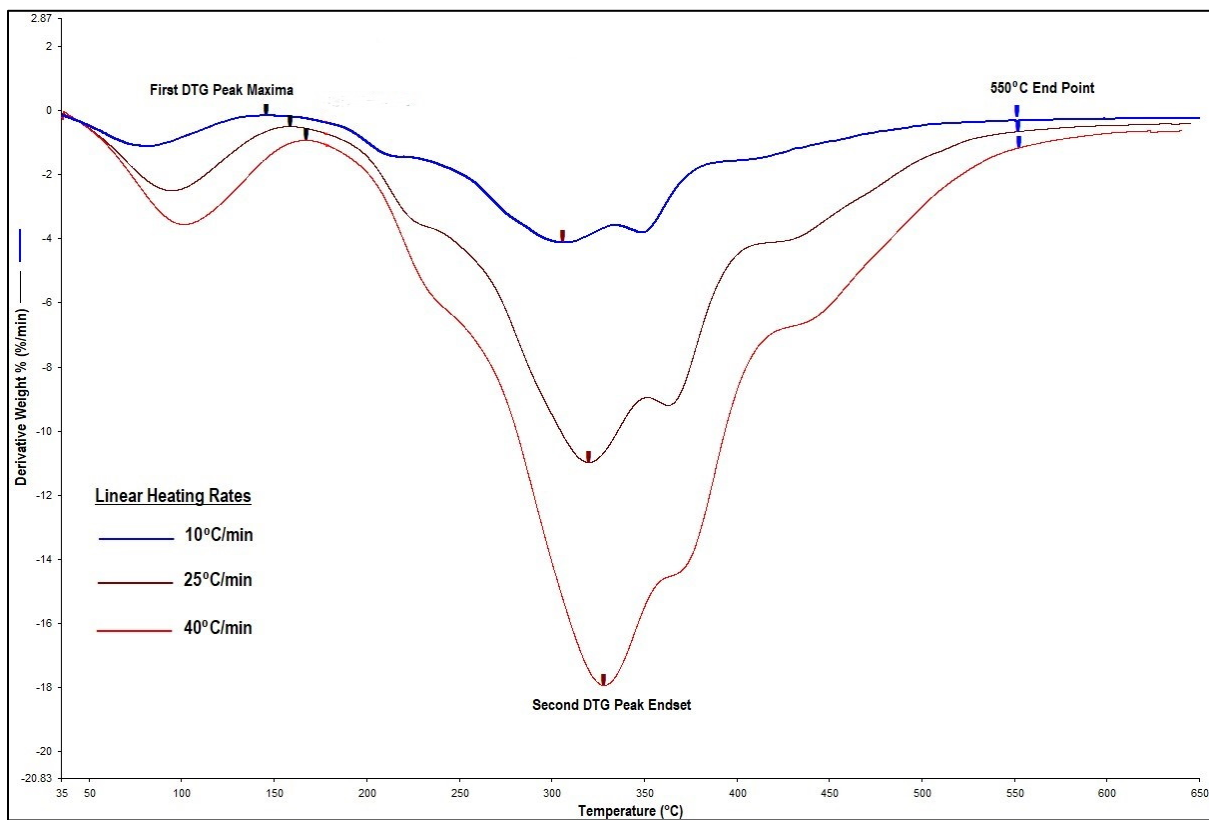


**Figure 13.** Dormant season devolatilization thermogram depicting the first DTG peak endset, third DTG peak maxima, and 550°C end points for linear heating rates of 10°, 25°, and 40°C min<sup>-1</sup>.

## RESULTS

### Proximate Analysis

#### Pineywoods Ecoregion

Since lower percentages of inorganic ash generally indicate greater gas-phase combustibility, ash% will be described based on lower values. Eastern red cedar and greenbrier produced the greatest and least dormant season combustibility based on higher VM%(s). Dormant season foliar VM% exhibited a fairly consistent reciprocal relationship with FC%, while ash% was more variable. Dormant season southern red oak wood produced a higher VM% and lower FC% than Chinese tallow wood, whereas ash% was relatively similar for both species (Table 4).

Greenbrier and Chinese tallow produced the greatest and least combustibility relative to low VM% and high ash%. Growing season Chinese tallow and southern red oak wood produced similar VM%'s, while their FC% and ash% exhibited < 1.0% reciprocal fluctuations. Foliar VM% was greatest in the growing season with the exception of Chinese privet. Conversely, foliar FC% was significantly lower in the growing season, excluding Chinese privet. Chinese privet and greenbrier exhibited considerable seasonal shifts in VM% and FC%, with Chinese privet producing a respective 2.85% increase and 3.04% decrease in dormant season VM% and FC%, while greenbrier produced a respective 7.13% increase and 6.13% decrease in

growing season VM% and FC%. Seasonal ash% did not follow a seasonal trend and varied in both seasons. Chinese tallow and southern red oak wood exhibited greater mean growing season VM%.

#### Post Oak Savannah Ecoregion

Post Oak Savannah dormant season foliar analysis for VM% and ash% indicated eastern red cedar and greenbrier had the greatest and least combustibility. In general, greater dormant season foliar VM%(s) correlated well with lower reciprocal FC%(s). Dormant season foliar ash% exhibited the greatest variability and produced no discernable relationships between VM%. Growing season foliar analysis for VM% and ash% indicated eastern red cedar and greenbrier had the greatest and least combustibility (Table 4). Growing season foliar VM%(s) did not exhibit a very strong correlation with low FC% and ash%.

All Post Oak Savannah foliar VM%(s) were higher in the dormant season as opposed to the growing season. Eastern red cedar exhibited the greatest seasonal shift in dormant season VM% (1.76%) and FC% (2.78%), while Chinese privet exhibited significant seasonal shifts in dormant season FC% (3.44%) and ash% (2.39%). Chinese tallow wood yielded a greater dormant season VM% and followed the same seasonal foliage VM%-FC% trend (Table 4).

### Blackland Prairie Ecoregion

Blackland Prairie dormant season foliar analysis for VM% and ash% indicated eastern red cedar and escarpment live oak had the greatest and least combustibility. Similar to previous ecoregions, greater dormant season foliar VM%(s) exhibited a strong inverse relationship with FC%(s). Growing season foliar analysis for VM% and ash% indicated eastern red cedar and escarpment live oak had the greatest and least combustibility (Table 4). Growing season foliage exhibited a reciprocal VM%-FC% relationship except Chinese tallow, whereas ash% showed no discernable correlation with VM%.

All foliar VM%(s) were higher in the growing season, with escarpment live oak exhibiting the greatest increase of 1.32% (Table 4). Foliar VM%-FC% trends were relatively the same in both seasons. The Blackland Prairie VM%-FC% trends were similar to the Post Oak Savannah, but VM% highs occurred in opposite seasons. Foliar ash% varied considerably with respect to season and exhibited no discernable relationship with VM%. Chinese tallow wood was significantly more combustible in the growing season based on a higher VM%(s).

### Ecoregion-wide Comparison

Foliar VM% was consistently higher in eastern red cedar, yaupon, and Chinese privet across all ecoregions, with the exception of greenbriers' higher growing season VM% in the Pineywoods. Seasonal foliar VM% was generally higher

in Blackland Prairie and lower in the Post Oak Savannah, whereas the Pineywoods seasonal VM% was more variable, especially in the growing season. Pineywoods growing season semi/evergreen foliage exhibited significant shifts in mean FC%, especially in Chinese privet and greenbrier. Foliar ash% trends were quite variable across ecoregions, especially in the growing season. Lastly, mean seasonal VM%, FC%, and ash% for Chinese tallow wood exhibited significant variation across ecoregions.

**Table 4.** Seasonal proximate analyses for volatile matter %, fixed carbon %, and ash % according to ecoregion. Standard deviation and wood samples (w) are denoted in parentheses.

<i>Proximate-Ecoregion Season-Species</i>	VM%	FC%	Ash%
Pineywoods			
<i>Dormant</i>			
Yaupon	79.55 (1.07)	16.51 (1.37)	3.93 (0.78)
Chinese privet	79.14 (1.73)	15.59 (2.22)	5.27 (0.60)
Greenbrier	78.51 (0.64)	17.65 (0.53)	3.84 (0.19)
E. Red Cedar	80.49 (0.89)	15.51 (0.83)	3.92 (0.46)
Chinese tallow (w)	83.56 (2.07)	14.47 (1.79)	1.97 (0.34)
S. Red Oak (w)	84.46 (1.17)	13.39 (1.10)	2.16 (0.56)
<i>Growing</i>			
Yaupon	79.91 (1.29)	16.01 (0.74)	4.08 (1.79)
Chinese Privet	76.29 (2.33)	18.63 (1.35)	5.07 (1.21)
Greenbrier	85.64 (0.76)	11.52 (0.70)	2.79 (0.21)
E. Red Cedar	81.35 (1.14)	14.78 (0.87)	3.87 (0.65)
S. Red Oak	74.99 (0.83)	22.25 (0.89)	2.75 (0.30)
Chinese Tallow	74.83 (1.68)	20.41 (1.37)	4.77 (0.64)
Chinese Tallow (w)	85.57 (1.78)	13.25 (1.17)	1.18 (0.64)
S. Red Oak (w)	85.39 (1.25)	12.59 (1.11)	2.03 (0.47)
Post Oak Savannah			
<i>Dormant</i>			
Yaupon	80.14 (0.68)	16.04 (0.84)	3.83 (0.91)
Chinese Privet	77.85 (1.12)	14.79 (1.12)	7.36 (0.38)
Greenbrier	76.59 (0.59)	19.14 (1.02)	4.26 (0.53)
E. Red Cedar	81.58 (0.42)	14.72 (0.36)	3.41 (0.33)
E. Live Oak	77.82 (0.41)	18.30 (0.69)	3.88 (0.55)
Chinese Tallow (w)	80.28 (0.76)	16.52 (0.76)	3.20 (0.25)

**Table 4.** Continued

<i>Growing</i>			
Yaupon	77.66 (0.55)	16.93 (0.54)	5.41 (0.90)
Chinese Privet	76.80 (0.77)	18.23 (0.55)	4.97 (0.29)
Greenbrier	76.51 (0.33)	19.40 (0.53)	4.09 (0.38)
E. Red Cedar	79.82 (0.38)	17.50 (0.59)	2.68 (0.88)
E. Live Oak	76.70 (0.95)	19.06 (1.04)	4.24 (0.35)
Chinese Tallow	76.75 (1.64)	17.06 (1.72)	6.19 (0.67)
Chinese Tallow (w)	79.13 (1.62)	18.01 (1.50)	2.86 (0.55)
<i>Ecoregion</i>	Blackland Prairie		
<i>Dormant</i>			
Yaupon	81.15 (0.78)	15.17 (0.59)	3.67 (0.33)
Chinese Privet	78.26 (1.22)	16.39 (1.26)	5.41 (0.36)
Greenbrier	77.43 (0.49)	17.58 (0.42)	4.98 (0.40)
E. Red Cedar	81.38 (0.67)	14.90 (0.93)	3.77 (0.74)
E. Live Oak	74.75 (1.11)	19.39 (1.08)	5.86 (1.33)
Chinese Tallow (w)	80.24 (1.15)	17.60 (0.89)	2.16 (0.29)
<i>Growing</i>			
Yaupon	81.27 (0.47)	14.37 (0.70)	4.36 (0.57)
Chinese Privet	79.04 (1.12)	16.15 (1.42)	4.81 (0.77)
Greenbrier	78.01 (0.40)	17.10 (0.41)	4.88 (0.12)
E. Red Cedar	81.36 (0.30)	14.68 (0.49)	3.96 (0.31)
E. Live Oak	76.07 (0.72)	19.85 (0.50)	4.08 (0.92)
Chinese Tallow	76.61 (0.30)	16.56 (0.38)	6.84 (0.50)
Chinese Tallow (w)	84.94 (1.05)	13.13 (0.86)	1.93 (0.58)

## Oxygen Bomb Calorimetry

### Pineywoods Ecoregion

Mean dormant and growing season foliar NHC-A ranged from 16.18-17.76 and 16.98-17.81 MJ kg<sup>-1</sup>, respectively, with greenbrier and eastern red cedar producing the greatest dormant and growing season NHC-A (Table 5). Mean dormant and growing season foliar NHC-AF ranged from 17.35-18.43 and 17.76-18.29 MJ kg<sup>-1</sup>, respectively (Table 6). Greenbrier and eastern red cedar produced the greatest mean dormant season NHC-AF, while Chinese privet, eastern red cedar, and southern red oak produced the greatest growing season NHC-AF (Figure 14). Southern red oak foliage yielded a greater mean NHC-A and NHC-AF compared to Chinese tallow foliage; however, Chinese tallows' greater ash% resulted in a significant increase in NHC-AF, which consequently became much closer to southern red oaks NHC-AF. Chinese tallow wood NHC-A and NHC-AF were significantly greater in the growing season, whereas southern red oak wood varied little with respect to season. Southern red oak wood exhibited considerably higher NHC-A and NHC-AF than Chinese tallow wood in both seasons (Tables 5-6).

### Post Oak Savannah Ecoregion

Mean dormant and growing season foliar NHC-A ranged from 17.03-18.61 and 16.82-18.29 MJ kg<sup>-1</sup>, respectively, with yaupon and eastern red cedar producing the greatest seasonal NHC-A (Figure 14). Mean dormant and growing season foliar



NHC-AF ranged from 17.95-19.42 and 17.84-19.26 MJ kg<sup>-1</sup>, with yaupon and eastern red cedar producing the greatest dormant season NHC-AF, and yaupon and Chinese privet producing the greatest growing season NHC-AF. Greenbrier and escarpment live oak consistently yielded the least mean seasonal NHC-AF, with the exception Chinese tallow foliage. Chinese tallows' high foliage ash% (6.19%) yielded a significant increase in mean NHC-AF, but it still retained the least amount of mean NHC-AF among species. Chinese tallow wood exhibited slightly greater growing season NHC-A and NHC-AF, but remained fairly consistent between seasons (Tables 5-6).

#### Blackland Prairie Ecoregion

Mean dormant and growing season foliar NHC-A ranged from 17.03-19.12 and 16.66-19.10 MJ kg<sup>-1</sup>, respectively, with yaupon and eastern red cedar producing the greatest seasonal NHC-A. Dormant and growing season foliar NHC-AF ranged from 18.01-19.81 and 17.78-19.92 MJ kg<sup>-1</sup>, respectively, with yaupon and eastern red cedar producing the greatest seasonal NHC-AF. In contrast, Chinese tallow and greenbrier foliage produced the lowest growing season foliage NHC-AF. Chinese tallow wood exhibited a slightly higher growing season NHC-A and NHC-AF, but remained relatively consistent both seasons.

### Ecoregion-wide Comparison and Statistics

Foliar NHC-A values were significantly different between species, ecoregion, species-season, species-ecoregion, and season-ecoregion, and foliar NHC-AF values were significantly different between species, season, ecoregion, species-season, species-ecoregion, and season-ecoregion (Table 7). Post hoc testing of significant independent factors for semi/evergreen foliar NHC-A and NHC-AF ruled out respective non-significant pairwise differences between Chinese privet-escarpment live oak and Chinese privet-greenbrier. Chinese tallow wood NHC-A and NHC-AF were significantly different between season, ecoregion, and season-ecoregion (Table 8); however, post hoc testing revealed a non-significant pairwise difference between the Post Oak Savannah and Blackland Prairie ecoregions for both NHC-A and NHC-AF.

Pineywoods yaupon, Chinese privet, eastern red cedar, and Chinese tallow foliage produced the lowest NHC-AF across ecoregions (Figure 13). Yaupon and eastern red cedar exhibited the greatest overall NHC-AF values in the Post Oak Savannah and Blackland Prairie, with the exception of eastern red cedar in the Post Oak Savannah growing season. Chinese Privets' high ash% (4.81-7.36%) consistently produced the greatest NHC-AF increases across ecoregions, especially in the Post Oak Savannah. Chinese tallow foliage also exhibited considerable increases in growing season NHC-AF across ecoregions due to high ash% (4.77-

6.84%), whereas Chinese tallow wood NHC-A and NHC-AF remained fairly consistent across ecoregions, with the exception of the Pineywoods dormant season. Foliar water vaporization corrections based on oxidative TGA ranged from 1.00-1.56 MJ kg<sup>-1</sup> and 0.96-1.68 MJ Kg<sup>-1</sup> in the dormant and growing season, respectively. Mean seasonal water vaporization corrections for all foliar samples were 1.24 MJ kg<sup>-1</sup> and 1.25 MJ kg<sup>-1</sup> in dormant and growing season, respectively, which is consistent with Williams and Agee (2002) 1.26 MJ kg<sup>-1</sup> correction factor. The majority of species foliar and wood NHC(s) fell below the standard NHC of 18.61 MJ kg<sup>-1</sup> used in common fire behavior models (Tables 5-6). Species meeting or exceeding the NHC standard were exclusive to the Post Oak Savannah and Blackland Prairie, and included yaupon, eastern red cedar, greenbrier, and Chinese privet.

**Table 5.** Mean seasonal NHC-A for foliar and wood samples according to ecoregion. Standard deviations and wood samples (w) are denoted in parentheses. Underlined values meet or exceed the standard NHC value of 18.61 MJ kg<sup>-1</sup> used in common fire models. All foliar samples were significantly different with respect to species (p<0.05), except Chinese tallow and southern red oak. Significant seasonal and regional differences for foliar and wood samples are denoted as: A: season; B: ecoregion; C: season and ecoregion.

<i>Ecoregion</i>	Pineywoods	Post Oak Savannah	Blackland Prairie
<i>Species</i>	<i>NHC-A (MJ kg<sup>-1</sup>)</i>		
<i>Dormant</i>			
Yaupon <sup>B</sup>	17.05 (0.53)	18.40 (0.29)	<u>19.12</u> (0.27)
C. Privet <sup>B</sup>	16.49 (0.57)	17.03 (0.30)	17.45 (0.27)
Greenbrier <sup>B</sup>	17.76 (0.23)	17.48 (0.29)	17.86 (0.23)
E. Red Cedar <sup>B</sup>	17.63 (0.54)	<u>18.61</u> (0.27)	18.30 (0.35)
E. Live Oak <sup>B</sup>	-	17.29 (0.33)	17.03 (0.45)
C. Tallow (w) <sup>C</sup>	14.68 (0.43)	16.74 (0.24)	16.96 (0.19)
S. Red Oak (w)	16.94 (0.28)	-	-
<i>Growing</i>			
Yaupon <sup>B</sup>	17.09 (0.92)	18.29 (0.42)	<u>19.10</u> (0.24)
C. Privet <sup>B</sup>	17.14 (0.89)	17.97 (0.31)	17.70 (0.26)
Greenbrier <sup>B</sup>	17.50 (0.24)	17.16 (0.28)	17.07 (0.34)
E. Red Cedar <sup>B</sup>	17.34 (0.54)	18.03 (0.28)	17.96 (0.33)
E. Live Oak <sup>B</sup>	-	17.28 (0.38)	17.30 (0.27)
C. Tallow <sup>B</sup>	16.98 (0.90)	16.82 (0.37)	16.66 (0.37)
S. Red Oak	17.81 (0.36)	-	-
C. Tallow (w) <sup>C</sup>	16.20 (1.45)	16.46 (0.24)	16.81 (0.28)
S. Red Oak (w)	16.84 (0.20)	-	-

**Table 6.** Mean seasonal NHC-AF for foliar and wood samples according to ecoregion. Standard deviations and wood samples (w) are denoted in parentheses. Underlined values meet or exceed the standard NHC value of 18.61 MJ kg<sup>-1</sup> used in common fire models. All species foliar samples were significantly different with respect to species ( $p < 0.05$ ), except Chinese tallow and southern red oak. Significant seasonal and regional differences for foliar and wood samples are denoted as: A: season; B: ecoregion; C: season and ecoregion.

<i>Ecoregion</i>	Pineywoods	Post Oak Savannah	Blackland Prairie
<i>Species</i>	<i>NHC-AF (MJ kg<sup>-1</sup>)</i>		
<i>Dormant</i>			
Yaupon <sup>c</sup>	17.72 (0.60)	<u>19.09</u> (0.31)	<u>19.81</u> (0.25)
C. Privet <sup>c</sup>	17.35 (0.62)	18.27 (0.30)	18.38 (0.28)
Greenbrier <sup>c</sup>	18.43 (0.25)	18.21 (0.34)	<u>18.74</u> (0.26)
E. Red Cedar <sup>c</sup>	18.30 (0.52)	<u>19.42</u> (0.28)	<u>18.98</u> (0.37)
E. Live Oak <sup>c</sup>	-	17.95 (0.36)	18.01 (0.33)
C. Tallow (w) <sup>c</sup>	14.97 (0.47)	17.27 (0.25)	17.32 (0.20)
S. Red Oak (w)	17.30 (0.28)	-	-
<i>Growing</i>			
Yaupon <sup>c</sup>	17.76 (0.77)	<u>19.26</u> (0.34)	<u>19.92</u> (0.25)
C. Privet <sup>c</sup>	17.99 (0.84)	<u>18.84</u> (0.29)	18.54 (0.29)
Greenbrier <sup>c</sup>	17.98 (0.26)	17.85 (0.29)	17.89 (0.35)
E. Red Cedar <sup>c</sup>	17.99 (0.48)	18.51 (0.36)	<u>18.66</u> (0.32)
E. Live Oak <sup>c</sup>	-	18.00 (0.36)	17.99 (0.28)
C. Tallow	17.77 (0.98)	17.84 (0.32)	17.78 (0.38)
S. Red Oak	18.29 (0.39)	-	-
C. Tallow (w) <sup>c</sup>	16.39 (1.48)	16.93 (0.27)	17.13 (0.25)
S. Red Oak (w)	17.17 (0.18)	-	-

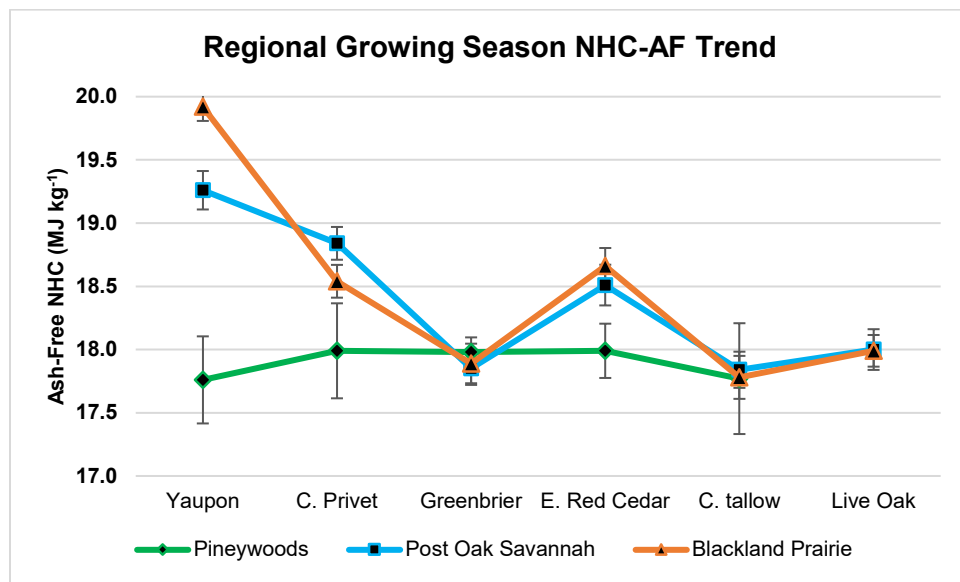
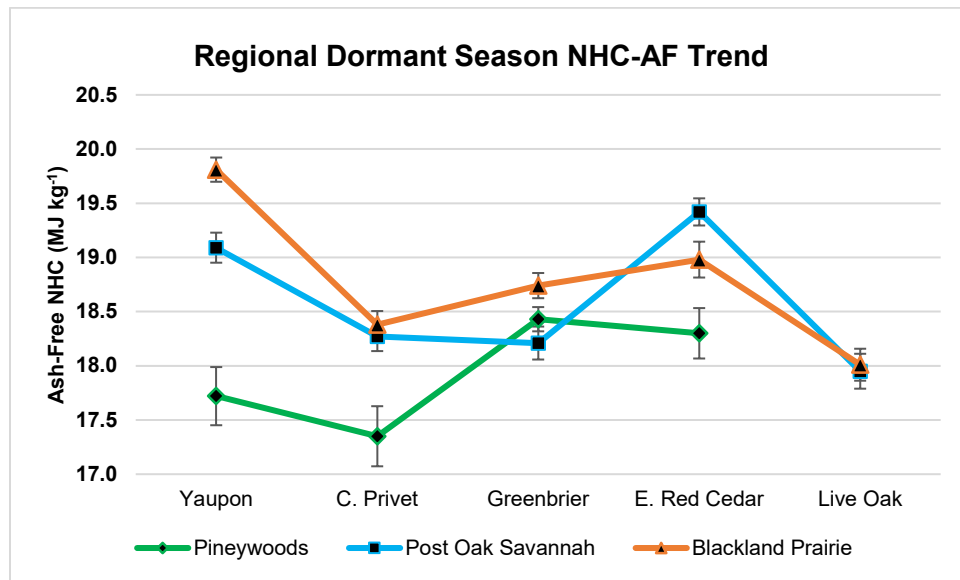


**Figure 14.** Regional and seasonal NHC-AF trends for semi/evergreen species foliar samples. The error bars represent the standard error of the mean.

**Table 7.** ANOVA table representing NHC-A and NHC-AF indices for semi/evergreen foliar samples. A Tukey's Studentized Range Test was applied to all significant factors ( $p < 0.05$ ). Post hoc testing revealed the following non-significant pairwise differences: *NHC-A*: Chinese privet-escarpment live oak; *NHC-AF*: Chinese privet-greenbrier.

Source of Variation	<i>df</i>	<i>Type III SS</i>	<i>MS</i>	<i>F</i>	<i>p</i>
NHC-A					
Species	4	120.45	30.11	128.25	0.0001
Season	1	0.17	0.17	0.71	0.4005
Ecoregion	2	71.92	35.96	153.14	0.0001
Species*Season	4	27.38	6.84	29.15	0.0001
Species*Ecoregion	7	73.88	10.55	44.95	0.0001
Season*Ecoregion	2	1.18	0.59	2.51	0.0819
Error	671	157.55	0.24		
NHC-AF					
Species	4	105.55	26.39	112.79	0.0001
Season	1	1.58	1.58	6.76	0.0095
Ecoregion	2	95.64	47.82	204.40	0.0001
Species*Season	4	27.30	6.83	29.18	0.0001
Species*Ecoregion	7	67.23	9.60	41.05	0.0001
Season*Ecoregion	2	1.12	0.56	2.38	0.0930
Error	671	156.97	0.23		

**Table 8.** ANOVA table representing NHC-A and NHC-AF for Chinese tallow wood samples. A Tukey's Studentized Range Test was applied to all significant factors ( $p < 0.05$ ). Post hoc testing revealed the following non-significant pairwise differences: *NHC-A*: Post Oak Savannah-Blackland Prairie; *NHC-AF*: Post Oak Savannah-Blackland Prairie.

Source of Variation	<i>df</i>	<i>Type III SS</i>	<i>MS</i>	<i>F</i>	<i>p</i>
NHC-A					
Season	1	4.64	4.64	11.09	0.0011
Ecoregion	2	58.10	29.05	69.46	0.0001
Season*Ecoregion	2	25.62	12.81	30.63	0.0001
Error	144	60.22	0.42		
NHC-AF					
Season	1	3.04	3.04	6.92	0.0094
Ecoregion	2	72.90	36.45	82.96	0.0001
Season*Ecoregion	2	24.50	12.25	27.88	0.0001
Error	144	63.27	0.44		



## Oxidative Thermogravimetric Analysis

### Pineywoods Ecoregion

Dormant season foliar RSIT, GP-MMLR, and GP-CD ranged from 160.75-174.04°C, 3.04-4.72 % min<sup>-1</sup>, 20.87-23.77 min., respectively (Table 9). Eastern red cedar and Chinese privet produced the greatest and least ignitability according to >RSIT(s), yaupon and Chinese privet produced the greatest and least combustibility relative to >GP-MMLR(s), and eastern red cedar and Chinese privet produced the greatest and least combustibility relative to <GP-CD(s) (Figure 15). Greater dormant season RSIT(s) exhibited a general correlation with greater GP-MMLR(s) and lower GP-CD(s). Foliar GP-CD(s) can infer greater degrees of sustainability as evidenced by yaupons' high GP-CD. Dormant season southern red oak wood yielded a greater RSIT, but lower GP-MMLR compared to Chinese tallow wood, indicating greater dormant season ignitability with a concurrent reduction in combustibility.

Growing season foliar RSIT, GP-MMLR, and GP-CD ranged from 156.44-175.78 °C, 3.19-5.19 % min.<sup>-1</sup>, and 20.00-23.06 min., respectively (Table 9). Eastern red cedar and Chinese privet produced the greatest and least growing season RSIT, greenbrier and Chinese tallow produced the greatest and least GP-MMLR, and Chinese privet and greenbrier produced the greatest and least GP-CD (Figure 16). Similar to the dormant season, there was a general correlation between greater growing season RSIT(s) and GP-MMLR(s), as well as lower GP-CD(s). Growing

season Chinese tallow wood yielded the greatest RSIT and GP-MMLR, indicating greater ignitability and combustibility compared to southern red oak wood.

Yaupon and eastern red cedar RSIT(s) exhibited little variability between seasons, whereas Chinese privet and greenbrier produced significant seasonal variability. Seasonal foliar ignitability was fairly consistent for eastern red cedar and yaupon, whereas greenbrier and Chinese privet exhibited significant shifts in seasonal ignitability, with greenbrier and Chinese privet exhibiting much greater respective growing and dormant season ignitability. Seasonal foliar GP-MMLR(s) and GP-CD(s) were fairly consistent between seasons, with the exception of greenbrier, which exhibited significant growing season shifts in GP-MMLR ( $\sim 1.54\%$   $\text{min}^{-1}$ ) and GP-CD (1.55 min). Seasonal foliar combustibility was consistently greater in the growing season based on high GP-MMLR(s) and low GP-CD(s). Greater seasonal RSIT(s) correlated fairly well with higher GP-MMLR(s) and lower GP-CD(s). Chinese tallow wood was more ignitable and combustible in the growing season, whereas southern red oak was significantly more ignitable in the dormant season, but relatively consistent in terms of seasonal combustibility (Table 9).

#### Post Oak Savannah Ecoregion

Dormant season foliar RSIT, GP-MMLR, and GP-CD ranged from 162.51-176.78 °C, 3.31-4.92 %  $\text{min}^{-1}$ , and 18.74-22.45 min., respectively (Table 9). Escarpment live oak and greenbrier produced the greatest and second lowest

dormant season RSIT and GP-MMLR, respectively, which correlates well in terms of ignitability and combustibility. GP-MMLR(s) and GP-CD(s) exhibited a reciprocal relationship, indicating greater degrees of combustibility based on rapid decomposition rates commensurate with decreasing GP-CD(s) (Figure 15).

Growing season foliar RSIT, GP-MMLR, and GP-CD ranged from 157.00-178.86 °C, 3.19-5.02 % min.<sup>-1</sup>, and 18.43-22.88 min. Escarpment live oak and Chinese privet produced the greatest and second lowest growing season RSIT and GP-MMLR, respectively, which correlates well with ignitability and combustibility metrics. Escarpment live oak and Chinese privet growing season GP-MMLR(s) were inversely related to GP-CD(s), and is consistent with greater degrees of combustibility. Furthermore, all growing season GP-MMLR(s) and GP-CD(s) displayed a fairly consistent reciprocal relationship, reaffirming greater overall combustibility. In terms of sustainability, yaupon and eastern red cedar yielded high GP-CD(s) combined with intermediate to high GP-MMLR(s), indicating high sustainability and combustibility.

Seasonal foliar RSIT(s) for yaupon, Chinese privet, and greenbrier were quite variable, with yaupon and Chinese privet exhibiting much greater dormant season ignitability, while greenbrier exhibited significantly greater growing season ignitability. The majority of species exhibited greater growing season combustibility, with GP-MMLR(s) and GP-CD(s) following an inverse trend. Chinese tallow wood exhibited a

significantly greater growing season RSIT coupled with a higher GP-MMLR and lower GP-CD, indicating significantly greater growing season ignitability and combustibility.

#### Blackland Prairie Ecoregion

Dormant season foliar RSIT, GP-MMLR, and GP-CD ranged from 161.82-178.84 °C, 3.74-5.05 % min.<sup>-1</sup>, and 18.78-22.12 min, respectively. Escarpment live oak and greenbrier produced the greatest and least growing season RSIT and the second greatest and least GP-MMLR, respectively, which correlates fairly well with ignitability and combustibility metrics. Subsequent dormant season GP-CD(s) did not exhibit a strong reciprocal correlation with GP-MMLR (Figure 15). Eastern red cedar and yaupon were the most combustible and sustainable dormant season species based on high GP-MMLR(s) and GP-CD(s).

Growing season foliar RSIT, GP-MMLR, and GP-CD ranged from 157.39-178.25 °C, 3.28-5.35 % min.<sup>-1</sup>, 18.53-22.55 min, respectively. Escarpment live oak and Chinese privet produced the greatest and least growing season RSIT and the second greatest and least GP-MMLR, respectively, and is consistent with the dormant season trend. Similar to the dormant season, growing season GP-CD(s) did not yield a strong reciprocal relationship with GP-MMLR(s). Yaupon and eastern red cedar produced significantly greater growing season GP-MMLR(s) and GP-CD(s), indicating greater degrees of combustibility and sustainability.

Seasonal foliar RSIT trends varied considerably, with eastern red cedar and escarpment live oak exhibiting the greatest seasonal RSIT(s), and Chinese privet producing the least seasonal RSIT(s) (Table 9). Seasonal foliar GP-MMLR(s) were consistently greater in the growing season, indicating greater growing season combustibility. Foliar GP-CD(s) were fairly consistent between seasons, with the majority of species exhibiting lower growing season GP-CD(s). Chinese tallow wood exhibited a significantly greater growing season RSIT and GP-MMLR coupled with a lower GP-CD, indicating significantly greater growing season ignitability and combustibility.

#### Ecoregion-wide Comparison and Statistics

Yaupon and Chinese privet produced greater dormant season RSIT(s) across ecoregions, whereas eastern red cedar, greenbrier, and escarpment live oak produced greater growing season RSIT(s). The majority GP-MMLR(s) trended higher in the growing season, but there was significant variability between ecoregions (Figure 16). Yaupon, eastern red cedar, and escarpment live oak consistently produced the greatest dormant season GP-MMLR(s) across ecoregions, while growing season foliar GP-MMLR(s) were more varied. Chinese privet and Chinese tallow consistently produced the lowest mean growing season foliar GP-MMLR(s) across ecoregions, while eastern red cedar and escarpment live oak produced the greatest seasonal GP-MMLR(s). GP-CD(s) were more variable in

the dormant season, leading to greater ecoregion variability in the dormant season. Greenbrier exhibited the greatest seasonal and ecoregion variability with respect to RSIT, GP-MMLR, and GP-CD values.

Foliar RSIT(s) were significantly different with regard to species, ecoregion, species-season, species-ecoregion, and season-ecoregion (Table 10), whereas foliar GP-MMLR(s) and GP-CD(s) were significantly different relative to species, season, ecoregion, species-season, species-ecoregion, and season-ecoregion. Post hoc testing confirmed significant differences among all independent factors, with the exception of non-significant pairwise groupings for: *RSIT*: Post Oak Savannah-Blackland Prairie; *GP-MMLR*: eastern red cedar-escarpment live oak and Pineywoods-Post Oak Savannah; *GP-CD*: eastern red cedar-greenbrier and Post Oak Savannah-Blackland Prairie (Table 10). Chinese tallow foliage RSIT and GP-MMLR were significantly different relative to ecoregion (Table 11), while Chinese tallow wood RSIT(s), GP-MMLR(s), and GP-CD(s) were all significantly different relative to season, ecoregion, and season-ecoregion (Table 12). Post hoc testing of Chinese tallow foliage produced non-significant pairwise groupings for the following: *RSIT*: Pineywoods-Post Oak Savannah; *GP-MMLR*: Post Oak Savannah-Blackland Prairie. Post hoc testing of Chinese tallow wood produced non-significant pairwise groupings for the following parameters: *RSIT*: Post Oak Savannah-Blackland Prairie; *GP-MMLR*: Pineywoods-Blackland Prairie; *GP-CD*: Pineywoods-Post Oak Savannah

and Post Oak Savannah-Blackland Prairie. Southern red oak wood RSIT and GP-CD were significantly different relative to season.

**Table 9.** Regional oxidative differential thermogravimetric analysis (DTG) results displaying flammability parameters for relative spontaneous ignition temperature (RSIT), gas-phase maximum mass loss rate (GP-MMLR), and gas-phase combustion duration (GP-CD). Standard deviations and wood samples (w) are in parentheses. All species foliage except Chinese tallow and southern red oak were significantly different ( $p < 0.05$ ) based on RSIT, GP-MMLR, and GP-CD. Seasonal and regional significant differences are denoted as: A: season, B: ecoregion, and C: season and ecoregion.

<i>Ecoregion-DTG</i>			
<i>Season-Species</i>	RSIT (C°)	GP-MMLR (% min. <sup>-1</sup> )	GP-CD (min.)
Pineywoods			
<i>Dormant</i>			
Yaupon	169.75 <sup>B</sup> (1.37)	4.72 <sup>C</sup> (0.20)	23.58 <sup>C</sup> (0.48)
C. Privet	160.75 <sup>B</sup> (1.04)	3.04 <sup>C</sup> (0.17)	23.77 <sup>C</sup> (0.91)
Greenbrier	164.23 <sup>B</sup> (0.46)	3.65 <sup>C</sup> (0.09)	21.55 <sup>C</sup> (0.25)
E. Red Cedar	174.04 <sup>B</sup> (1.23)	4.36 <sup>C</sup> (0.36)	20.87 <sup>C</sup> (0.21)
C. Tallow (W)	184.25 <sup>C</sup> (1.30)	9.93 <sup>C</sup> (1.72)	20.74 <sup>C</sup> (0.17)
S. Red Oak (W)	201.54 <sup>A</sup> (0.57)	8.85 (0.48)	16.39 <sup>A</sup> (0.18)
<i>Growing</i>			
Yaupon	168.54 <sup>B</sup> (1.25)	4.60 <sup>C</sup> (0.07)	21.94 <sup>C</sup> (0.27)
C. Privet	156.44 <sup>B</sup> (0.34)	3.54 <sup>C</sup> (0.07)	23.06 <sup>C</sup> (0.64)
Greenbrier	170.58 <sup>B</sup> (0.27)	5.19 <sup>C</sup> (0.17)	20.00 <sup>C</sup> (0.79)
E. Red Cedar	175.78 <sup>B</sup> (0.76)	4.94 <sup>C</sup> (0.38)	20.37 <sup>C</sup> (0.13)
C. Tallow	159.54 <sup>B</sup> (0.42)	2.58 <sup>B</sup> (0.09)	21.98 (0.38)
S. Red Oak	164.51 (0.81)	3.61 (0.08)	20.13 (0.47)
C. Tallow (W)	198.98 <sup>C</sup> (1.52)	11.91 <sup>C</sup> (0.89)	18.12 <sup>C</sup> (0.55)
S. Red Oak (W)	187.79 <sup>A</sup> (1.12)	8.69 (0.64)	16.96 <sup>A</sup> (0.37)
Post Oak Savannah			
<i>Dormant</i>			
Yaupon	176.00 <sup>B</sup> (0.69)	4.05 <sup>C</sup> (0.23)	21.74 <sup>C</sup> (0.26)
C. Privet	163.28 <sup>B</sup> (1.06)	3.31 <sup>C</sup> (0.13)	22.45 <sup>C</sup> (0.49)
Greenbrier	162.51 <sup>B</sup> (1.23)	3.41 <sup>C</sup> (0.13)	21.73 <sup>C</sup> (0.21)



**Table 9.** Continued

E. Red Cedar	175.99 <sup>B</sup> (0.37)	4.64 <sup>C</sup> (0.16)	20.89 <sup>C</sup> (0.16)
E. Live Oak	176.78 <sup>B</sup> (0.60)	4.92 <sup>C</sup> (0.14)	18.74 <sup>C</sup> (0.21)
C. Tallow (W)	183.48 <sup>C</sup> (1.79)	7.85 <sup>C</sup> (1.29)	21.13 <sup>C</sup> (0.51)
<i>Growing</i>			
Yaupon	169.21 <sup>B</sup> (1.57)	4.11 <sup>C</sup> (0.17)	22.15 <sup>C</sup> (0.92)
C. Privet	157.00 <sup>B</sup> (0.71)	3.37 <sup>C</sup> (0.08)	22.88 <sup>C</sup> (0.22)
Greenbrier	170.79 <sup>B</sup> (1.13)	4.50 <sup>C</sup> (0.11)	19.94 <sup>C</sup> (0.31)
E. Red Cedar	176.05 <sup>B</sup> (0.93)	4.78 <sup>C</sup> (0.25)	20.44 <sup>C</sup> (0.19)
E. Live Oak	178.86 <sup>B</sup> (0.47)	5.02 <sup>C</sup> (0.14)	18.43 <sup>C</sup> (0.29)
C. Tallow	159.02 <sup>B</sup> (0.81)	3.19 <sup>B</sup> (0.22)	22.59 (0.70)
C. Tallow (W)	203.97 <sup>C</sup> (1.18)	9.09 <sup>C</sup> (0.84)	16.84 <sup>C</sup> (0.70)
Blackland Prairie			
<i>Dormant</i>			
Yaupon	173.99 <sup>B</sup> (0.78)	4.27 <sup>C</sup> (0.15)	22.12 <sup>C</sup> (0.24)
C. Privet	165.77 <sup>B</sup> (0.44)	3.74 <sup>C</sup> (0.17)	21.70 <sup>C</sup> (0.68)
Greenbrier	161.82 <sup>B</sup> (0.91)	3.95 <sup>C</sup> (0.12)	20.97 <sup>C</sup> (0.32)
E. Red Cedar	173.93 <sup>B</sup> (0.89)	5.05 <sup>C</sup> (0.54)	21.00 <sup>C</sup> (0.17)
E. Live Oak	178.84 <sup>B</sup> (0.82)	4.40 <sup>C</sup> (0.31)	18.78 <sup>C</sup> (0.25)
C. Tallow (W)	185.59 <sup>C</sup> (0.78)	8.63 <sup>C</sup> (1.24)	20.08 <sup>C</sup> (0.67)
<i>Growing</i>			
Yaupon	166.89 <sup>B</sup> (0.41)	4.55 <sup>C</sup> (0.18)	22.55 <sup>C</sup> (0.32)
C. Privet	157.39 <sup>B</sup> (0.47)	3.94 <sup>C</sup> (0.24)	22.31 <sup>C</sup> (0.20)
Greenbrier	170.85 <sup>B</sup> (0.59)	4.46 <sup>C</sup> (0.12)	19.78 <sup>C</sup> (0.34)
E. Red Cedar	176.02 <sup>B</sup> (0.38)	5.35 <sup>C</sup> (0.35)	20.50 <sup>C</sup> (0.20)
E. Live Oak	178.25 <sup>B</sup> (0.32)	4.75 <sup>C</sup> (0.34)	18.53 <sup>C</sup> (0.13)
C. Tallow	157.95 <sup>B</sup> (0.86)	3.28 <sup>B</sup> (0.12)	22.06 (0.39)
C. Tallow (W)	202.21 <sup>C</sup> (1.16)	12.67 <sup>C</sup> (0.76)	17.05 <sup>C</sup> (1.04)

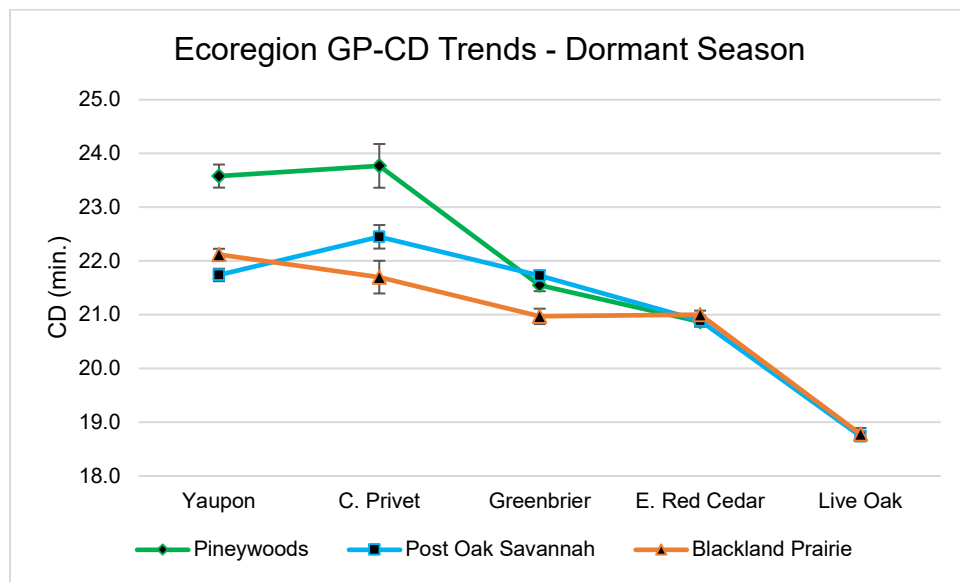
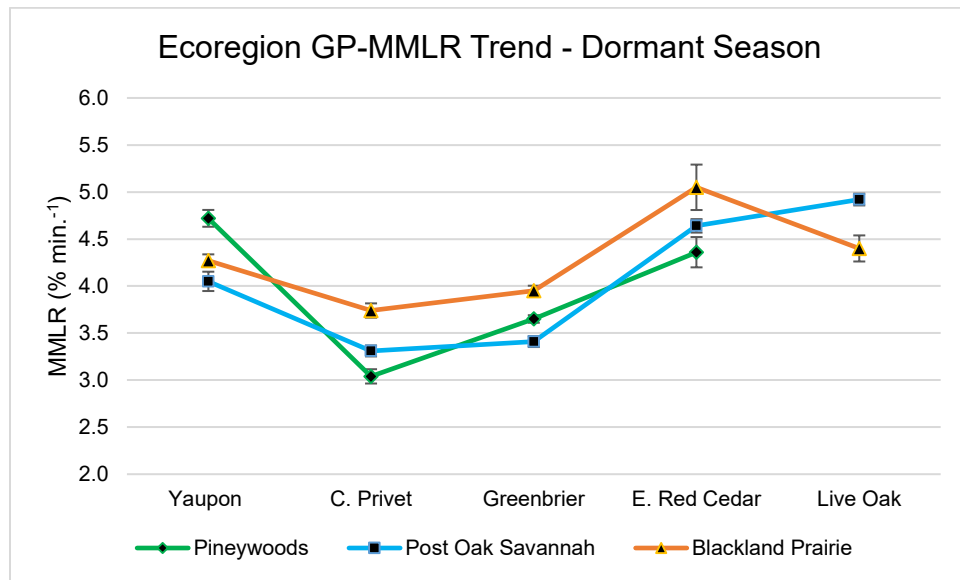


**Figure 15.** Regional dormant season GP-MMLR and GP-CD trends for semi/evergreen species foliar samples. The error bars represent the standard error of the mean.

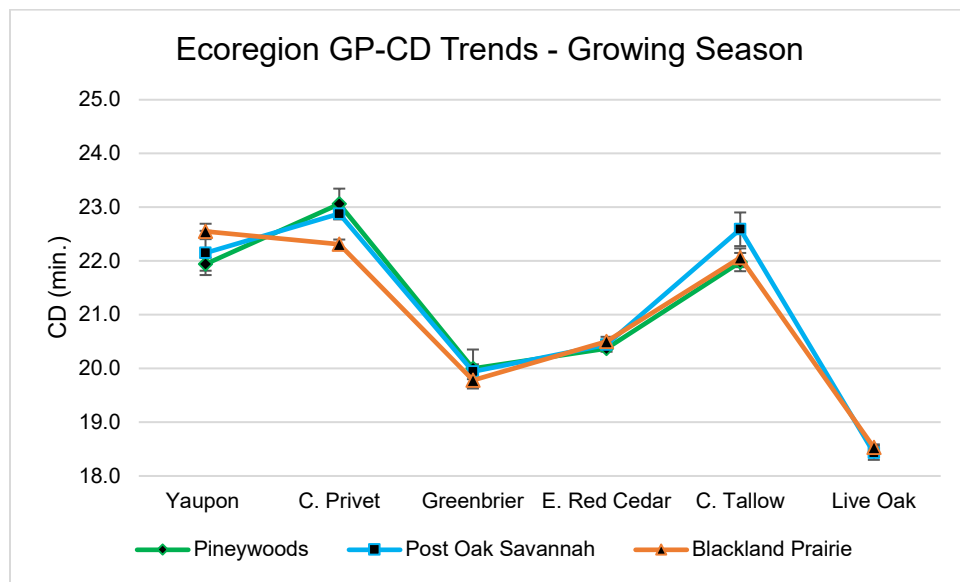
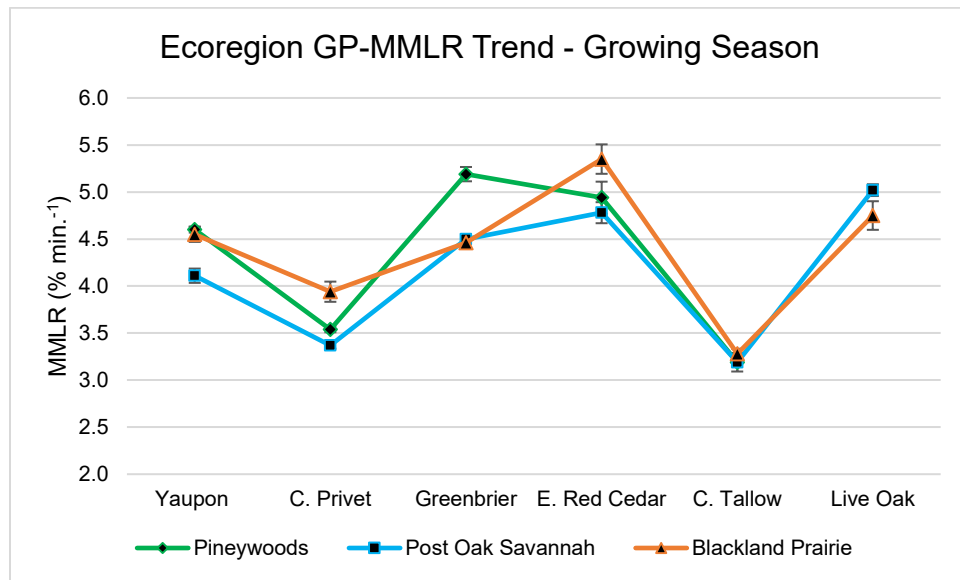


**Figure 16.** Regional growing season GP-MMLR and GP-CD trends for semi/evergreen species foliar samples. The error bars represent the standard error of the mean.

**Table 10.** ANOVA table representing RSIT, GP-MMLR, and GP-CD indices for semi/evergreen foliar samples. A Tukey's Studentized Range Test was applied to all significant factors ( $p < 0.05$ ). Post hoc testing revealed the following non-significant pairwise differences: *RSIT*: Post Oak Savannah-Blackland Prairie; *GP-MMLR*: eastern red cedar-escarpment live oak, Pineywoods-Post Oak Savannah; *GP-CD*: eastern red cedar-greenbrier, Post Oak Savannah-Blackland Prairie.

Source of Variation	<i>df</i>	<i>Type III SS</i>	<i>MS</i>	<i>F</i>	<i>p</i>
RSIT					
Species	4	5071.87	1267.97	989.91	0.0001
Season	1	4.43	4.43	3.46	0.0656
Ecoregion	2	22.55	11.27	8.80	0.0003
Species*Season	4	1021.89	255.47	199.45	0.0001
Species*Ecoregion	7	79.74	11.39	8.89	0.0001
Season*Ecoregion	2	13.93	6.96	5.44	0.0056
Error	112	143.46	1.28	8.27	
GP-MMLR					
Species	4	33.76	8.44	163.55	0.0001
Season	1	5.65	5.65	109.47	0.0001
Ecoregion	2	1.37	0.69	13.29	0.0001
Species*Season	4	4.15	1.04	20.09	0.0001
Species*Ecoregion	7	5.82	0.83	16.12	0.0001
Season*Ecoregion	2	0.56	0.28	5.46	0.0054
Error	112	5.78	0.05		
GP-CD					
Species	4	232.26	58.07	335.41	0.0001
Season	1	9.70	9.70	56.05	0.0001
Ecoregion	2	5.56	2.78	16.07	0.0001
Species*Season	4	10.76	2.69	15.54	0.0001
Species*Ecoregion	7	8.94	1.28	7.38	0.0001
Season*Ecoregion	2	4.89	2.44	14.12	0.0001
Error	112	19.39	0.17		

**Table 11.** ANOVA table representing RSIT, GP-MMLR, and GP-CD indices for Chinese tallow foliage. A Tukey’s Studentized Range Test was applied to all significant factors ( $p < 0.05$ ). Post hoc testing revealed the following non-significant pairwise differences: *RSIT*: Pineywoods-Post Oak Savannah; *GP-MMLR*: Post Oak Savannah and-Blackland Prairie.

Source of Variation	<i>df</i>	<i>Type I SS</i>	<i>MS</i>	<i>F</i>	<i>p</i>
RSIT					
Ecoregion	2	6.56	3.28	6.26	0.0138
Error	12	6.29	0.52		
GP-MMLR					
Ecoregion	2	1.43	0.71	31.04	0.0001
Error	12	0.28	0.02		
GP-CD					
Ecoregion	2	1.10	0.55	2.11	0.1645
Error	12	3.14	0.26		

**Table 12.** ANOVA table representing RSIT, GP-MMLR, and GP-CD indices for Chinese tallow wood. A Tukey's Studentized Range Test was applied to all significant factors ( $p < 0.05$ ). Post hoc testing revealed the following non-significant pairwise differences: *RSIT*: Post Oak Savannah-Blackland Prairie; *GP-MMLR*: Pineywoods-Blackland Prairie; *GP-CD*: Pineywoods-Post Oak Savannah and Post Oak Savannah-Blackland Prairie.

Source of Variation	<i>df</i>	<i>Type III SS</i>	<i>MS</i>	<i>F</i>	<i>p</i>
RSIT					
Season	1	2241.04	2241.04	1273.40	0.0001
Ecoregion	2	32.38	16.19	9.20	0.0011
Season*Ecoregion	1	43.11	21.55	12.25	0.0002
Error	24	42.24	1.76		
GP-MMLR					
Season	1	44.02	44.02	32.04	0.0001
Ecoregion	2	36.20	18.10	13.17	0.0001
Season*Ecoregion	1	10.60	5.30	3.86	0.0352
Error	24	32.98	1.37		
GP-CD					
Season	1	82.20	82.20	188.38	0.0001
Ecoregion	2	3.78	1.89	4.33	0.0248
Season*Ecoregion	1	3.75	1.87	4.29	0.0254
Error	24	10.47	0.44		

## Thermal Kinetic Analysis

### Pineywoods Ecoregion

Friedman and OFW dormant season foliar global  $E\alpha(s)$  ranged from 179.03-211.96 KJ mol<sup>-1</sup> and 172.27-204.69 KJ mol<sup>-1</sup>, respectively, with Chinese privet and yaupon exhibiting the greatest (< $E\alpha$ ) and least (> $E\alpha$ ) combustibility (Tables 13-14). Friedman and OFW mean dormant season foliar GPC  $E\alpha(s)$  ranged from 139.50-177.83 KJ mol<sup>-1</sup> and 137.45-169.58 KJ mol<sup>-1</sup>, with Chinese privet and yaupon again exhibiting the greatest and least combustibility (Tables 15-16). Friedman dormant season global and GPC  $E\alpha(s)$  were consistently higher than OFW, and yielded the same  $E\alpha$  combustibility order. Chinese privet exhibited an unexpected shift in global and GPC  $E\alpha(s)$ , indicating a significant increase in overall combustibility, whereas eastern red cedar maintained a relatively high to moderate combustibility.

Friedman and OFW growing season foliar global  $E\alpha(s)$  ranged from 176.46-256.35 KJ mol<sup>-1</sup> and 167.83-244.59 KJ mol<sup>-1</sup>, respectively, with Chinese privet and Chinese tallow producing the greatest and least combustibility (Tables 17-18). Friedman and OFW growing season GPC  $E\alpha(s)$  ranged from 134.25-209.81 KJ mol<sup>-1</sup> and 132.67-200.87 KJ mol<sup>-1</sup>, with Chinese privet and Chinese tallow producing the greatest and least combustibility (Tables 15-16). Yaupon and greenbrier exhibited significant shifts to greater dormant season gas-phase combustibility, whereas eastern red cedar and Chinese privet varied the least relative to season.

Friedman and OFW global  $E\alpha(s)$  for southern red oak wood yielded lower growing season  $E\alpha(s)$  (Table 19), indicating slightly greater growing season combustibility. Southern red oak wood exhibited little difference ( $\sim 1.0 \text{ KJ mol}^{-1}$ ) among seasonal GPC  $E\alpha(s)$ . Friedman and OFW global and GPC  $E\alpha(s)$  for Chinese tallow wood were significantly lower in the growing season, indicating a possible substantial increase in combustibility (Tables 15-16,20). In contrast, dormant season southern red oak and Chinese tallow wood exhibited little variation in global and gas-phase combustibility. Southern red oak foliage exhibited greater combustibility compared to Chinese tallow foliage, as evidenced by its much lower global and GPC  $E\alpha(s)$ .

#### Post Oak Savannah Ecoregion

Friedman and OFW dormant season foliar global  $E\alpha$ 's ranged from 176.62-208.37  $\text{KJ mol}^{-1}$  and 166.84-199.19  $\text{KJ mol}^{-1}$ , respectively, with Chinese privet and yaupon producing the greatest and least combustibility (Tables 13-14). Friedman and OFW dormant season foliar GPC  $E\alpha(s)$  ranged from 137.9-180.81 and 134.01-173.76  $\text{KJ mol}^{-1}$ , with Chinese privet and escarpment live oak producing the greatest and least combustibility (Tables 15-16). Friedman global and GPC  $E\alpha(s)$  were consistently higher than OFW  $E\alpha(s)$ , and produced the same  $E\alpha$  combustibility order for each method. Species global and GPC foliar  $E\alpha(s)$  were consistent with respect



to combustibility order, with the exception of yaupon and escarpment live oak which exhibited significant differences in mean GPC  $E\alpha(s)$ .

Friedman and OFW growing season foliar global  $E\alpha(s)$  ranged from 177.21-240.11 KJ mol<sup>-1</sup> and 168.60-223.62 KJ mol<sup>-1</sup>, respectively, with Chinese privet and Chinese tallow yielding the greatest and least combustibility (Tables 17-18).

Friedman and OFW growing season foliar GPC  $E\alpha(s)$  ranged from 135.61-192.88 and 132.15-181.54 KJ mol<sup>-1</sup>, with Chinese Privet and Chinese tallow yielding the greatest and least combustibility (Tables 15-16). Friedman global and GPC  $E\alpha(s)$  were consistently higher than OFW  $E\alpha(s)$ , and were mostly consistent with respect to  $E\alpha$  combustibility order, with the exception of yaupon and greenbrier which exhibited slight variations in mean  $E\alpha(s)$ . Friedman and OFW global and GPC  $E\alpha(s)$  for Chinese tallow wood exhibited the greatest seasonal difference in mean  $E\alpha(s)$  while producing the lowest dormant season  $E\alpha$  among ecoregions (Table 20).

#### Blackland Prairie Ecoregion

Friedman and OFW dormant season foliar global  $E\alpha(s)$  ranged from 176.22-211.38 and 168.62-201.17 KJ mol<sup>-1</sup>, respectively, with eastern red cedar and escarpment live oak producing the greatest and least combustibility (Tables 13-14).

Friedman and OFW dormant season foliar GPC  $E\alpha(s)$  ranged from 140.19-183.50 and 138.45-172.77 KJ mol<sup>-1</sup>, with Chinese privet and escarpment live oak yielding the greatest and least combustibility (Tables 15-16). Friedman global and GPC

$E\alpha(s)$  were consistently lower than OFW  $E\alpha(s)$  and produced the same  $E\alpha$  combustibility order for each method. Dormant season global  $E\alpha(s)$  displayed considerable variability among all species, with the exception of Chinese privet and eastern red cedar.

Friedman and OFW growing season foliar global  $E\alpha(s)$  ranged from 165.47-225.15 and 155.66-213.80 KJ mol<sup>-1</sup>, respectively, with eastern red cedar and Chinese tallow producing the greatest and least combustibility (Tables 17-18). Friedman and OFW growing season foliar GPC  $E\alpha(s)$  ranged from 139.31-191.85 and 132.61-181.53 KJ mol<sup>-1</sup>, respectively. Eastern red cedar and Chinese privet produced the greatest GPC, and Chinese tallow foliage produced the least (Tables 15-16). Mean growing season global and GPC  $E\alpha$  trends exhibited considerable variability among species. Friedman global  $E\alpha$  for Chinese tallow wood was lower in the growing season, while the OFW global  $E\alpha$  was slightly lower in the dormant season (Table 20). Friedman and OFW GPC  $E\alpha(s)$  for Chinese tallow wood yielded significantly lower dormant season GPC  $E\alpha(s)$ , indicating greater dormant season combustibility.

#### Ecoregion-wide Global and Gas-Phase Combustion $E\alpha(s)$

##### *Species foliage samples*

General seasonal and ecoregion trends for Friedman foliar global  $E\alpha$ 's indicated higher combustibility ( $<E\alpha$ ) associated with Chinese privet and eastern red

cedar, while species with intermediate to low combustibility were more variable (Tables 13 and 17). By contrast, Friedman growing season global  $E\alpha(s)$  for escarpment live oak and Chinese tallow consistently produced low combustibility's ( $>E\alpha$ ). Friedman seasonal global  $E\alpha(s)$  for Chinese privet and escarpment live oak varied by  $<1.0 \text{ KJ mol}^{-1}$  in the Post Oak Savannah and Blackland Prairie, which suggests season and region had little effect on combustibility.

Friedman foliar GPC  $E\alpha(s)$  exhibited a general seasonal trend of greater combustibility associated with Chinese privet and eastern red cedar across all ecoregions (Table 15). Yaupon and greenbrier comprised the intermediate range of GPC  $E\alpha(s)$ , while escarpment live oak and Chinese tallow comprised the lower range of GPC  $E\alpha(s)$ . The majority of Friedman foliar GPC  $E\alpha(s)$  exhibited greater dormant season combustibility across ecoregions, with the exception of Chinese privet that produced greater growing season combustibility in all ecoregions.

Similar to Friedman, seasonal foliar combustibility for OFW global  $E\alpha(s)$  trended higher for Chinese privet and eastern red cedar across all ecoregions, whereas escarpment live oak and Chinese tallow foliage produced the least combustibility (Tables 14 and 18). Growing season foliar combustibility for OFW global  $E\alpha(s)$  varied considerably across all ecoregions, with yaupon, greenbrier, and Chinese tallow exhibiting the greatest variation (Table 16). No discernable seasonal global  $E\alpha$  trends were noted across ecoregions due to significant variability.

Seasonal OFW GPC  $E\alpha$  combustibility trends indicated high GPC for Chinese privet and eastern red cedar, intermediate GPC for yaupon and greenbrier, and low GPC for escarpment live oak and Chinese tallow across all ecoregions. Chinese privet and yaupon shared relatively the same seasonal pyrolytic MMLR conversion degree ( $\alpha$ ), but differed significantly with regard to GPC  $E\alpha(s)$  and DTG curves (Figure 17). Likewise, dormant season pyrolytic MMLR conversion degrees ( $\alpha$ ) for greenbrier and eastern red cedar were relatively close, but greenbriers' DTG thermogram shifted significantly throughout 150-330°C range during the growing season (Figure 18). Greenbrier and Chinese privet were the only species across ecoregions to produce a consistent seasonal  $E\alpha$  trend, with greenbrier and Chinese privet yielding greater respective dormant and growing season combustibility.

#### *Chinese tallow wood and foliage samples*

Friedman and OFW dormant season global  $E\alpha(s)$  for Chinese tallow wood ranged from 195.25-213.92 and 184.42-209.51 KJ mol<sup>-1</sup>, respectively, with the Post Oak Savannah yielding the greatest combustibility (Tables 20). Friedman and OFW growing season global  $E\alpha(s)$  for Chinese tallow wood ranged from 190.01-225.61 and 181.00-221.05 KJ mol<sup>-1</sup>, with the Pineywoods yielding the greatest combustibility. OFW global  $E\alpha(s)$  were consistently lower than Friedman global  $E\alpha(s)$ , and produced the same seasonal  $E\alpha$  trend across ecoregions, with the exception of the Blackland Prairie. Chinese tallow wood produced greater growing

season combustibility in the Pineywoods, while the Post Oak Savannah produced greater combustibility in the dormant season.

Friedman and OFW dormant season GPC  $E\alpha(s)$  for Chinese tallow wood ranged from 176.98-207.51 and 169.35-199.80 KJ mol<sup>-1</sup>, respectively, with the Post Oak Savannah yielding the greatest combustibility (Tables 15-16). Friedman and OFW growing season GPC  $E\alpha(s)$  for Chinese tallow wood ranged from 178.97-223.99 and 170.51-217.25 KJ mol<sup>-1</sup>, with the Pineywoods producing the greatest combustibility. Seasonally, Chinese tallow wood produced greater dormant season Friedman and OFW GPC  $E\alpha(s)$  in the Post Oak Savannah and Blackland Prairie, while the Pineywoods yielded a greater growing season GPC  $E\alpha$ . However, Chinese tallow wood GPC  $E\alpha(s)$  were not in complete agreement with corresponding seasonal and regional thermograms (Figure 19), which indicate all ecoregions had a significant increase in devolatilization MMLR(s) in the growing season. Pineywoods Chinese tallow consistently produced lower seasonal wood GPC  $E\alpha(s)$  than southern red oak, indicating Chinese tallow may be more combustible, especially in the growing season. Although growing season GPC  $E\alpha(s)$  yielded a clear difference in growing season combustibility, the corresponding seasonal devolatilization DTG thermograms didn't exhibit much separation in terms of MMLR(s), but did show a greater percent mass loss (Figure 17).

Friedman and OFW global  $E\alpha(s)$  for Chinese tallow foliage ranged from 225.15-256.35 and 213.80-244.59 KJ mol<sup>-1</sup>, respectively, with the Blackland Prairie yielding the greatest combustibility (Tables 17-18). Friedman and OFW GPC  $E\alpha(s)$  for Chinese tallow foliage ranged from 191.85-209.81 and 181.53-200.87 KJ mol<sup>-1</sup> (Tables 15-16), with the Blackland Prairie yielding the greatest combustibility. Friedman global and GPC  $E\alpha(s)$  were consistently lower than OFW  $E\alpha(s)$ , and produced the same  $E\alpha$  trend across ecoregions. Chinese tallow foliage consistently produced the lowest gas-phase combustibility among tree species foliage (Figure 21).

#### Species Ignitability

Friedman dormant season foliar  $E\alpha$  ignitability order was the same across ecoregions, with the exception of greenbrier and eastern red cedar in the Blackland Prairie. The Post Oak Savannah had the majority of species with the greatest dormant season ignitability, including Chinese privet, greenbrier, and escarpment live oak. Friedman dormant season foliar  $E\alpha$  ignitability for Chinese tallow wood ranged from 156.02-179.51 KJ mol<sup>-1</sup> (Table 21), with the Post Oak Savannah yielding the greatest ignitability. Dormant season Chinese tallow wood was significantly more ignitable than southern red oak wood in the Pineywoods ecoregion.

Friedman growing season foliar  $E\alpha$  ignitability ranged from 128.59-176.72 KJ mol<sup>-1</sup>, with Chinese privet exhibiting a general trend of greater ignitability and escarpment live oak and Chinese tallow producing the least ignitability. Regional Friedman ignitability trends were indiscernible due to considerable growing season variability. The Post Oak Savannah had the majority of species with the greatest growing season ignitability, whereas the Pineywoods produced the majority of species with the least ignitability. Southern red oak produced the greatest Friedman foliar ignitability of the tree species, whereas escarpment live oak and Chinese tallow exhibited considerable variability. Friedman  $E\alpha$  ignitability for growing season Chinese tallow wood ranged from 152.71-213.74 KJ mol<sup>-1</sup>, with the Pineywoods producing the greatest overall ignitability (Table 21). Similar to the dormant season, Chinese tallow wood was significantly more ignitable than southern red oak wood, except in the Post Oak Savannah. In general, the majority of species exhibited greater Friedman foliar ignitability in the dormant season, with the exception of Chinese privet which consistently produced greater growing season ignitability. Chinese tallow wood generally produced greater dormant season ignitability, with the exception of the Pineywoods.

OFW dormant season foliar  $E\alpha$  ignitability ranged from 128.58-152.02 KJ mol<sup>-1</sup>, with Chinese privet, greenbrier, and eastern red cedar producing the greatest ignitability, and escarpment live oak the least (Table 22). The Post Oak Savannah

and Pineywoods produced the majority of species with the greatest and least dormant season ignitability, respectively. OFW dormant season  $E\alpha$  ignitability for Chinese tallow wood ranged from 148.66-173.43 KJ mol<sup>-1</sup>, with the Post Oak Savannah yielding the greatest ignitability.

OFW growing season foliar  $E\alpha$  ignitability ranged from 120.00-167.70 KJ mol<sup>-1</sup>, with Chinese privet and eastern red cedar producing the greatest ignitability. OFW growing season foliar ignitability varied considerably across ecoregions, but the Pineywoods consistently produced the least foliar ignitability among ecoregions. Southern red oak foliage exhibited the greatest growing season OFW ignitability among tree species. Growing season OFW  $E\alpha(s)$  for Chinese tallow wood ranged from 145.85-205.76 KJ mol<sup>-1</sup>, with the Pineywoods yielding the greatest ignitability (Table 22). In general, Chinese tallow wood was significantly more ignitable than southern red oak wood, with the exception of the Post Oak Savannah. The majority of species exhibited greater dormant season ignitability, with the exception of Chinese privet which exhibited greater growing season ignitability.



**Table 13.** Mean Friedman dormant season foliar global  $E\alpha$ (s) based on conversion degrees ( $\alpha$ ) ranging from 0.02-0.80. Underlined  $E\alpha$  values indicate rough estimations of species maximum mass loss rates that correlate with peak devolatilization and gas-phase combustion. Note that escarpment live oak was not collected in the Pineywoods.

<i>Eα-Spp.</i>	<i>KJ mol<sup>-1</sup></i>				
	<i>Yaupon</i>	<i>C. Privet</i>	<i>Smilax</i>	<i>Red Cedar</i>	<i>Live Oak</i>
<i>Conversion (α)</i>					
	<i>Pineywoods</i>				
0.02	144.66	129.95	131.40	111.18	-
0.05	152.62	133.22	135.67	144.64	-
0.10	181.29	136.36	143.61	158.53	-
0.20	200.72	143.24	187.13	164.66	-
0.30	<u>213.28</u>	<u>143.93</u>	199.02	172.79	-
0.40	229.90	161.97	<u>214.26</u>	<u>194.44</u>	-
0.50	233.03	198.27	216.08	195.57	-
0.60	232.42	233.25	215.01	192.79	-
0.70	238.84	244.85	248.60	228.46	-
0.80	292.81	265.27	304.94	289.83	-
<i>Mean Eα</i>	<i>211.96</i>	<i>179.03</i>	<i>199.57</i>	<i>185.29</i>	-
	<i>Post Oak Savannah</i>				
0.02	136.46	127.78	126.31	134.40	144.99
0.05	151.46	131.64	135.66	146.72	152.29
0.10	166.36	135.82	146.91	159.57	166.56
0.20	184.61	140.92	178.21	157.48	180.40
0.30	<u>198.11</u>	<u>147.77</u>	189.28	175.27	196.81
0.40	219.98	170.53	<u>204.41</u>	<u>198.28</u>	<u>209.90</u>
0.50	245.49	201.47	206.72	197.96	216.08
0.60	245.18	223.14	209.35	193.41	197.40
0.70	249.18	229.19	246.71	237.58	205.58
0.80	286.87	257.92	316.69	297.72	393.00
<i>Mean Eα</i>	<i>208.37</i>	<i>176.62</i>	<i>196.02</i>	<i>189.84</i>	<i>206.30</i>

**Table 13.** Continued

---

	<i>Blackland Prairie</i>				
0.02	142.74	131.90	125.74	126.90	133.36
0.05	146.84	135.38	140.67	137.83	169.26
0.10	160.96	141.38	154.80	151.22	184.80
0.20	178.04	143.53	176.98	147.63	187.60
0.30	<u>193.94</u>	<u>149.41</u>	187.19	164.65	206.24
0.40	215.42	167.92	<u>195.46</u>	<u>190.38</u>	<u>221.47</u>
0.50	229.28	204.94	192.32	185.19	222.31
0.60	231.55	227.33	193.74	177.76	201.86
0.70	235.71	228.48	232.64	211.88	220.07
0.80	285.68	258.92	300.55	268.76	366.89
<i>Mean E<math>\alpha</math></i>	<i>202.02</i>	<i>178.92</i>	<i>190.01</i>	<i>176.22</i>	<i>211.38</i>

---

**Table 14.** Mean Ozawa-Flynn-Wall dormant season foliar global  $E\alpha$ (s) based on conversion degrees ( $\alpha$ ) ranging from 0.02-0.80. Underlined  $E\alpha$  values indicate rough estimations of species maximum mass loss rates that correlate with peak devolatilization and gas-phase combustion. Note that escarpment live oak was not collected in the Pineywoods.

<i>E<math>\alpha</math>-Spp.</i>	KJ mol <sup>-1</sup>					
	<i>Conversion (<math>\alpha</math>)</i>	Yaupon	C. Privet	Greenbrier	Red Cedar	Live Oak
		<i>Pineywoods</i>				
	0.02	139.99	129.46	132.46	103.19	-
	0.05	144.45	131.91	127.72	138.95	-
	0.10	168.18	135.15	139.30	151.03	-
	0.20	193.96	141.88	176.00	163.37	-
	0.30	<u>203.10</u>	<u>142.00</u>	188.69	166.42	-
	0.40	217.59	152.04	<u>208.64</u>	<u>182.44</u>	-
	0.50	226.64	177.92	214.31	191.02	-
	0.60	239.95	216.04	215.33	192.77	-
	0.70	234.69	234.85	227.95	205.55	-
	0.80	278.31	261.42	288.81	274.22	-
	<i>Mean E<math>\alpha</math></i>	<i>204.69</i>	<i>172.27</i>	<i>191.92</i>	<i>176.90</i>	<i>-</i>
		<i>Post Oak Savannah</i>				
	0.02	142.66	122.13	121.50	118.58	137.73
	0.05	141.99	129.03	129.86	139.09	147.67
	0.10	158.95	134.58	138.58	155.01	163.52
	0.20	177.48	138.55	170.71	155.66	176.92
	0.30	<u>187.23</u>	<u>141.49</u>	180.79	164.35	185.75
	0.40	204.77	154.60	<u>195.56</u>	<u>183.51</u>	<u>201.55</u>
	0.50	226.95	179.02	204.57	196.76	211.48
	0.60	237.67	204.20	207.79	195.14	210.92
	0.70	243.12	222.77	222.72	210.04	202.22
	0.80	271.05	241.99	296.60	277.63	342.11
	<i>Mean E<math>\alpha</math></i>	<i>199.19</i>	<i>166.84</i>	<i>186.87</i>	<i>179.58</i>	<i>197.99</i>

**Table 14.** Continued

---

	<i>Blackland Prairie</i>				
0.02	142.72	130.96	116.73	113.95	118.31
0.05	146.91	133.99	132.57	129.09	159.59
0.10	154.08	140.51	146.25	143.61	178.16
0.20	171.99	142.26	171.58	150.54	178.95
0.30	<u>182.74</u>	<u>144.77</u>	177.82	154.07	193.16
0.40	200.75	152.73	<u>189.98</u>	<u>176.90</u>	<u>211.50</u>
0.50	221.11	178.21	193.43	187.77	221.87
0.60	224.85	212.33	193.30	182.73	215.91
0.70	232.74	223.42	210.16	190.55	208.38
0.80	264.57	249.14	272.17	256.98	325.83
<i>Mean E<math>\alpha</math></i>	<i>194.24</i>	<i>170.83</i>	<i>180.40</i>	<i>168.62</i>	<i>201.17</i>

---

**Table 15.** Mean regional Friedman gas-phase combustion (GPC)  $E\alpha$  estimates based on species maximum mass loss rates,  $E\alpha(s)$  ranged from 0.02-0.52 $\alpha$ . Wood samples (w) are denoted in parentheses.

<i>E<math>\alpha</math>/Ecoregion</i>	KJ mol <sup>-1</sup>			
	Species	Pineywoods	Post Oak Savannah	Blackland Prairie
			<i>Dormant</i>	
Yaupon	177.83	167.25	163.88	
C. Privet	139.50	137.90	140.19	
Greenbrier	168.33	163.00	163.21	
E. Red Cedar	157.63	161.95	159.19	
E. Live Oak	-	180.81	183.50	
C. Tallow (w)	207.51	176.98	190.41	
S. Red Oak (w)	205.53	-	-	
			<i>Growing</i>	
Yaupon	187.43	167.45	187.95	
C. Privet	134.25	135.61	139.31	
Greenbrier	177.23	167.45	163.86	
E. Red Cedar	158.34	165.38	142.92	
C. Tallow	209.81	192.88	191.85	
E. Live oak	-	183.24	187.16	
S. Red Oak	175.46	-	-	
C. Tallow (w)	178.97	223.99	198.77	
S. Red Oak (w)	204.59	-	-	

**Table 16.** Mean regional Ozawa-Flynn-Wall gas-phase combustion (GPC)  $E\alpha$  estimates based on species maximum mass loss rates,  $E\alpha(s)$  ranged from 0.02-0.52 $\alpha$ . Wood samples (w) are denoted in parentheses.

<i>E<math>\alpha</math>/Ecoregion</i>	KJ mol <sup>-1</sup>			
	Species	Pineywoods	Post Oak Savannah	Blackland Prairie
			<i>Dormant</i>	
Yaupon	169.58	161.74	159.24	
C. Privet	137.45	134.01	138.45	
Greenbrier	161.90	155.58	155.20	
E. Red Cedar	150.76	152.70	149.19	
E. Live Oak	-	173.76	172.77	
C. Tallow (w)	199.80	169.35	182.84	
S. Red Oak (w)	201.72	-	-	
			<i>Growing</i>	
Yaupon	178.10	159.79	178.36	
C. Privet	132.67	132.15	135.49	
Greenbrier	171.01	156.27	155.10	
E. Red Cedar	149.51	153.05	132.61	
C. Tallow	200.87	181.54	181.53	
E. Live oak	-	176.35	181.21	
S. Red Oak	165.67	-	-	
C. Tallow (w)	170.51	217.25	194.96	
S. Red Oak (w)	199.46	-	-	

**Table 17.** Mean Friedman growing season foliar global  $E\alpha(s)$  based on conversion degrees ( $\alpha$ ) ranging from 0.02-0.80. Underlined values indicate rough estimations of species maximum mass loss rates that correlate with peak devolatilization and gas-phase combustion.

$E\alpha$ - <i>Spp.</i>	KJ mol <sup>-1</sup>					
<i>Conv.</i> ( $\alpha$ )	Yaupon	C. Privet	Greenbrier	Red Cedar	Live Oak	C. Tallow
	<i>Pineywoods</i>					
0.02	160.02	127.42	150.72	133.49	-	148.05
0.05	180.60	130.85	165.20	148.22	-	160.64
0.10	189.55	133.89	181.88	160.89	-	194.40
0.20	196.46	140.67	178.49	152.79	-	233.66
0.30	<u>214.18</u>	<u>143.62</u>	186.15	171.36	-	261.40
0.40	224.74	159.22	<u>202.49</u>	<u>186.54</u>	-	<u>259.42</u>
0.50	229.25	197.95	205.56	194.33	-	268.07
0.60	214.38	232.26	220.68	196.01	-	268.39
0.70	226.38	242.06	315.00	240.45	-	321.49
0.80	260.78	256.70	420.45	306.95	-	447.96
<i>Mean E<math>\alpha</math></i>	209.63	176.46	222.66	189.10	-	256.35
	<i>Post Oak Savannah</i>					
0.02	140.15	126.38	115.58	135.80	144.33	146.93
0.05	157.69	129.05	154.00	148.01	165.75	162.72
0.10	170.21	134.43	170.77	156.70	175.25	184.61
0.20	179.32	143.50	175.33	152.44	185.53	209.38
0.30	<u>197.95</u>	<u>146.23</u>	<u>192.56</u>	169.96	196.41	225.86
0.40	211.66	167.49	204.40	<u>197.36</u>	<u>206.97</u>	<u>228.45</u>
0.50	209.42	207.45	198.25	205.86	217.50	250.36
0.60	204.84	226.71	209.97	192.63	196.96	236.31
0.70	217.30	239.68	257.29	215.43	202.59	290.06
0.80	266.17	251.21	344.59	283.50	371.80	466.41
<i>Mean E<math>\alpha</math></i>	195.47	177.21	202.27	185.77	206.31	240.11

**Table 17.** Continued

---

	<i>Blackland Prairie</i>					
0.02	144.99	125.63	123.88	118.95	158.96	139.69
0.05	168.37	129.86	155.61	133.40	175.22	153.55
0.10	191.05	137.58	168.07	133.42	182.88	178.55
0.20	194.53	145.44	167.44	132.43	189.73	209.50
0.30	<u>212.80</u>	<u>148.61</u>	181.66	153.25	202.71	<u>233.63</u>
0.40	226.56	175.27	<u>189.45</u>	<u>187.49</u>	<u>214.41</u>	232.97
0.50	215.68	211.22	187.89	185.06	211.62	230.76
0.60	205.07	214.68	190.20	170.75	199.44	226.83
0.70	219.74	245.86	230.73	192.13	224.50	260.81
0.80	277.10	251.97	289.44	247.84	348.25	385.24
<i>Mean E<math>\alpha</math></i>	205.59	178.61	188.44	165.47	210.77	225.15

---



**Table 18.** Mean Ozawa-Flynn-Wall growing season foliar global  $E\alpha$ (s) based on conversion degrees ( $\alpha$ ) ranging from 0.02-0.80. Underlined values indicate rough estimates of species maximum mass loss rates that correlate with peak devolatilization and gas-phase combustion.

$E\alpha$ -Spp. Conv.( $\alpha$ )	KJ mol <sup>-1</sup>					
	Yaupon	C. Privet	Greenbrier	Red Cedar	Live Oak	C. Tallow
<i>Pineywoods</i>						
0.02	149.57	126.37	145.65	122.68	-	138.97
0.05	171.19	127.74	156.82	137.71	-	149.43
0.10	182.35	131.30	175.45	155.76	-	187.05
0.20	189.26	139.24	180.71	152.62	-	221.99
0.30	<u>202.03</u>	<u>139.11</u>	178.58	159.72	-	249.67
0.40	216.32	148.03	<u>191.00</u>	<u>172.12</u>	-	<u>257.96</u>
0.50	223.73	172.19	198.92	183.88	-	262.81
0.60	226.16	211.16	205.28	192.13	-	273.74
0.70	224.30	230.23	251.86	211.72	-	292.94
0.80	247.54	252.95	416.00	281.95	-	411.37
<i>Mean E<math>\alpha</math></i>	<i>203.25</i>	<i>167.83</i>	<i>210.03</i>	<i>177.03</i>	-	<i>244.59</i>
<i>Post Oak Savannah</i>						
0.02	131.48	125.91	99.52	117.82	136.12	131.41
0.05	150.09	126.61	139.14	136.60	161.34	154.92
0.10	162.30	130.47	165.06	152.00	171.41	179.93
0.20	173.96	135.57	165.92	150.07	179.25	190.60
0.30	<u>186.38</u>	<u>142.54</u>	<u>182.53</u>	158.43	186.95	211.57
0.40	202.53	152.86	193.33	<u>178.26</u>	<u>199.70</u>	<u>224.47</u>
0.50	211.10	181.21	201.81	198.66	211.96	231.27
0.60	208.47	215.89	200.21	198.34	211.37	236.97
0.70	214.61	230.28	237.35	198.08	198.97	258.81
0.80	248.98	244.66	318.01	261.45	296.69	416.24
<i>Mean E<math>\alpha</math></i>	<i>188.99</i>	<i>168.60</i>	<i>190.29</i>	<i>174.97</i>	<i>195.38</i>	<i>223.62</i>

**Table 18.** Continued

---

	<i>Blackland Prairie</i>					
0.02	129.69	124.39	107.27	105.76	149.17	130.68
0.05	158.84	126.73	143.29	124.60	172.65	142.65
0.10	182.58	131.60	162.97	129.63	181.14	167.96
0.20	192.26	143.94	165.77	129.74	184.22	198.93
0.30	<u>202.11</u>	<u>141.96</u>	173.20	142.32	195.55	<u>221.90</u>
0.40	218.03	156.93	<u>182.93</u>	<u>164.69</u>	<u>206.25</u>	232.83
0.50	224.22	187.28	187.30	183.66	212.86	230.85
0.60	214.55	207.71	190.48	171.05	208.62	233.09
0.70	212.77	228.90	209.67	179.44	209.90	238.57
0.80	251.51	246.50	265.66	225.73	316.07	340.50
<i>Mean E<math>\alpha</math></i>	198.66	169.59	178.85	155.66	203.64	213.80

---

**Table 19.** Mean seasonal Friedman and Ozawa-Flynn-Wall (OFW) global  $E_{\alpha}(s)$  (0.02-0.80) for southern red oak wood and foliage. Underlined values indicate rough estimations of species maximum mass loss rates that correlate with peak devolatilization and gas-phase combustion.

<i>Kinetics</i> $E(\alpha)/season$	Friedman (KJ mol <sup>-1</sup> )			OFW (KJ mol <sup>-1</sup> )		
	Dormant <sup>W</sup>	Growing <sup>W</sup>	Growing <sup>F</sup>	Dormant <sup>W</sup>	Growing <sup>W</sup>	Growing <sup>F</sup>
0.02	196.54	189.50	130.95	194.21	181.71	115.00
0.05	198.27	202.34	152.29	198.02	199.49	139.82
0.10	192.31	204.25	176.56	193.55	199.65	169.20
0.20	197.58	198.32	188.80	186.74	196.44	181.44
0.30	215.27	212.22	198.08	203.58	198.66	190.75
0.40	221.62	215.64	<u>211.38</u>	215.95	212.02	<u>202.70</u>
0.50	<u>216.29</u>	<u>207.18</u>	222.77	<u>220.16</u>	<u>214.17</u>	218.21
0.60	201.17	195.23	221.29	215.48	209.16	222.72
0.70	193.72	185.64	269.19	207.13	200.59	234.85
0.80	256.69	240.10	417.34	211.32	201.12	380.71
<i>Mean E<sub>α</sub></i>	<i>208.95</i>	<i>205.04</i>	<i>218.86</i>	<i>204.61</i>	<i>201.30</i>	<i>205.54</i>

Dormant<sup>W</sup> and Growing<sup>W</sup>; wood samples; Growing<sup>F</sup>: foliage samples

**Table 20.** Mean Friedman and Ozawa-Flynn-Wall (OFW) global  $E\alpha$ (s) (0.02-0.80) for Chinese tallow wood based season and ecoregion. Underlined values indicate rough estimations of species maximum mass loss rates that correlate with peak devolatilization and gas-phase combustion. Ecoregions are abbreviated as: PW: Pineywoods, POS: Post Oak Savannah, and BP: Blackland Prairie.

<i>Kinetics/<math>E\alpha</math></i> <i>Conversion (<math>\alpha</math>)</i>	Friedman (KJ mol <sup>-1</sup> )			OFW (KJ mol <sup>-1</sup> )		
	PW	POS	BP	PW	POS	BP
	<i>Dormant</i>					
0.02	153.22	132.40	148.48	152.27	128.68	153.46
0.05	165.92	145.17	153.44	159.42	139.95	149.29
0.10	188.78	161.48	173.69	179.95	153.00	164.11
0.20	210.14	185.02	197.71	202.08	173.01	185.09
0.30	224.00	200.01	215.29	213.84	187.56	201.42
0.40	234.18	205.76	232.56	225.81	198.87	207.88
0.50	<u>245.83</u>	<u>211.99</u>	<u>223.24</u>	<u>238.13</u>	<u>206.80</u>	<u>219.35</u>
0.60	242.42	212.73	227.47	246.54	214.14	222.80
0.70	225.32	221.46	225.28	238.98	208.84	227.57
0.80	249.35	276.38	256.17	238.07	233.29	235.18
<i>Mean <math>E\alpha</math></i>	<i>213.92</i>	<i>195.24</i>	<i>205.33</i>	<i>209.51</i>	<i>184.42</i>	<i>196.62</i>
	<i>Growing</i>					
0.02	129.68	217.22	165.44	129.31	196.07	161.22
0.05	142.34	208.66	185.59	136.71	208.08	173.94
0.10	158.14	210.81	183.49	149.46	208.79	190.44
0.20	180.66	218.25	199.17	167.92	210.12	187.62
0.30	192.77	235.53	215.87	179.85	223.71	203.40
0.40	198.08	240.50	219.49	188.76	235.51	214.31
0.50	<u>217.33</u>	<u>236.55</u>	<u>213.79</u>	<u>203.99</u>	<u>239.25</u>	<u>216.99</u>
0.60	221.23	228.12	202.87	216.99	237.22	213.74
0.70	210.53	210.33	196.82	217.46	226.92	208.06
0.80	249.36	250.16	236.02	219.51	224.87	208.01
<i>Mean <math>E\alpha</math></i>	<i>190.01</i>	<i>225.61</i>	<i>201.85</i>	<i>181.00</i>	<i>221.05</i>	<i>197.77</i>

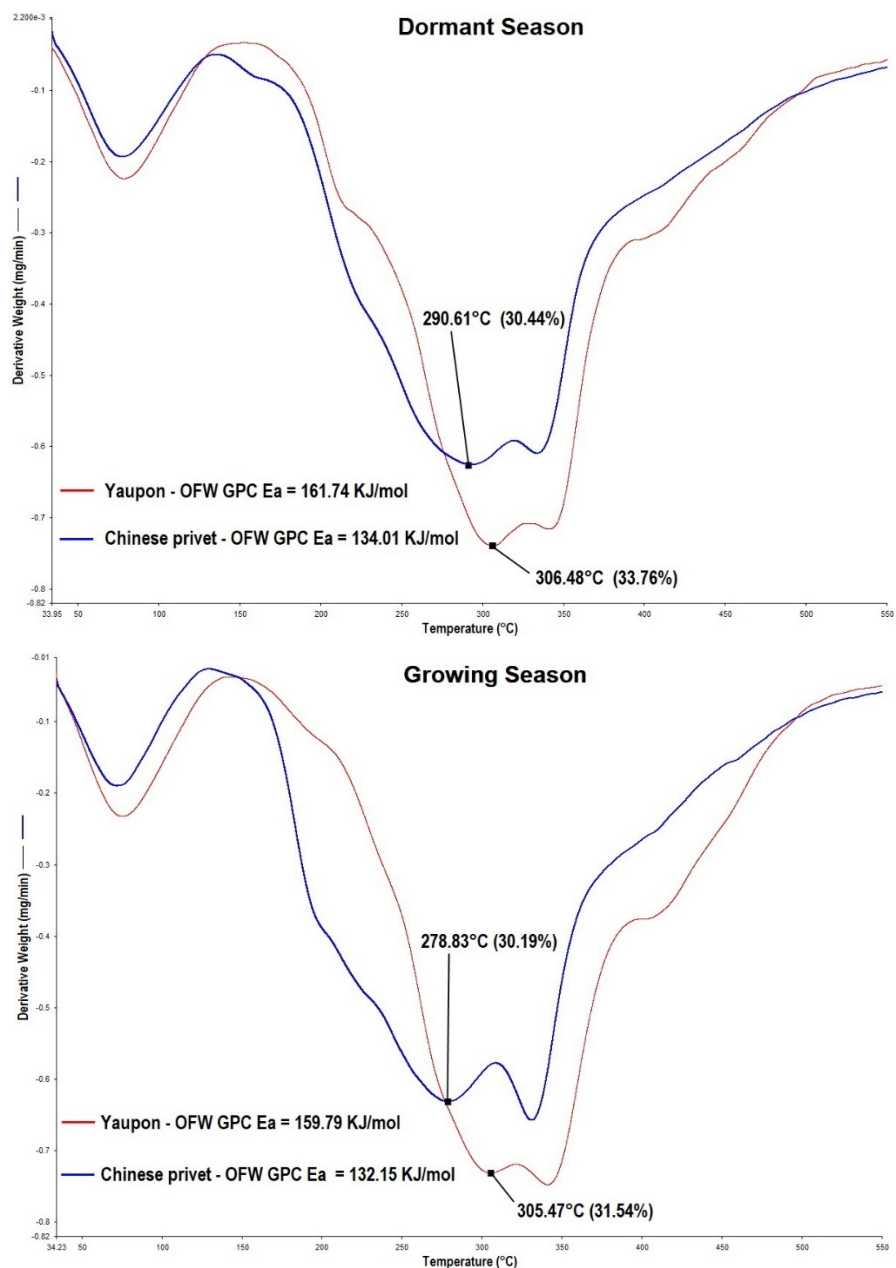


**Figure 17.** Seasonal DTG devolatilization thermograms displaying gas-phase combustion (GPC)  $E_a$ , maximum mass loss rate temperature, and percent mass loss for Post Oak Savannah yaupon and Chinese privet.

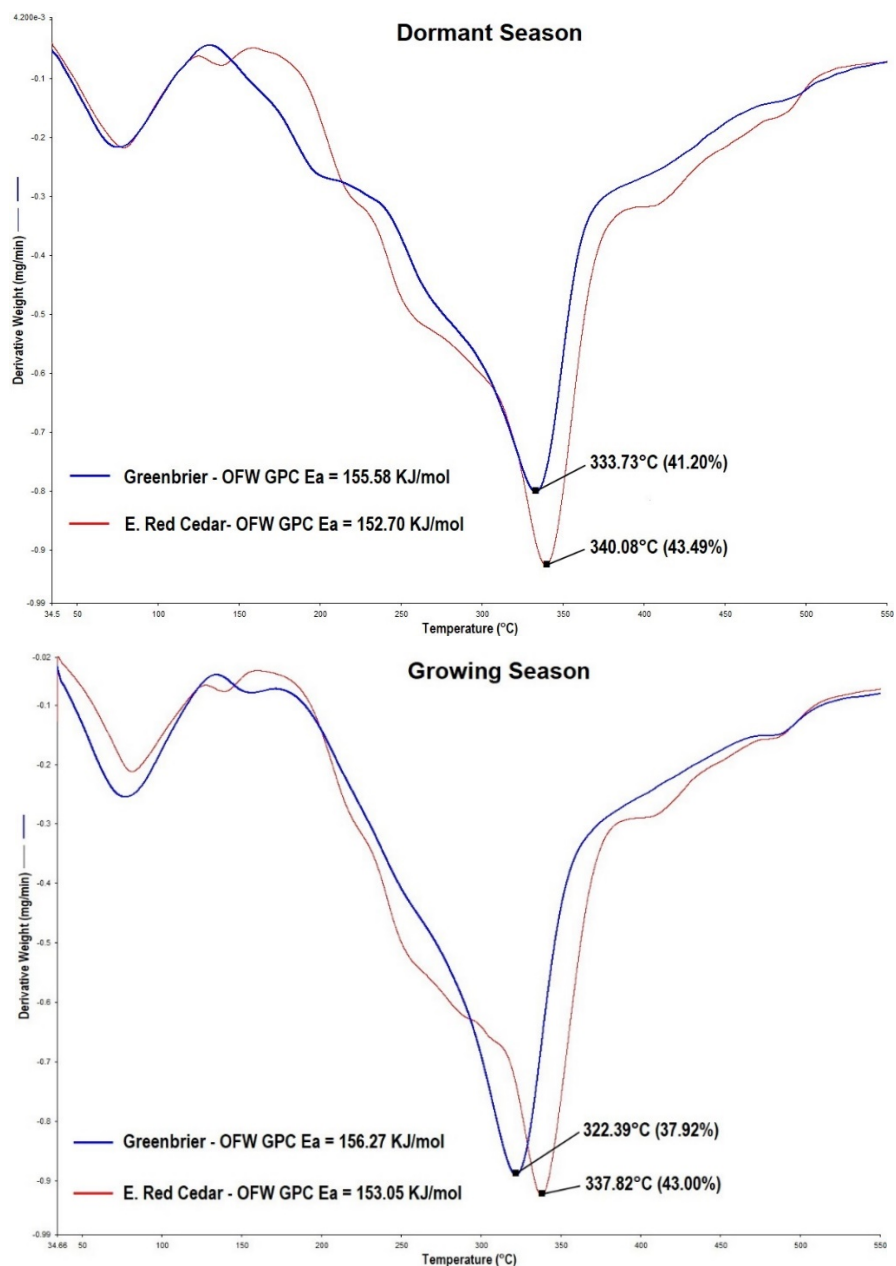


**Figure 18.** Seasonal DTG devolatilization thermograms displaying gas-phase combustion (GPC)  $E_a$ , maximum mass loss rate temperature, and percent mass loss for Post Oak Savannah greenbrier and eastern red cedar.

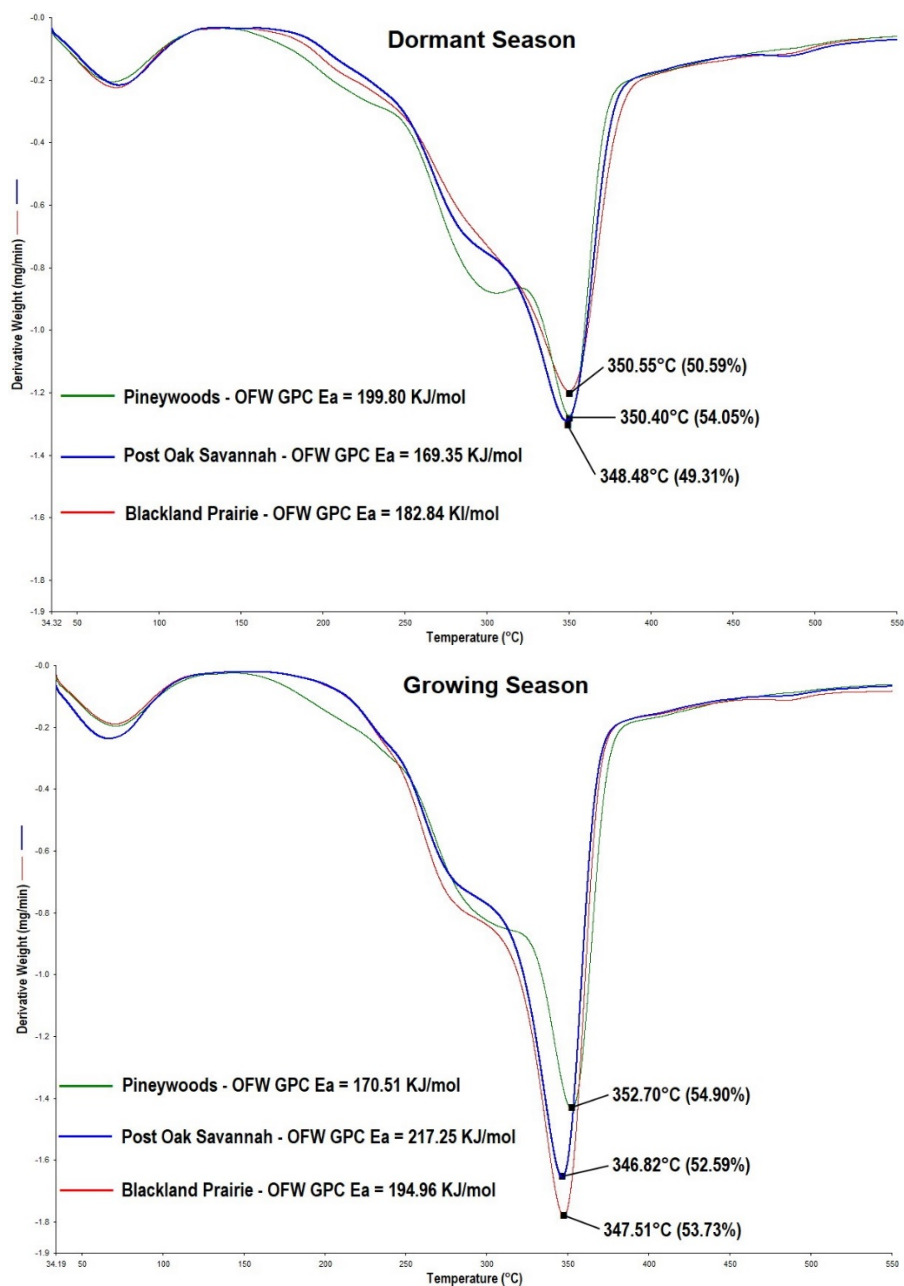


**Figure 19.** Seasonal and regional DTG devolatilization thermograms displaying gas-phase combustion  $E_a$ , maximum mass loss rate temperature, and percent mass loss for Chinese tallow wood in the Pineywoods, Post Oak Savannah, and Blackland Prairie ecoregions.

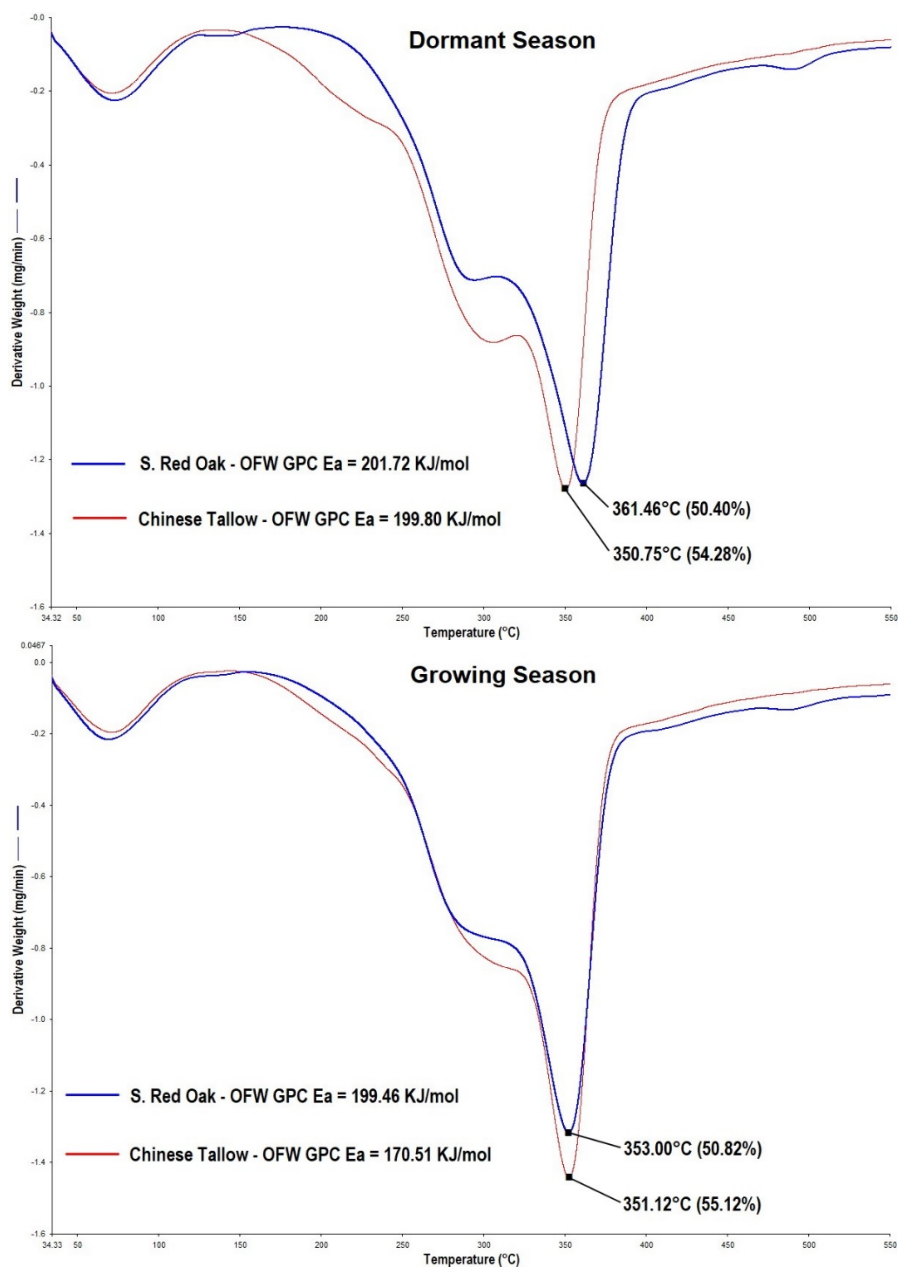


**Figure 20.** Seasonal DTG devolatilization thermograms displaying gas-phase combustion (GPC)  $E\alpha$ , maximum mass loss rate temperature, and percent mass loss for Pineywoods Chinese tallow and southern red oak wood.



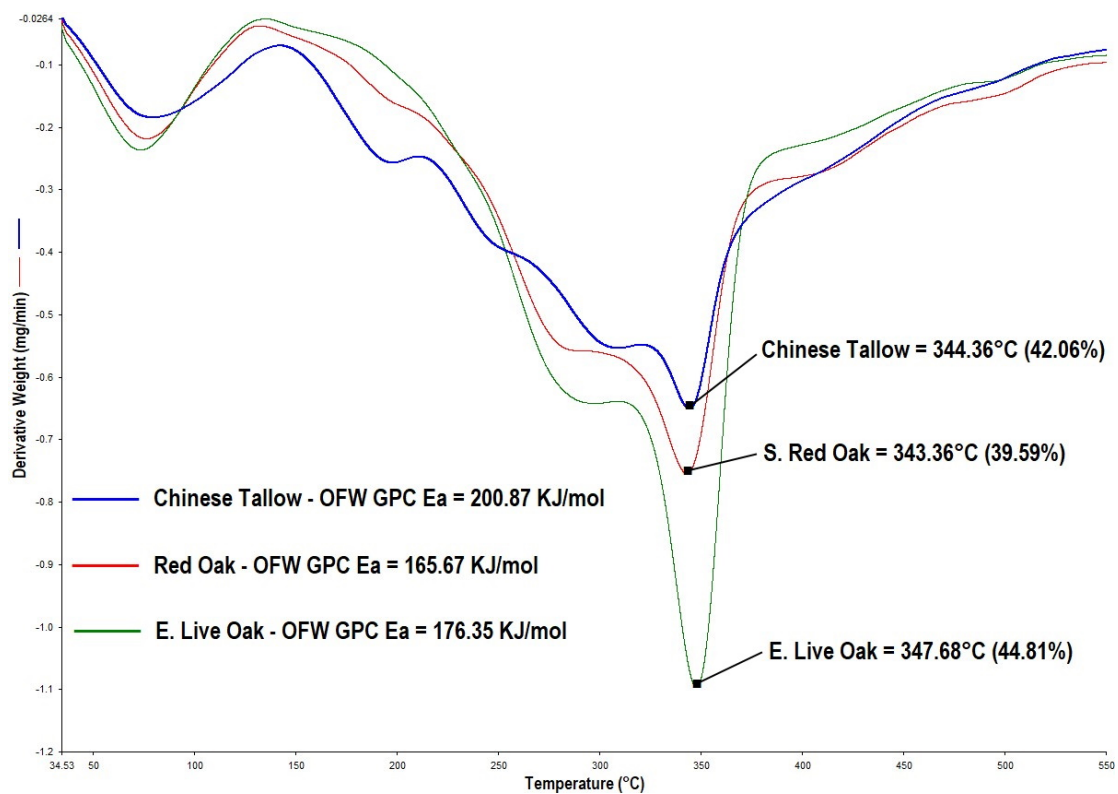


**Figure 21.** DTG devolatilization thermograms displaying gas-phase combustion (GPC)  $E_a$ , maximum mass loss rate temperature, and percent mass loss for Pineywoods Chinese tallow and southern red oak and Post Oak Savannah escarpment live oak.

**Table 21.** Mean ignitability estimates based on Friedman global  $E\alpha(s)$  ranging from 0.02-0.10 and 0.02-0.20 for foliar and wood samples, respectively. Wood samples (w) are denoted in parentheses.

<i>E<math>\alpha</math>/Ecoregion</i>	KJ mol <sup>-1</sup>		
	Pinewoods	Post Oak Savannah	Blackland Prairie
	<i>Dormant</i>		
Yaupon	159.52	151.43	150.18
C. Privet	133.18	131.75	136.22
Greenbrier	136.90	136.29	140.41
E. Red Cedar	138.12	146.90	138.65
E. Live Oak	-	154.61	162.47
C. Tallow (w)	179.51	156.02	168.33
S. Red Oak (w)	196.18	-	-
	<i>Growing</i>		
Yaupon	176.72	156.02	168.13
C. Privet	130.72	129.96	131.02
Greenbrier	165.39	146.79	149.19
E. Red Cedar	147.53	146.84	128.59
C. Tallow	167.70	164.75	157.26
E. Live oak	-	161.78	172.35
S. Red Oak	153.26	-	-
C. Tallow (w)	152.71	213.74	183.42
S. Red Oak (w)	198.60	-	-

**Table 22.** Mean ignitability estimates based on Ozawa-Flynn-Wall global  $E\alpha(s)$  ranging from 0.02-0.10 and 0.02-0.20 for foliar and wood samples, respectively. Wood samples (w) are denoted in parentheses.

<i>E<math>\alpha</math>/Ecoregion</i>	<i>KJ mol<sup>-1</sup></i>			
	<i>Species</i>	Pineywoods	Post Oak Savannah	Blackland Prairie
			<i>Dormant</i>	
Yaupon	150.87	147.87	147.90	
C. Privet	133.53	128.58	135.15	
Greenbrier	133.16	129.98	131.85	
E. Red Cedar	131.06	137.56	128.88	
E. Live Oak	-	149.64	152.02	
C. Tallow (w)	173.43	148.66	162.99	
S. Red Oak (w)	193.13	-	-	
			<i>Growing</i>	
Yaupon	167.70	147.96	157.04	
C. Privet	128.47	127.67	127.58	
Greenbrier	159.31	134.57	137.84	
E. Red Cedar	138.71	135.48	120.00	
C. Tallow	158.48	155.42	147.10	
E. Live oak	-	156.29	167.65	
S. Red Oak	141.34	-	-	
C. Tallow (w)	145.85	205.76	178.3	
S. Red Oak (w)	194.32	-	-	

## DISCUSSION

### Proximate Analysis

Proximate analyses are often used in heat content and TGA studies to help elucidate differences in thermochemical and thermal kinetic properties of natural, lignocellulosic fuels (Munir et al. 2009, Rivera et al. 2012). The low cost and accessibility of proximate analysis data has also led to several linear and nonlinear regression models that predict the heat content of biomass feedstock for the bio-energy industry (Nhuchhen and Salam 2012). Studies have also linked greater heat content and volatile extract production in natural fuels with peak growing season conditions and subsequent changes in soil moisture and maximum temperatures (Philpot 1971, Chrosciewicz 1986). Proximate analysis data trends can provide insight into natural fuel combustibility based on seasonal climatic trends relative to VM%, FC%, and ash%.

VM% was the only parameter that was a general indicator of greater NHC and GP-MMLR(S), and may offer limited insight into general species flammability. However, VM% does contain some non-combustible constituents such as CO<sub>2</sub> and H<sub>2</sub>O (Ozyuguran and Yaman 2017), thereby adding a small degree of uncertainty to actual proportions of combustible constituents available to burn in VM% estimates. Greater proportions of FC% in woody plant tissue have been linked to increased

NHC (Ozyuguran and Yaman 2017, Uzun et al. 2017), but this trend may not relate to foliar NHC values as evidenced by Safdari et al. (2018) who reported a much greater degree of FC% and heat content variability in Southern US shrubs. This trend was also noted for the majority of foliar FC%(s) in this study; therefore, no discernable relationships were observed between species foliar FC% and NHC. Ash% has been linked to reduced fuel flammability by interfering with the formation of volatile compounds and reducing the proportion of organic matter available to burn (Rivera et al. 2012); therefore, lower proportions of ash% generally indicate greater flammability. In theory, greater VM% in combination with lower ash% would lead to greater foliar gas-phase flammability. After analyzing inverse trends between VM% relative to ash%, ash% exhibited considerable variability and a weak inverse relationship to VM%, which suggests this combination is not an ideal predictor of combustibility. Most foliage proximate analysis parameters exhibited a weak relationship with respect to mean seasonal and regional precipitation and maximum temperatures. Irrespective of weak seasonal and regional climate trends, VM% may provide some insight into possible foliar combustibility trends, but further testing is needed to confirm these potential trends.

Foliar flammability estimates based on VM% were consistently greater for eastern red cedar and yaupon relative to season and ecoregion, which is not surprising based on anecdotal accounts attesting to their flammability. On the

other hand, greenbrier and escarpment live oak were on the lower end of VM% combustibility, except Pineywoods greenbrier, which exhibited the greatest growing season VM% of all foliar samples. Reasons for greenbrier's very high VM% in the Pineywoods growing season is unclear, but could have possibly been influenced by increased growth from above normal precipitation and maximum temperatures that occurred in the 2016 growing season. The potential increased growing season growth associated with Pineywoods greenbrier may have led to greater proportions of bound inter-molecular water, which may be explained by its very high VM% and low Friedman and OFW ignitability ( $>E\alpha$ ). As expected, foliar VM% generally trended higher in the growing season across ecoregions, except in the Post Oak Savannah where all foliar samples exhibited greater dormant season VM%. This unexpected shift in the Post Oak Savannah could be related to increased dormant season growth from above normal temperatures and reduced tree canopy shading from a deciduous overstory. Regionally, VM% did not exhibit any general trends, and remained quite variable across ecoregions. Chinese privet exhibited the greatest ash% among species, yet retained moderate flammability with respect to season and ecoregion compared to native species. This potentially highlights a significant physiological difference between Chinese privets' ability to sequester inorganic nutrients as compared to native species. Moreover, Chinese privets' consistent intermediate

combustibility relative to VM% may potentially increase fire intensity in mixed stands given favorable fire weather and low live fuel moisture.

Seasonal foliar VM% for escarpment live oak ranged from ~ 75-78%, with the Post Oak Savannah yielding the greatest VM% and the Blackland Prairie the least. Although escarpment live oak is considered evergreen, they do shed their leaves in the spring to accommodate new growth; as new leaves develop and growth continues throughout the growing season, greater proportions of VM% are generated from primary cell wall growth, which is primarily comprised of hemicellulose and cellulose. Conversely, at the cessation of leaf growth, secondary cell walls begin to develop in order to strengthen and support the leaf structure (Cosgrove 1997, Alonso et al. 2012). To maintain leaf structural integrity, secondary cell walls are comprised of hemicellulose, cellulose, and lignin (Cosgrove 2005). In theory, escarpment live oaks VM% should be higher in the dormant season prior to leaf abscission, which is consistent with escarpment live oak VM% in the Post Oak Savannah, but not in the Blackland Prairie. A possible explanation for the higher dormant season VM% in the Post Oak Savannah could be increased seasonal growth from +35 mm of above normal growing season rainfall and +3°C above normal dormant season maximum temperature at Lake Somerville in 2017, as well as increased soil productivity associated with Alfisol soils (Brady and Weil 2008). Escarpment live

oak in the Blackland Prairie may have had reduced dormant season growth due to lower soil moisture from – 22 mm below normal rainfall, combined with a +2.3°C above normal maximum temperature, as well as lower soil productivity associated with Inceptisol soils (Brady and Weil 2008). Chinese tallow and escarpment live oak foliage in Post Oak Savannah and Blackland Prairie exhibited similar growing season VM%; however, similar to Chinese privet, Chinese tallow exhibited a significant shift in ash%, potentially decreasing flammability. Chinese tallow and southern red oak foliage in the Pineywoods shared similar VM%(s), but significantly differed in ash%, with southern red oak foliage exhibiting the lowest ash% among tree species. Southern red oaks low foliar ash% also aligns well with the lowest Friedman and OFW GPC and ignition  $E\alpha(s)$ , making it the most ignitable and combustible foliage of the broad leaf trees.

Chinese tallow wood VM%, FC%, and ash% varied considerably with respect to season and ecoregion. However, Chinese tallow wood VM% and ash% were inversely related in the growing season, with significantly higher growing season VM% values recorded in the Pineywoods and Blackland Prairie ecoregions. Consequently, Chinese tallow wood appears to be much more combustible in the growing season in both the Pineywoods and Blackland Prairie. Chinese tallow and southern red oak wood shared similar growing



season VM% in the Pineywoods, but significantly differed in ash%, with Chinese tallow yielding the lowest ash% of all wood samples. Southern red oaks increase in dormant season VM% in the Pineywoods ecoregion as compared to Chinese tallow, could be related to an abundance of growing season rainfall (+32 mm) in 2018.

### Oxygen Bomb Calorimetry

As expected, based on anecdotal observations, yaupon and eastern red cedar consistently produced the greatest seasonal NHC-A content across ecoregions, with the exception of yaupon in the Pineywoods ecoregion. Pineywoods yaupon exhibited the greatest NHC-A variability of all species within the study; therefore, any assumptions attempting to explain yaupon's low NHC-A values will be avoided, other than the dormant season drought of 2013 may have contributed to yaupons' high variability. Greenbrier consistently exhibited the greatest seasonal NHC-A in the Pineywoods, potentially increasing the risk of torching and crown fire initiation in unmanaged forest stands and streamside management zones where greenbrier vines have extended in to the mid-story canopy. In contrast, greenbrier in the Post Oak Savannah and Blackland Prairie exhibited a significant shift from an intermediate dormant season NHC-A to a low growing season NHC-A. One possible explanation for greenbriers seasonal shift in NHC-A, could be its semi-evergreen characteristics, which may allow it to

access more dormant season site resources when all other deciduous competitors have slowed their growth. Although greenbriers reduced growing season NHC-A would likely reduce the risk of torching and crown fire initiation in hardwood stands, it would still seem prudent to exercise caution when prescribed burning in hardwood stands in the early growing season when greenbrier may still exhibit intermediate heat content that could result in crown scorch of desirable hardwoods. Chinese tallow and southern red oak foliage produced greater NHC-A(s) than stem wood samples, which is consistent with Rivera et al. (2012). It is also worth noting that mean TGA-derived foliar water vaporization corrections were  $1.24 \text{ MJ kg}^{-1}$ , and are consistent with Williams and Agee (2002) standard water vaporization correction of  $1.26 \text{ MJ kg}^{-1}$ . All species foliar NHC-A(s) fell well below the  $18.61 \text{ MJ kg}^{-1}$  used in common fire behavior models, with the exception of Blackland Prairie yaupon; therefore, common fire modeling programs like BehavePlus will likely over predict fire behavior based on the majority of species NHC-A(s) in this study.

Chinese tallows' mean GHC of  $17.09 \text{ MJ kg}^{-1}$  was fairly consistent with the mean GHC ( $17.65 \text{ MJ Kg}^{-1}$ ) reported by Scheld and Cowles (1981). On average, southern red oak and Chinese tallow wood yielded similar NHC-A(s). Chinese tallow wood NHC-A also varied little across ecoregions, except in the Pineywoods dormant season. Southern red oak

wood yielded a mean GHC of 18.07 MJ kg<sup>-1</sup>, which was ~ 1 MJ kg<sup>-1</sup> lower than small oak branch wood (19.20 MJ kg<sup>-1</sup>) reported by Nhuchhen and Salam (2012). Foliar NHC-A values for Chinese tallow and southern red oak were consistently greater than their corresponding wood NHC-A values, and is consistent with previous reports by Rivera et al. (2012).

Dormant and growing season foliar NHC-A corrections ranged from 3.41-7.36% and 2.68-6.84%, respectively, whereas respective dormant and growing season wood NHC-A corrections ranged from 1.97-3.20% and 1.18-2.86%. Previous research by Monti et al. (2008) reported a two-fold increase in foliar ash% compared to wood ash%, which is consistent with the aforementioned ash% corrections. Foliar NHC-AF(s) also yielded significant differences with respect to species, season, and ecoregion, which may facilitate improved comparative analysis. Mean seasonal and regional NHC-AF values for Post Oak Savannah and Blackland Prairie yaupon and escarpment live oak were 19.52 and 17.98 MJ kg<sup>-1</sup>, respectively, and are fairly consistent with Safdari et al. (2018) who reported mean NHC-AF(s) of 19.79 MJ kg<sup>-1</sup> for yaupon and 18.21 MJ kg<sup>-1</sup> for southern live oak. The slightly lower mean NHC-AF(s) for yaupon and escarpment live oak in this study compared to Safdari et al. (2018) could be related to their use of nurse stock in their study, which was likely grown with fertilizer under ideal conditions, as well as differences between live oak species.

As expected, yaupon and eastern red cedar consistently produced the greatest seasonal NHC-AF values, while escarpment live oak and Chinese tallow foliage consistently yielded the lowest NHC-AF values. Chinese tallow foliage produced some of the greatest ash% corrections in the Post Oak Savannah (6.19%) and Blackland Prairie (6.84%), but produced some of the lowest NHC-AF values, indicating a likely reduction in foliar flammability. In terms of seasonality, yaupon and Chinese privet consistently produced greater growing season NHC-AF, which was expected due to greater growth potential; however, greenbrier and eastern red cedar exhibited consistently greater NHC-AF values in the dormant season, indicating the possibility of active dormant season growth, potentially enhanced by reduced deciduous plant competition and above normal temperatures. For example, eastern red cedars'  $\sim 1.0 \text{ MJ kg}^{-1}$  increase in dormant season NHC-AF in the Post Oak Savannah could be related to greatly improved soil moisture from +54.36 mm above normal growing season rainfall combined with a +3.0°C increase in dormant season maximum temperature in 2017. Greenbriers' semi-evergreen traits may also be related to increased dormant season NHC-AF due to the partial senescence of intact foliage that may increase NHC-AF during the early stages of decomposition (Bocock 1964), but this possible explanation requires further testing. Chinese privets' intermediate to high growing season NHC-AF is similar to greenbrier,

and could potentially increase fire intensity in mixed midstory fuel beds under favorable conditions. Seasonal and regional foliar NHC-AF values for the majority of species fell well below the standard  $18.61 \text{ MJ kg}^{-1}$  (Andrews 1986, Finney 1998), with the exception of Post Oak Savannah and Blackland Prairie yaupon and eastern red cedar. Based on the majority of species low NHC-AF values, fire behavior will be essentially over-predicted, which could be misleading when developing low intensity prescribed fire prescriptions, possibly resulting in significantly reduced fire intensity that doesn't meet the desired management goals.

Significant regional differences in foliar NHC-AF values were especially apparent with yaupon, Chinese privet, and eastern red cedar. The Post Oak Savannah and Blackland Prairie generally produced significantly greater seasonal NHC-AF values, which may be attributed to increased growth from more open stand conditions with less overstory shading from deciduous hardwoods as well as less evapotranspiration culminating from reduced tree density and increased grass cover. By contrast, understory shrub growth in the Pineywoods may be inhibited by greater overstory shading and an overall increase in tree and shrub density resulting in greater evapotranspiration. Further increases in NHC-AF maybe related to an increase in leaf cuticle waxes as a response to drier conditions to mitigate non-stomatal water loss (Burghardt

and Riederer 2003, Hasanuzzaman et al. 2017). Owens et al. (1998) reported a significant increase in monoterpenoid content in west Texas Ashe juniper as compared to lower, more stable monoterpenoid contents in central Texas Ashe juniper. This increase in monoterpene concentration maybe be related to enhanced cuticular wax control on leaf tissue in drier regions, where oil and resin secretion facilitates the clearing of thicker layers of cuticular wax to clear stomatal apertures during infrequent wet periods (Scahde et al. 1999, Schulz et al. 2007). The juxtaposition of this trend could be applied to the Pineywoods and Post Oak Savannah ecoregions, where the climatic moisture gradient declines in a westerly direction (Figure 2).

Mean dormant season NHC-AF for Chinese tallow wood was significantly lower in the Pineywoods, while the Post Oak Savannah and Blackland Prairie were not significantly different according to post hoc testing. The low dormant season wood NHC-AF for Pineywoods Chinese tallow might be related to diminished growth from prolonged drought and below normal dormant season rainfall (-31.56 mm), combined with an above normal maximum temperature (+2°C). Conversely, NHC-AF for Pineywoods Chinese tallow wood rebounded significantly in the 2013 growing season, which correlates well with drought recovery and an increase in rainfall. Growing season Chinese tallow wood in the Pineywoods was highly variable, and it still remains unclear as to how much

improved soil moisture may have impacted NHC-AF. Chinese tallow wood NHC-AF in the Post Oak Savannah and Blackland Prairie were greater in the dormant season as opposed to the growing season. This shift in dormant season Chinese tallow wood NHC-AF did not correlate with any proximate analysis indices or climate data, and the underlying cause remains unclear; however, the low magnitude of the shift in NHC-AF is unlikely to have a significant impact on wood flammability. Southern red oak wood NHC-AF was consistently greater than Chinese tallow wood in the Pineywoods, and is consistent with previous studies (Scheld and Cowles 1981, Miranda et al. 2009). Southern red oak woods' greater NHC-AF may be related to its greater specific gravity (0.52; Jenkins et al. 2003) as compared to Chinese tallow woods' mean specific gravity (0.44; Scheld and Cowles 1981).

Significant regional differences in foliar NHC-A(s) were likely associated with regional precipitation (Figure 2) and temperature gradients, as well as soil characteristics in terms of more specific taxonomic classifications that give a more detailed account of soil properties. By contrast, NHC-AF(s) were significantly different with respect to season and ecoregion. In this case, seasonal differences may be influenced by differences in local temperatures from variable frontal movement and localized rainfall from convective storms. It is also worth noting that seasonal variations in temperature and rainfall are

much more likely in the Post Oak Savannah and Blackland Prairie due to their greater north-south extent, especially in the northern reaches of the regions. For example, the majority of foliar NHC-AF(s) were greater at the northernmost collection site in the Blackland Prairie, which may be related to lower seasonal temperatures and subsequent reductions in evapotranspiration rates. Significant interactions between species\*season and species\*ecoregion are likely related to physiologic and life cycle differences among species and their respective response to changes in rainfall, temperature, photoperiod, and edaphic conditions. Chinese tallow wood was also significantly different relative to season and ecoregion, but post hoc testing revealed a nonsignificant difference between the Post Oak Savannah and Blackland Prairie. These seasonal and regional similarities may be related to their persistence in smaller riparian systems that exhibit similar soil diversity and flooding regimes as opposed to more extensive bottomland systems in the Pineywoods that tend to flood more frequently and with greater duration.

#### Oxidative Thermogravimetric Analysis

Foliar and wood RSIT(s) were significantly different with respect to species, season, and ecoregion; however, data was highly variable for many species, making it challenging to discern trends in RSIT. High RSIT variability associated with some species maybe be related to the superposition of



hemicellulose and lignin devolatilization that occurs from 200-350°C and 200-450° C, respectively (Collard and Blin 2014). Species with significant differences in hemicellulose and lignin composition may have presented a challenge identifying appropriate tangential points to base RSIT onset temperatures from due to several inflection points presented on the second DTG peak ranging from ~ 150°C - 320°C. In addition to high variability, species foliar and wood RSIT's were weakly related to proximate analysis data.

Yaupon and Chinese privet unexpectedly produced greater dormant season RSIT(s), indicating greater ignitability. Differences in yaupon RSIT's were much more pronounced in the Post Oak Savannah and Blackland Prairie, which also coincided with significant reductions in dormant season ash%. In this case, yaupons slowed dormant season growth may have resulted in reduced foliar ash% by a potential shift in the translocation of inorganic nutrients from foliar to meristematic tissue (Monti et al. 2008). Chinese privets' greater dormant season RSIT may indicate continued dormant season growth with sustained primary and secondary cell wall development (Cosgrove 1997, Alonso et al. 2012). Greenbrier also exhibited a significant increase in growing season RSIT, which may be related to an increase in seasonal growth as well.

Chinese tallow wood produced significantly greater growing season RSIT(s), which correlated well with a respective increase and decrease in VM% and ash% in

the Pineywoods and Blackland Prairie. Chinese tallow wood in the Post Oak Savannah growing season yielded the greatest RSIT, but growing season VM% and ash% did not correspond with the high RSIT estimate. Despite high seasonal and regional RSIT variability associated with Chinese tallow wood, a significant difference in growing season RSIT still remains, which suggests that Chinese tallow wood is significantly more ignitable in the growing season. Greater growing season ignitability may aid in integrated control efforts using prescribed fire to burn masticated wood residue generated in the growing season. Southern red oak wood produced a significantly greater mean dormant season RSIT, but no correlations with VM% and ash% were noted that supported this significant increase in RSIT; therefore, the difference in southern red oaks' seasonal wood RSIT(s) remain unclear.

As expected, all species foliar GP-MMLR(s) were greater in the growing season, with the exception of Pineywoods yaupon. Eastern red cedar and escarpment live oak were not significantly different and consistently produced the greatest GP-MMLR(s) relative to season and region. Escarpment live oaks' high foliar combustibility was unexpected, and may lead to greater fire intensity in grassland ecosystems where young stands may be more susceptible to torching and crown fire initiation depending on stand density, spatial arrangement, and crown height. Seasonal GP-MMLR(s) for yaupon, Chinese privet, and eastern red

cedar did not produce large variations in GP-MMLR, which may be related to their evergreen characteristics and similarities in stand-level competition given their common occurrence in dense understory stands and thickets. Greenbrier on the other hand, yielded a significantly greater growing season GP-MMLR, especially in the Pineywoods. Significant increases in growing season GP-MMLR for Pineywoods greenbrier is likely related to increased growth with a concurrent increase in VM%. Further differences in greenbriers' combustibility may also be related to greenbriers semi-evergreen traits that lead to slowed dormant season growth and a subsequent drop in bound inter-molecular water. Chinese privet and Chinese tallow both yielded the least combustible foliage evidenced by their low GP-MMLR(s). Chinese tallow has already been linked to suppressing the fire cycle in fire-dependent ecosystems (Pile et al. 2017), and the very low foliar combustibility in this study provides further evidence of Chinese tallows' resistance to fire, especially in mature stands. By contrast, Chinese privet likely requires repeated prescribed fire treatments of moderate intensity in order to gain any appreciable control (Faulkner et al. 1989, Caspary and Affolter 2012). Any efforts to control Chinese privet resprouting may be better served with the integrated use of herbicides and prescribed fire because multiple prescribed fire treatments may lack the necessary fuels to carry fire, as well as the capacity to generate sufficient fire

intensity required to effectively control Chinese privet given its low foliar combustibility.

Chinese tallow wood yielded significantly greater growing season GP-MMLR(s) in the Post Oak Savannah and Blackland Prairie, and were consistent with concomitant increases in growing season VM%. This significant shift in growing season wood combustibility may be related to a shift in the translocation of non-structural carbohydrates necessary to support late growing season seed development of highly lipid-rich seeds (Picou and Bolder 2012, Pile et al. 2017). Picou and Bolder (2012) reported that Chinese tallow seeds can contain >50% lipids by mass, making them a good candidate for biofuel production given their prolific seeding characteristics. It seems reasonable that a significant shift in the translocation of non-structural carbohydrates is likely during late summer seed development for Chinese tallow. The lower growing season GP-MMLR for Chinese tallow wood in the Post Oak Savannah may be associated with less productive Inceptisol soils as compared to the more productive Alfisol and Mollisol soils (Brady and Weil 2008) associated with the Pineywoods and Blackland Prairie sites. As previously mentioned, greater growing season Chinese tallow wood combustibility may aid in the burning of masticated wood residue, but further analysis is required to confirm that larger diameter bole wood is equally as combustible as small diameter stem wood. In contrast, southern red oak wood yielded a much lower

seasonal GP-MMLR, which may be associated with its greater specific gravity compared to Chinese tallow (Scheld and Cowles 1981, Jenkins et al. 2003). In addition to wood density, southern red oaks' late growing season translocation of non-structural carbohydrates for acorn development is likely much less than Chinese tallow due to a significant reduction in acorn lipid content (22.7% by weight; Short 1976).

GP-CD can be used to measure both combustibility and sustainability when compared with GP-MMLR(s). Species yielding high GP-MMLR(s) in combination with lower GP-CD(s) can be classified as very combustible based on the rapidity of oxidative decomposition. Conversely, species with low GP-MMLR(s) in combination with long GP-CD(s) suggests reduced combustibility and a higher degree of sustainability. Species with high GP-MMLR(s) and GP-CD(s) can indicate both greater degrees of combustibility and sustainability, making fuels more hazardous in terms of sustained heat yield and greater flame residence times. As expected, the majority of species foliar samples produced lower growing season GP-CD(s) that correlated with corresponding higher GP-MMLR(s), confirming greater degrees of combustibility. Dormant season yaupon and Chinese privet in the Post Oak Savannah and Blackland Prairie produced lower GP-CD(s), possibly indicating greater dormant season combustibility. Greenbrier exhibited the greatest growing

season shift in combustibility by yielding the lowest GP-CD(s) combined with high GP-MMLR(s). As previously mentioned, greenbriers' high growing season combustibility could lead to greater amounts of overstory crown scorch when conducting early growing season prescribed burns in forest stands with high densities of greenbrier extending into the midstory strata. The majority of species exhibited similar GP-CD(s) across ecoregions, with the exception of Post Oak Savannah yaupon and Pineywoods eastern red cedar, which produced significantly lower GP-CD(s). In this case, the reduction in GP-CD for yaupon and eastern red cedar is likely related to their high GP-MMLR(s). It is also worth noting that the majority of species GP-CD(s) did not correlate with mean VM% and ash% values.

In terms of high GP-CD(s) relative to sustainability estimates, yaupon and eastern red cedar exhibited the greatest combined values for GP-CD and GP-MMLR, translating into a higher degree of overall flammability. Conversely, Chinese privets' high GP-CD, combined with its low GP-MMLR, is likely a reflection of lower combustibility as opposed to greater sustainability due to its significantly reduced oxidative decomposition rate. The combination of Chinese privets' decreased GP-MMLR and increased GP-CD would still likely produce a less effective PHRR for a longer duration, limiting the amount of heat intensity generated during peak gas-phase combustion. The PHRR associated with GP-MMLR and the latter portion of GP-CD are likely key determinants for increased fire intensity given the large

amounts of heat release within this temperature range from all three biopolymers, especially cellulose (Yang et al. 2007, Dorez et al. 2014). In the case of yaupon and eastern red cedar, anecdotal observations of appreciable fire intensity align well with corresponding GP-CD and GP-MMLR data. In addition to yaupon and eastern red cedar, growing season greenbrier also yielded high GP-MMLR(s) in combination with fairly high GP-CD(s), possibly leading to similar increases in fire intensity. Subsequent post hoc testing revealed nonsignificant pairwise differences between eastern red cedar and escarpment live oak for GP-MMLR, and greenbrier and eastern red cedar for GP-CD. Although escarpment live oak exhibits a similar GP-MMLR as eastern red cedar, it is unlikely to produce the same PHRR as eastern red cedar due to its significantly lower GP-CD. On the other hand, greenbriers' high growing season GP-MMLR and GP-CD seems more likely to yield and increase in fire intensity due to accelerated decomposition rates over a longer duration. Given the potential for greenbriers increased growing season flammability, care should be taken while conducting prescribed burns in late spring to early summer. Additionally, escarpment live oaks' potential for a high intensity, shorter duration PHRR should not be discounted, especially in dense stands with a continuous mixed fuel bed of shrubs and grasses.

Chinese tallow wood consistently produced greater growing season GP-MMLR(s) and low GP-CD(s), indicating greater growing season combustibility. The

Blackland Prairie yielded the greatest growing season GP-MMLR for Chinese tallow wood, which may be possibly be related to greater growth associated with a more fertile Mollisol soil. Collectively, Chinese tallow wood exhibited considerable regional variability in terms of GP-MMLR and GP-CD. This variability may be linked to differences in soil properties and flood regimes associated with the riparian and bottomland systems where samples were collected. By contrast, southern red oak produced a significantly lower growing season GP-MMLR as compared to Chinese tallow wood, likely resulting in a lower combustion rate. However, dormant season southern red oak wood GP-MMLR(s) were similar to Chinese tallow, and differed only slightly from the growing season. Both GP-MMLR and GP-CD for southern red oak wood varied only slightly with respect to season, and appears to have very similar seasonal combustibility.

### Thermal Kinetic Analysis

All foliar devolatilization DTG thermograms displayed four distinct peaks (Figure 13) that are consistent with previous studies (Tihay and Gillard 2011, Amini et al. 2019). The four corresponding DTG peaks are consistent with sample dehydration and thermal devolatilization of hemicellulose, cellulose, and lignin. Increasing  $E\alpha$ (s) were consistent with greater degrees of conversion ( $\alpha$ ) associated with increasing bond strengths from the aforementioned biopolymers in conjunction



with any parallel reactions that may have occurred with increasing temperatures (Collard and Blin 2014, Amini et al. 2019). As a result, mean  $E\alpha(s)$  used to estimate GPC and ignition were significantly lower than mean global  $E\alpha(s)$ . Mean global and GPC  $E\alpha(s)$  for Friedman and OFW followed a relatively similar species  $E\alpha$  combustibility trend with respect to season and ecoregion. Though a few species'  $E\alpha(s)$  varied slightly between methods, both model-free kinetic methods appear to be reasonably consistent for evaluating kinetic parameters. All Friedman model-free  $E\alpha(s)$  were consistently greater than OFW model-free  $E\alpha(s)$  which was expected based on previous reports from Tihay and Gillard (2011).

Amini et al. (2019) reported respective mean global  $E\alpha(s)$  of 130.6 and 160.3 KJ mol<sup>-1</sup> for yaupon and live oak using the KAS model-free method. The KAS and OFW model-free methods generally yield similar  $E\alpha$  trends (Tihay and Gilard 2011), but in this study, mean OFW global  $E\alpha(s)$  for yaupon (197.98 KJ mol<sup>-1</sup>) and escarpment live oak (199.55 KJ mol<sup>-1</sup>) were significantly higher. A possible explanation for these large discrepancies may be related to the higher linear heating rate of 40°C min<sup>-1</sup> used in this study. Linear TGA heating rates  $\leq 20^\circ\text{C min}^{-1}$  are generally considered low enough to precisely determine the onset of pyrolytic reactions (Collard and Blin 2014), and the simultaneous devolatilization of hemicellulose, cellulose, and lignin during gas-phase combustion (150-330°C) has

been confirmed by previous works (Collard and Blin 2014). Comparatively, Amini et al. (2019) used linear heating rates of 10, 15, 20, 25, and 30°C min<sup>-1</sup>, whereas this study used linear heating rates of 10, 25, and 40°C min<sup>-1</sup> to simulate fast pyrolysis. As a result, the increased linear heating rate of 40 °C min<sup>-1</sup> may have forced pyrolytic reactions to occur at higher temperatures (Figure 13), potentially increasing  $E\alpha(s)$  across all conversions ( $\alpha$ ), especially within the 0.40-0.80  $\alpha$  range (Tables 13-14). The generation of higher  $E\alpha(s)$  may also be linked to accelerated depolymerization of the three primary biopolymers, which may have led to the recondensation (parallel reactions) of volatile compounds to higher molecular weight molecules such as secondary char (Collard and Blin 2014). In addition to higher heating rates, the greater sample mass of ~20 mg used in this study may have also led to differences in heat and mass transfer as compared to Amini et al. (2019), who used a sample mass of 6 mg.

The majority of species mean foliar Friedman and OFW global  $E\alpha(s)$  generally trended lower in the growing season, with the exception of greenbrier. Chinese privet unexpectedly produced the lowest mean global  $E\alpha$  among species, indicating potentially high combustibility, which is inversely related to its low oxidative TGA combustibility exhibiting a low mean GP-MMLR and VM%. Chinese privets' significant drop in global  $E\alpha$  remains unclear; however, lower proportions of

bound inter-molecular water associated with the primary cell wall (hemicellulose) may explain the significant drop in  $E\alpha$  given the greater amount of energy required to dehydrate water molecules. For example, hemicellulose constitutes the primary biopolymer associated with GPC, but it contains more water (20-30%) than cellulose and lignin (5-15%) (Collard and Blin 2014). Hemicellulose dehydration becomes significant at 200°C, while cellulose dehydration peaks between 260-300°C (Collard and Blin 2014), meaning peak dehydration can occur throughout the range of GPC. Visualization of this potential trend can easily be seen by examining the seasonal DTG thermogram of yaupon and Chinese privet within the 150-280°C range (Figure 17); note the increasing distance between the DTG curves. This subsequent increase in yaupons' early onset devolatilization temperature may indicate a greater degree of bound inter-molecular water during the growing season compared to the dormant season. Another possible explanation for Chinese privets' lower composite  $E\alpha(s)$  compared to yaupon, is its significantly thinner leaves. Previous studies have reported leaf thickness as having a damping effect on ignitability and a synergistic effect on sustainability (Grootemaat et al. 2017, Ganteaume 2018), which is consistent with yaupons' thicker leaves, higher composite  $E\alpha(s)$ , and greater GP-CD(s). It is also worth noting, that Chinese privet had the thinnest leaves of all the evergreen species in this study.

Post Oak Savannah greenbrier and eastern red cedar also exhibited similar seasonal MMLR thermograms and  $E\alpha(s)$ , but greenbrier differed significantly relative to season (Figure 18). Although greenbriers' GPC  $E\alpha$  is slightly lower in dormant season, its lower growing season MMLR endset temperature and significantly greater MMLR suggest much greater growing season combustibility, meaning small variations in GPC  $E\alpha(s)$  may be limited as a primary determinant of combustibility estimates. Greenbriers' secondary growing season DTG peak occurring from 150-190°C (Figure 18) may indicate the devolatilization of a greater concentration of low molecular weight volatiles. A similar trend can be visualized when comparing growing season southern red oak and escarpment live oak, but with much less pronounced secondary peaks occurring in the 130-200°C range (Figure 21). Alternatively, Chinese tallow can be easily visualized as the least combustible foliage compared to the oak species (Figure 21), yet it correlates well with the ascribed GPC  $E\alpha$  combustibility order. Dorez et al. (2014) conducted a HRR test for xylan (hemicellulose), cellulose, and lignin in a pyrolysis combustion flow calorimeter, and found that xylan yielded two HRR peaks at 250°C (34  $Wg^{-1}$ ) and 300°C (48  $Wg^{-1}$ ), cellulose HRR peaked at 370°C (141  $Wg^{-1}$ ), and lignin HRR peak at 350°C (36  $Wg^{-1}$ ). The combination of increased volatile and hemicellulose production in the growing season may slightly dampen the rapidity of devolatilization in the 150-200°C range by requiring greater  $E\alpha(s)$  to overcome the

initial dehydration of greater amounts bound inter-molecular water associated with increased primary cell wall growth and hemicellulose production. Yet when this initial  $E\alpha$  is reached within this range, a much greater devolatilization rate of all biopolymers occurs, which may be the case for Post Savannah greenbrier (Figure 18).

Mean seasonal global  $E\alpha(s)$  displayed considerable variability, and no significant seasonal relationships were noted. However, the majority of mean foliar GPC  $E\alpha(s)$  were lower in the dormant season using both kinetic methods, with the exception of Chinese privet. This general trend may also be related to a decrease in bound inter-molecular water caused by a reduction in primary cell wall growth during the dormant season (Cosgrove 1997, Alonso et al. 2012). Chinese privets' lower growing season  $E\alpha$  trends align well with greater GP-MMLR(s), but  $E\alpha$  and GP-MMLR values in the Post Oak Savannah and Blackland Prairie varied slightly, and may be related to sample testing variation. Pineywoods greenbrier exhibited the greatest growing season shift to greater mean global and GPC  $E\alpha(s)$ , which was inversely related to corresponding mean devolatilization and oxidative MMLR(s). This seasonal shift was similar to Post Oak Savannah greenbrier (Figure 18), which displayed a significant growing season peak between the 150-200°C range where low molecular weight volatiles are generally decomposed. The

potential increase in growing season volatiles was likely accompanied by an increase in primary cell wall development and subsequent hemicellulose production. Since hemicellulose is the primary biopolymer that contains the greatest proportion of water (Collard and Blin 2014), subsequent increases in growing season hemicellulose water content may require a greater  $E\alpha$  to overcome the dehydration of bound inter-molecular water. When this reaction is sped up in an oxidative environment, the addition of volatile vapors may possibly facilitate ignition and the necessary  $E\alpha$  to catalyze rapid combustion. Higher temperatures required to dehydrate bound inter-molecular water during early onset  $E\alpha(s)$  may therefore lead to greater combustion and sustainability rates in some species due to increased production of low molecular weight volatiles and hemicellulose during peak growing conditions.

Mean global and GPC  $E\alpha$  trends displayed considerable variability relative to ecoregion, though some trends were noted in Post Oak Savannah and Blackland Prairie. Specifically, eastern red cedar and Chinese tallow foliage in the Blackland Prairie consistently produced the lowest regional global and GPC  $E\alpha(s)$  in combination with greater GP-MMLR(s). Escarpment live oak in the Post Oak Savannah also produced the same trend. Reasons for regional differences associated with eastern red cedar are unclear, given precipitation was not severely

limited and all samples were collected on Alfisol soils with similar stand density across all ecoregions. Variations in escarpment live oak and Chinese tallow combustibility may have been influenced by edaphic changes across ecoregions. For example, escarpment live oak was sampled on Alfisol and Inceptisol soils in the Post Oak Savannah and Blackland Prairie, respectively. Since Alfisol soils are generally more productive than Inceptisol soils (Brady and Weil 2008), escarpment live oak in the Post Oak Savannah may have benefited from improved growth. Similarly, Chinese tallow was collected on three different soil orders across ecoregions: Alfisols-Pineywoods, Inceptisols-Post Oak Savannah, and Mollisols-Blackland Prairie. Chinese tallows' greatest foliar combustibility was associated with the Blackland Prairie, which correlates with Mollisol soils greater productivity (Brady and Weil 2008).

Global and GPC  $E\alpha(s)$  for Chinese tallow wood displayed considerable variability relative to season and ecoregion, with the Post Oak Savannah and Blackland Prairie producing the greatest seasonal  $E\alpha$  variability. As previously mentioned, differences in regional soil orders and rainfall may explain some of the variation. Seasonal and regional DTG thermograms for Chinese tallow wood displayed a clear trend of greater growing season combustibility (Figure 19), but showed no correlation with lower GPC  $E\alpha(s)$ . Differences in growing season

devolatilization MMLR(s) and GPC  $E\alpha(s)$  for Post Oak Savannah and Blackland Prairie Chinese tallow may have been more readily influenced by soil productivity (Table 2) rather than soil moisture, given the above normal precipitation within both ecoregions. Southern red oaks' seasonal DTG thermograms were relatively similar to Chinese tallow in terms of peak onset temperatures (Figures 20), but produced considerably lower decomposition rates throughout the low to intermediate temperature range, leading to considerably lower devolatilization MMLR(s) that were consistent with greater composite GPC  $E\alpha(s)$ . These contrasting thermal properties may potentially be linked to differences in wood density (Scheld and Cowles 1981, Jenkins et al. 2003) and translocation of non-structural carbohydrates (Short 1976, Picou and Boldor 2012).

Chinese privet unexpectedly produced the lowest foliar ignition  $E\alpha(s)$  of all species, while yaupon produced some of the greatest ignition  $E\alpha(s)$  and was among some of the least ignitable species, which is contrary to general flammability characterizations (Long et al. 2006, Wimberly et al. 2008) and anecdotal accounts attesting to its flammability. Although Chinese privet appears to be more ignitable, yaupon clearly exhibits greater combustibility as evidenced by its seasonal devolatilization and oxidative GP-MMLR(s) (Figures 15-17). The combination of yaupons' high combustibility metrics and NHC-AF values likely contribute to its high



flammability hazard classification. In general, Chinese privet, greenbrier, and eastern red cedar all shared similar dormant season ignitability, but differed considerably in the growing season. Increasing growing season ignition  $E\alpha(s)$  for greenbrier appeared to be linked to greater low molecular weight volatile production as evidenced by the dramatic shift in the seasonal devolatilization thermogram within the 150-200°C range (Figure 18). In addition to low molecular weight volatiles, potential increases in bound inter-molecular water may further influence seasonal ignition  $E\alpha(s)$  in the early stages of devolatilization. Differences in the first DTG peak and corresponding dehydration temperatures of Post Oak Savannah yaupon and Chinese privet can be visualized in Figure 17. In terms of overall ignitability, estimates derived from low foliar ignition  $E\alpha(s)$  did not correlate with high RSIT(s) and clearly need more definitive testing.

Southern red oak wood ignitability  $E\alpha(s)$  were relatively consistent with regard to season, and align well with corresponding devolatilization thermograms (Figure 20), which suggests southern red oak ignitability may be less affected by season. Compared to Chinese tallow wood, southern red oak consistently produced greater ignition  $E\alpha(s)$  that were consistent with higher decomposition temperatures depicted in seasonal devolatilization thermograms ranging from 150-250°C (Figure 20). As previously mentioned, contrasting wood  $E\alpha$  ignitability between species

may be related to differences in wood density (Scheld and Cowles 1981, Jenkins et al. 2003). With the exception of the Pineywoods, Chinese tallow wood produced significantly lower dormant season ignition  $E\alpha(s)$  that were consistent with corresponding devolatilization thermograms (Figure 19). This trend suggests that Chinese tallow is more ignitable in the dormant season, but significantly more combustible in the growing season based on much greater MMLR(s) associated with devolatilization. Similar to foliar ignitability, wood ignitability may also be influenced by seasonal reductions in bound inter-molecular water. In this case, the cessation of growth associated with the dormant season may have resulted in lower cambial tissue water content leading to greater ignitability. Pineywoods Chinese tallow was recovering from a prolonged drought at the time of collection in 2013, possibly explaining the flat devolatilization curves in the 150-250°C range compared to the Post Oak Savannah and Blackland Prairie (Figure19), which had ample soil moisture at the time of collection. Chinese tallow may possibly present a unique fire management decision based on whether to exploit ignitability or combustibility characteristics; however, further bench-scale and large-scale testing is required to validate this potential thermal characteristic.

Though Chinese tallow wood appears to have significant growing season combustibility, an important question remains: does smaller diameter stem wood transfer similar flammability properties to increasing branch and bole diameters?

Nhuchhen and Salam (2012) reported similar GHC(s) for small (19.20 MJ kg<sup>-1</sup>), medium (19.24 MJ kg<sup>-1</sup>), and large (19.17 MJ/kg) oak branches, but proximate analysis values for small branch wood were 4.3% lower in VM%, 2.32% higher in FC%, and ~ 1-2% higher in ash% as compared to medium and large branches. These relatively small changes in proximate analysis values may suggest that the flammability properties of small diameter wood may be transferable to large diameter branch and bole wood that has been masticated to a finer fuel particle size. Further flammability testing will be required to elucidate any potential diameter-specific wood flammability trends.

The majority of species seasonal foliar ignition  $E\alpha(s)$  tended to be lower in the dormant season, with the exception of Chinese privet and eastern red cedar. Contrasting seasonal changes in ignitability can be easily visualized in the devolatilization thermograms for Chinese privet and greenbrier throughout the 120-200°C range (Figures 17-18). These differences are likely associated with variations in low molecular weight volatiles, bound inter-molecular water, and leaf thickness (Collard and Blin 2014, Popovic et al. 2021). Based on ignition  $E\alpha(s)$  and devolatilization thermograms (120-200°C) for yaupon and eastern red cedar, it appears that eastern red cedar retains a relatively similar ignitability, whereas yaupon and greenbrier exhibit significant shifts in seasonal ignitability. In this case,

yaupons' greater dormant season ignitability combined with relatively minor changes in devolatilization and oxidative MMLR(s) suggest that yaupon may be more flammable in the dormant season. Greenbrier exhibits lower growing season ignitability, but exhibits significantly greater growing season combustibility, likely translating into greater growing season fire intensity. Escarpment live oak also exhibits greater dormant season ignitability with a negligible difference in seasonal MMLR(s), following a similar trend as yaupon, with a potentially greater dormant season flammability. Collectively, all species produced a mixed seasonal trend of ignitability that warrants further testing, specifically the combined use of STA and cone calorimetry, where visually confirmed ignitability can be linked to TGA and DTA data.

The majority of mean foliar ignition  $E\alpha(s)$  trended lower in the Post Oak Savannah, while the Blackland Prairie produced the second lowest ignition  $E\alpha$  results. Interestingly, there were three species that shifted to different ecoregions between the two kinetic model-free methods. These subsequent shifts in species ignition  $E\alpha(s)$  may be related to greater sensitivity of species-specific thermal decomposition behavior derived from the Friedman model-free method. Tihay and Gillard (2011) reported positive results using the Friedman model-free method, specifically their  $E\alpha$  results were highly correlated ( $R^2$  97.8-98.8%) with their

respective devolatilization thermograms spanning the 0.10-0.90  $\alpha$  range, indicating good representation of species-specific thermal properties. Alternatively, Tihay and Gillard (2011) reported more uniform, linear  $E\alpha$  distributions associated with the OFW and KAS model-free methods across the 0.10-0.90  $\alpha$  range. Regardless of kinetic method, the Post Oak Savannah generally produced the lowest regional ignition  $E\alpha(s)$  for yaupon, Chinese privet, and greenbrier. These three species were also collected on Alfisol soils and at the same time in the Blackland Prairie during the 2016 dormant and growing season, which produced above normal rainfall and maximum temperatures for both seasons; however, dormant season maximum temperatures were 0.7°C and 1.7°C above normal in the Blackland Prairie and Post Oak Savannah, respectively. Additionally, respective 10-year averaged maximum temperatures (normal) in the Post Oak Savannah were 2.0°C and 0.7°C higher in the dormant and growing season compared to the Blackland Prairie. Based on these species' evergreen characteristics, the Post Oak Savannahs' general trend of greater seasonal maximum temperatures may be related to changes in plant thermal behavior due to differences in evapotranspiration and growth between ecoregions.

## CONCLUSIONS AND MANAGEMENT IMPLICATIONS

### Oxygen Bomb Calorimetry

NHC-AF values significantly differed with respect to season and ecoregion; yaupon and Chinese privet yielded an expected increase in growing season NHC-AF, but greenbrier and eastern red cedar produced greater dormant season NHC-AF(s). The shift in greenbriers' and eastern red cedars' NHC-AF may be related to extended growing conditions from higher dormant season temperatures and improved access to site resources as deciduous competitors' transition into dormancy. Dormant season ash% was also greater in greenbrier and eastern red cedar, possibly indicating a continuation of growth and assimilation of inorganic nutrients into the dormant season. The Pineywoods ecoregion consistently produced the lowest NHC-AF(s) among ecoregions, with the exception of greenbrier, which may be linked to greater competitive interactions and evapotranspiration rates associated with dense forest cover. Significant interactions among species and season could possibly be linked to variable temperatures and localized rainfall from variances in seasonal frontal movement and the stochastic development of convective storms. By contrast, significant species and ecoregion interactions might be more readily influenced

by the regional precipitation gradient (Figure 2) and more site-specific edaphic characteristics beyond the soil order classification

Chinese privet and Chinese tallow foliage produced the greatest ash% and subsequent NHC-AF ash corrections. Since Chinese privet and Chinese tallow are exotic invasive species, greater ash% may possibly be linked to greater competitive fitness related to sequestering inorganic resources through unique physiological traits as compared to its native competitors. Chinese privets' significant NHC-AF correction ( $\sim 1 \text{ MJ kg}^{-1}$ ) placed it relatively close to yaupons' growing season NHC-AF in the Pineywoods and Post Oak Savannah, which may potentially increase fire intensity in stands infested with Chinese privet.

Conversely, Chinese tallow foliage produced the lowest NHC-AF of all species, and will likely produce low intensity canopy fires if sufficient surface fuels are present. Eastern red cedar and yaupon appear to be year-round hazardous fuels given their high seasonal NHC-AF(S) and GP-MMLR(s). Greenbrier produced greater dormant season NHC-AF(s), though GP-MMLR(s) were significantly greater in the growing season, and will likely contribute more to fire intensity and become problematic in overgrown stands where vines serve as ladder fuels. All broad leaf tree species shared similar growing season NHC-AF(S), but escarpment live oak produced some of the greatest GP-MMLR(s), and will likely yield the greatest fire intensity. Escarpment live oaks' high NHC-AF and GP-

MMLR may lead to greater fire intensity in stands where sufficient ladder fuels are present, as well as increased spot fire potential from convectively entrained burning foliage.

The majority of species NHC-AF(s) were well below the standard heat content ( $18.61 \text{ MJ kg}^{-1}$ ) used in common fire models, with the exception of yaupon and eastern red cedar, and will likely result in an under-prediction of fire behavior in mixed stands. Subsequent predictions could result in reduced prescribed fire effectiveness and combustion efficiency. Reductions in combustion efficiency can lead to greater emissions of carbon monoxide, particulate matter, and other toxic compounds that can significantly impact air quality in sensitive airsheds. As hazardous fuels management issues continue to be problematic in suburban and urban areas, fire managers will require accurate fire behavior, smoke management, and emissions predictions to support prescribed fire programs.

#### Oxidative Thermogravimetric Analysis

Foliar and wood RSIT(s) were difficult to determine between some species due to significant shifts associated with second DTG thermogram peaks. These subsequent shifts added a level of complexity in placing tangential points used to estimate onset temperatures for RSIT. Peak variability among second DTG



thermograms is unclear, but may be related to variations in bound inter-molecular water, low molecular weight volatiles, proportions of hemicellulose (xylan) and lignin, and leaf age or location on the plant, or any combination thereof. Leaf age would likely be more applicable to evergreen shrubs like yaupon and Chinese privet, while leaf location would likely be linked to deciduous trees in terms of shade and sun leaves. Some species RSIT(s) were loosely correlated with variations in ash%, which suggests ignitability may be linked to variations in seasonal growth, as well as localized precipitation and site-specific edaphic characteristics associated with each ecoregion. In general, the majority of species exhibited slight variations in seasonal and regional RSIT ignitability, with the exception of yaupon, greenbrier, and Chinese tallow wood, which exhibited significant changes in seasonal ignitability. Specifically, yaupon exhibited greater dormant season ignitability and greenbrier and Chinese tallow wood exhibited greater growing season ignitability.

The methodology for assigning greater ignitability to species with higher RSIT(s) was inversely related to  $E\alpha$  ignitability ( $<E\alpha$ ). Despite this inverse relationship, greater RSIT(s) were highly correlated with species exhibiting the greatest combustibility based on greater GP-MMLR(s). Conversely, species with the least ignitability ( $<RSIT$ ) were also the least combustible ( $<GP-MMLR$ ) when

tested in an oxidative atmosphere. Yet in an inert atmosphere,  $E\alpha$  ignitability was greater ( $<E\alpha$ ) for the least ignitable species tested under oxidative conditions. Though some species shared similar ignitability, there was a clear discrepancy between some species, especially yaupon and Chinese privet. Therefore, based on the mixed results in this study, further testing will be required to determine the efficacy of using TGA to estimate plant ignitability.

Foliar GP-MMLR(s) were all significantly higher in the growing season, indicating greater combustibility and potential for increased fire intensity. Yaupon, eastern red cedar, greenbrier, and escarpment live oak all yielded high growing season GP-MMLR(s). Some species also exhibited significant differences in regional GP-MMLR(s), with the Blackland Prairie generally producing the most species with the greatest seasonal GP-MMLR(s). Regional differences in GP-MMLR(s) remain unclear, while seasonal differences appear to be linked to greater seasonal growth. Notably, Chinese tallow foliage produced the lowest GP-MMLR, indicating low combustibility and confirming its low flammability that can suppress the fire cycle in fire-dependent ecosystems (Pile et al. 2017). Chinese privet produced the lowest seasonal GP-MMLR(s), but its low GPC  $E\alpha$ (s) may indicate greater combustibility that may potentially increase fire intensity, making it a good candidate for prescribed burning given sufficient

herbaceous fuel loading. Chinese tallow wood exhibited significantly greater growing season GP-MMLR(s), which may facilitate the burning of masticated wood if larger diameter wood displays the same thermal behavior as small diameter stem wood; however, further testing is required.

GP-CD can be a measure of combustibility and sustainability, dependent on the combination of values. In general, highly combustible biomass will exhibit high GP-MMLR(s) combined with lower GP-CD(s), signifying rapid combustion, while low combustibility materials exhibit the opposite trend. In some cases, biomass will yield high values for both GP-MMLR and GP-CD, indicating a highly combustible and sustainable fuel that is likely to substantially increase fire intensity. Eastern red cedar consistently exhibited high GP-MMLR(s) and GP-CD(s), potentially making it one of the most hazardous fuels. Yaupon and dormant season escarpment live oak also produced high GP-MMLR(s) and GP-CD(s) that may result in increased fire intensity, especially when mixed with eastern red cedar. Chinese tallow wood produced high growing season GP-MMLR(s) that are commensurate with low GP-CD(s), thus confirming its greater growing season combustibility.

RSIT(s) and GP-MMLR(s) were significantly different with respect to species, season, ecoregion, and all interactions between species, season and

ecoregion (Table 10). These significant differences are highlighted by the consistent production of greater RSIT(s) and GP-MMLR(s) in the Post Oak Savannah and Blackland Prairie, which consequently coincide with significant changes in plant community structure from forest to savannah and prairie ecosystems. As a result, significant differences in the regional rainfall gradient (Figure 2), soil characteristics, and plant community composition and structure likely played a role in individual plant growth and subsequent production of volatile compounds. Seasonal changes in plant growth were likely related to deciduous plant composition (overstory light and dormancy), and may be further affected by variable frontal movement resulting from heterogeneous temperature trends and localized rainfall for the stochastic development of convective storms. The latitudinal extent of the three ecoregions is roughly 3 degrees north, thus minor changes in seasonal photoperiods and the angle of incidence are unlikely to manifest significant differences in plant growth. On the other hand, the latitudinal extent of the ecoregions can be impacted by significant differences in seasonal temperatures and rainfall, with the northern extent of the ecoregions generally experiencing lower winter temperatures, while the southern extent generally receives more rainfall due to its closer proximity to the Gulf where moisture laden warm fronts are more likely to generate greater rainfall totals.

## Thermal Kinetic Analysis

Foliar devolatilization thermograms yielded four distinct peaks corresponding with sample dehydration and the devolatilization of hemicellulose, cellulose, and lignin. Subsequent  $E\alpha$  results were significantly higher than comparable  $E\alpha(s)$  for yaupon and southern live oak in a recent study by Amini et al. (2019). Two possible explanations for these  $E\alpha$  differences may include: 1) an increase in sample size of roughly ~14 mg may have led to differences in heat and mass transfer (Yang et al. 2007) and 2) the higher linear heating rate of 40°C min<sup>-1</sup> may have caused accelerated depolymerization of key biopolymers, possibly leading to the formation of less flammable secondary chars culminating from parallel recondensation reactions (Collard and Blin 2014). Nevertheless, corresponding species  $E\alpha(s)$  correlated well with devolatilization temperatures depicted in DTG thermograms. Species combustibility orders generally correlated well with Friedman and OPW Global and GPC  $E\alpha(s)$  since estimates were based on devolatilization MMLR(s) within each species global conversion ( $\alpha$ ) range. There were some minor differences in some species global and GPC  $E\alpha$  combustibility orders relative to Friedman and OFW model-free methods. These differences may be related to Friedman's greater sensitivity to species-specific  $E\alpha$  changes by using the differential method to define the conversion rate ( $\alpha$ ) as

opposed to OFW's approximation of the temperature integral (Tihay and Gillard 2011).

Mean foliar global  $E\alpha(s)$  exhibited considerable variability, but as expected, the majority species generally produced lower growing season  $E\alpha(s)$ . Chinese privet unexpectedly produced conflicting combustibility results related to producing the lowest global and GPC  $E\alpha(s)$  combined with the lowest GP-MMLR(s). Chinese privets' significant change in global and GPC  $E\alpha(s)$  remains unclear, but may be related to leaf thickness (Grootematt et al. 2017, Ganteaume 2018) or lower proportions of bound inter-molecular water associated with hemicellulose that requires less energy to dehydrate throughout the 150-280°C range. In contrast, yaupon unexpectedly produced significantly greater global and GPC  $E\alpha(s)$ , yet it produced some of the greatest devolatilization and oxidative MMLR(s) that indicate high combustibility. Based on yaupons' well-known flammability characteristics from anecdotal accounts, yaupon likely has greater amounts of volatile waxes on its leaf cuticle that contribute to its flammability, as well as a natural adaptation to preserve non-stomatal water loss. As such, yaupon may contain more hemicellulose water content and low molecular weight volatiles compared to Chinese privet, which may require more energy to dehydrate greater concentrations of bound inter-molecular water and

volatile waxes as compared to Chinese privet. Yaupons' subsequent increase in  $E\alpha(s)$  at lower conversions ( $\alpha$ ) may potentially catalyze a significant increase in hemicellulose devolatilization, possibly triggering a greater proportion of cellulose devolatilization at the MMLR, which is associated with the greatest heat release of all biopolymers.

Mean GPC  $E\alpha(s)$  exhibited the opposite seasonal trend as global  $E\alpha(s)$ , with the majority of species producing greater dormant season combustibility. This trend may be related to slowed dormant season growth and the subsequent decline in hemicellulose water content leading to less energy required for dehydration of bound inter-molecular water. Regionally, the Post Oak Savannah and Blackland Prairie generally produced the lowest global and GPC  $E\alpha(s)$ , which may be related to reduced evapotranspiration and competitive interactions from reduced forest overstory and midstory density, or regional variations in soil properties. Chinese privet, eastern red cedar, and greenbrier consistently produced the lowest seasonal GPC  $E\alpha(s)$  indicating high combustibility, especially for eastern red cedar and growing season greenbrier due to their high GP-MMLR(s). Chinese tallow yielded the lowest foliar combustibility and produced mixed seasonal wood combustibility, but generally produced lower GPC  $E\alpha(s)$  than southern red oak wood.

The majority of species foliar  $E\alpha(s)$  exhibited greater dormant season ignitability, potentially expanding prescribed burning opportunities throughout the dormant season. The Post Oak Savannah and Blackland Prairie generally produced greater species ignitability, which may facilitate greater year-round prescribed burning opportunities, as well as increase wildfire risk during seasonal dry periods. Chinese privet, eastern red cedar, and greenbrier exhibited the greatest seasonal ignitability, and may potentially accelerate fire spread and increase fire intensity. Chinese tallow wood produced mixed seasonal ignitability, but based on greater growing season combustibility, integrated control measures using prescribed fire will likely be more effective in the growing season.

Unexpectedly, mean seasonal ignitability  $E\alpha(s)$  were inversely related to greater RSIT(s). Chinese privet was the most ignitable species, yet it was the least combustible in terms of oxidative and devolatilization MMLR(s). Further examination of devolatilization thermogram MMLR(s) revealed a decreasing ignitability  $E\alpha$  trend ( $>E\alpha$ ) for the most combustible species, which is contrary to general flammability characteristics. To validate these differences and gain a clearer perspective into ignitability estimates using TGA, further bench-scale testing using the cone calorimeter or other combustion apparatus will be required



to visually confirm time to autoignition, as well as the corresponding ignition temperature.

### Management Implications

Yaupon is an aggressive, evergreen shrub native to East Texas ecoregions, and is capable of forming dense thickets, especially in the Pineywoods and Post Oak Savannah. Yaupon has been widely accepted as a highly flammable shrub and is generally not recommended for ornamental cultivation where high value infrastructure is intermixed in fire-prone ecosystems, particularly within the HIZ and defensible space zone. Though this study suggests yaupon has a lower degree of ignitability, its combustibility, sustainability, and heat content estimates were among some the greatest in the study, thereby confirming many reports attesting to its propensity to significantly increase fire intensity. Yaupon is commonly targeted for competition control in pine plantations and brush control in rangeland ecosystems to improve livestock forage. Aside from these control efforts and its high hazard classification in ornamental landscapes, yaupon generally does not need to be eradicated, and can be easily maintained with frequent prescribed burns at 1-3 year intervals. Frequent burning reduces shrub density and understory fire intensity, while providing flushes of new foliage that serve as excellent wildlife forage.

Chinese privet is an exotic, invasive, evergreen shrub commonly found in dense thickets where it can suppress native tree and shrub regeneration, as well as increase shrub fuel loading. To the authors knowledge, there has been no quantitative flammability testing done on Chinese privet, but a few studies have reported mixed results when using prescribed fire as a control measure. Flammability estimates in this study suggest Chinese privet may be highly ignitable, with low to moderate combustibility and moderate to high heat content. Although Chinese privets' combustibility appears to be fairly low, its potential high ignitability may serve as an initial catalyst to promote fire spread in mixed shrub stands, possibly leading to increased fire intensity and accelerated fire spread in dry, windy conditions. It is also worth noting Chinese privet produced the second and third greatest growing season heat contents in the Post Oak Savannah and Blackland Prairie, respectively, which may increase fire intensity. Based on these results, Chinese privet may be more receptive to control with prescribed fire in the Post Oak Savannah and Blackland Prairie where more contiguous herbaceous fuels are present to carry fire, as opposed to dense forest cover that tends to shade out herbaceous fuels. On the other hand, mixed stands of Chinese privet in the Post Oak Savannah and Blackland Prairie may become more hazardous when allowed to encroach near residential and commercial infrastructure.

Greenbrier is a semi-evergreen vine native to East Texas, and varies in density based on management intensity. In the absence of fire and other control measures, greenbrier can become quite dense and intrude into midstory tree canopies where it can act as a ladder fuel. Greenbrier produced mixed seasonal flammability, with the dormant and growing season yielding high ignitability and combustibility, respectively, while heat content was higher in the dormant season. Similar to yaupon, greenbrier is an excellent wildlife forage, and can be effectively controlled with frequent prescribed burns ranging from 1-3 year intervals. Repeated burning reduces fuel loads and ladder fuels and encourages new flushes of nutritious growth that is easily accessed by wildlife. Alternatively, in unmanaged, fire suppressed lands, greenbrier can increase in density and extend into midstory tree strata, adding to fuel loading and increasing the risk of canopy scorching and crown fire initiation.

Eastern red cedar is native evergreen tree common throughout East Texas, and is effectively managed with prescribed fire. Seasonal flammability estimates for eastern red cedar produced moderate to high ignitability and high combustibility and heat content. Eastern red cedar is generally targeted for control in the Post Oak Savannah and Blackland Prairie for the purpose of brush control and improved forage production for livestock. Dense thickets and mixed stands of eastern red cedar in and near the WUI, particularly in the Post Oak

Savannah and Blackland Prairie where tree densities are generally higher and can increase fire intensity, potentially threatening high value residential and commercial infrastructure. Fortunately, eastern red cedar can be effectively controlled with mechanical treatments in smoke-sensitive areas of the WUI, whereas carefully planned prescribed fires can also be an option.

Escarpment live oak is a native, semi-evergreen tree that can be found in varying densities across the Post Oak Savannah and Blackland Prairie. Greater tree densities are often associated with unmanaged land accompanied with infrequent fire return intervals. Seasonal foliar flammability appears to be of low ignitibility and high combustibility, while heat content is moderate. As escarpment live oaks mature, it is likely they are less susceptible to fire with increased canopy separation from herbaceous and shrub fuels. On the other hand, younger stands may become more susceptible to fire, potentially increasing fire intensity as canopy foliage is exposed to greater heat intensities from herbaceous and shrub fuels. In terms of ornamental vegetation, escarpment live oak is not likely to become problematic if grown in no contiguous horizontal and vertical fuel arrangements.

Chinese tallow is an exotic invasive tree that has expanded its range throughout East Texas, and is often targeted for control in both forest and

grassland ecosystems using a combination of herbicides, prescribed fire, and mechanical treatments. Chinese tallow foliar flammability appears to be of low ignitability and combustibility, which is consistent with previous research findings and its general classification as a fire suppressor as it invades fire-maintained ecosystems, most notably in the Gulf Coast Prairie. However, Chinese tallow wood appears to be very combustible in the growing season, which may warrant further investigation into a new management approach using a combination of mechanical treatments such as mastication and prescribed fire as means to control the seedbank and resprouting.

## LITERATURE CITED

- Absher J.D., Vaske J.J. 2011. The role of trust in residents' fire wise actions. *International Journal of Wildland Fire* 20 (2): 318-325.
- Akahira, T. and Sunrose T. 1971. Joint convention of four electrical institutes. Research report, Chiba Institute of Technology. *Science and Technology* 16: 22-34.
- Alonso, D.M., Wettstein, S.G. and Dumesic, J.A. 2012. Bimetallic catalysts for upgrading of biomass to fuels and chemicals. *Chemical Society Reviews* 41(24): 8075-8098.
- Amini, E., Safdari, M.S., Weise, D.R. and Fletcher, T.H. 2019. Pyrolysis kinetics of live and dead wildland vegetation from the Southern United States. *Journal of Analytical and Applied Pyrolysis* 142: 104613.
- Anderson, H.E. 1970. Forest fuel ignitability. *Fire Technology* 6: 312-319.
- Andreu, A.G., Shea, D., Parresol, B.R., and Ottmar, R.D. 2012. Evaluating fuel complexes for fire hazard mitigation planning in the southeastern United States. *Forest Ecology and Management* 273: 4-16.
- Andrews, P. L. 2007. BehavePlus fire modeling system: past, present, and future. In 'Proceedings of 7th Symposium on Fire and Forest Meteorological Society'. 23-25 October 2007, Bar Harbor, Maine. Boston, MA: American Meteorological Society. 13 p.
- Andrews, P.L. 1986. BEHAVE: Fire prediction and modeling system: Burn subsystem, part 1. USDA Forest Service, Intermountain Forest and Range Experiment Station General Technical Report INT-122. Ogden UT. 20 p.
- Barron, E. 2006. State of the Texas forest. Texas A&M Forest Service. August 2006
- Behm, A.L., Dureyea, M.L., Long, A.J., and Zipper, W.C. 2004. Flammability of native understory species in pine flatwood and hardwood hammock ecosystems and implications for the wildland-urban interface. *International Journal of Wildland Fire* 13: 355-365.

- Behm, A.L., Durey, M.L., Long, A.J., and Zipper, W.C. 2004. Flammability of native understory species in pine flatwood and hardwood hammock ecosystems and implications for the wildland-urban interface. *International Journal of Wildland Fire* 13: 355-365.
- Biagini, E., Barontini, F., and Tognotti, L. 2006. Devolatilization of biomass fuels and biomass components studied by TG/FTIR technique. *Industrial & Engineering Chemistry Research* 45: 4486-4493.
- Blank, R.R., White, R.H., and Ziska, L.H. 2006. Combustion properties of *Bromus tectorum* L.: influence of ecotype and growth under four CO<sub>2</sub> concentrations. *International Journal of Wildland Fire* 15: 227-236.
- Bocock, K.L. 1964. Changes in the amounts of dry matter, nitrogen, carbon and energy in decomposing woodland leaf litter in relation to the activities of the soil fauna. *The Journal of Ecology*: 273-284.
- Bomar, G.W., 1995. Texas weather. University of Texas Press.
- Brady, N.C. and Weil, R.R. 2008. The nature and properties of soils, 14<sup>th</sup> Edition. Upper Saddle River, NJ: Prentice hall.
- Brooks, M.L., D'Antonio, C.M., Richardson, D.M., Grace, J.B., Keeley, J.E., Ditomaso, J.M., Hobbs, R.J., Pellant, M., and Pyke, D. 2004. Effects of invasive alien plants on fire regimes. *Bioscience* 54: 677-687.
- Brooks, M.L. 2008. Plant invasions and fire regimes. *Wildland fire in ecosystems: effects of fire on flora*. USDA Forest Service, Rocky Mountain Research Station, General Technical Publication-42, Fort Collins, Colorado. 33-45.
- Brown, J.K. 2000. Introduction and fire regimes. In: Brown, J.K.; Smith, J.K., editors *Wildland fire in ecosystems: Effects of fire on flora*. Gen. Tech. Rep. RMRS-GTR-42-vol. 2. Ogden, UT: USDA, Forest Service, Rocky Mountain Research Station: 1-8.
- Brown, M.E., Dollimore, D., and Galeway, A.K. 1980. Reactions in the solid state. *Comprehensive Chemical Kinetics* Vol. 22, Elsevier Scientific Publishing Company, Amsterdam, Netherlands. 22: 41-109.

- Burgan, R.E. and Rothermel, R.C. 1984. BEHAVE: fire prediction and modeling system: fuel subsystem. USDA Forest Service, Intermountain Forest and Range Experiment Station General Technical Report INT-167. Ogden, UT. 126 p.
- Burgan, R. E. and Scott, R.A. 1991. Influence of sample processing techniques and seasonal variation on quantities of volatile compounds of gallberry, saw-palmetto, and wax myrtle. *International Journal Wildland Fire* 101: 57-62.
- Burghardt, M. and Riederer, M. 2003. Ecophysiological relevance of cuticular transpiration of deciduous and evergreen plants in relation to stomatal closure and leaf water potential. *Journal of Experimental Botany* 54(389): 1941-1949.
- Cantrell, K., Martin, J., and Ro, K. 2011. Application of thermogravimetric analysis for the proximate analysis of livestock wastes. In *Biofuels*. ASTM International.
- Carey, J.H. 1992. *Quercus falcata*, *Q. pagoda*. In: Fire Effects Information System. USDA, Forest Service, RMRS, Fire Sciences Laboratory. Located at: <https://www.fs.fed.us/database/feis/plants/tree/quefal/all.html> accessed on 12/18/2017.
- Carey, J.H. 1992. *Quercus virginiana*. In: Fire Effects Information System, USDA, Forest Service, RMRS, Fire Sciences Laboratory. Located at: <https://www.fs.fed.us/database/feis/plants/tree/quevir/all.html> accessed on 12/18/2017.
- Carey, J.H. 1994. *Smilax rotundifolia*. In: Fire Effects Information System, USDA, Forest Service, RMRS, Fire Sciences Laboratory. Located at: <https://www.fs.fed.us/database/feis/plants/vine/smirot/all.html> accessed on 12/18/2017.
- Caspary, M. and Affolter, J., 2012. Using prescribed burning to restore granite rock outcrop ecotones in the Piedmont of the southeastern United States. *Ecological Restoration* 30(3): 228-236.



- Carle, D. 2002. Burning questions: America's fight with nature's fire. Greenwood Publishing Group. pp 37-55.
- Chang, R.K., Raghavan, K.S. and Hussain, M.A., 1998. A study on gelatin capsule brittleness: moisture transfer between the capsule shell and its content. *Journal of Pharmaceutical Sciences* 87(5): 556-558.
- Christensen, N.L. 1981. Fire regimes in southeastern ecosystems. USDA Forest Service General Technical Report WO-26: 112-136.
- Chrosciewicz, Z. 1986. Foliar heat content variations in four coniferous tree species of central Alberta. *Canadian Journal of Forest Research* 16(1): 152-157.
- Collard, F.X. and Blin, J., 2014. A review on pyrolysis of biomass constituents: mechanisms and composition of the products obtained from the conversion of cellulose, hemicelluloses and lignin. *Renewable and Sustainable Energy Reviews* 38: 594-608.
- Cosgrove, D.J., 1997. Assembly and enlargement of the primary cell wall in plants. *Annual Review of Cell and Developmental Biology* 13(1):171-201.
- Cosgrove, D.J., 2005. Growth of the plant cell wall. *Nature Reviews Molecular Cell Biology* 6(11): 850-861.
- Daehler, C.C. 2003. Performance comparisons of co-occurring native and alien invasive plants: implications for conservation and restoration. *Annual Review of Ecology, Evolution, and Systematics* 34: 183-211.
- D'Antonio, C.M. and Vitousek, P.M. 1992. Biological invasions by exotic grasses, the grass/fire cycle and global change. *Annual Review of Ecology and Systematics* 23: 63-87.
- D'Antonio C.M., Dudley, T.L., and Mack, M. 1999. Disturbance and biological invasions: direct effects and feedbacks. *Ecosystems of the World 1999*: 413-452.
- Debano, L.F., Neary, D.G., and Ffolliott, P.F. 1998. Fire's effects on ecosystems. New York: John Wiley and Sons.

- Demirbaşı, A. 2003. Relationships between lignin contents and fixed carbon contents of biomass samples. *Energy Conversion and Management* 44(9): 1481-1486.
- Diamond, D.D., and Smeins, F.E. 1993. The native plant communities of the Blackland Prairie. In: M. R. Sharpless and J. C. Yelderman [EDS.]. *The Texas Blackland Prairie: Land, history, and culture*. Waco, TX: Baylor University Press. p 66-68.
- Dibble, A.C., White, R.H., and Lebow, P.K. 2007. Combustion characteristics of north-eastern USA vegetation tested in the cone calorimeter: invasive versus non-invasive plant. *International Journal of Wildland Fire* 16: 426-443.
- Diggs, G.M., Lipscomb, B.L., O'Kennon, R.J., Mahler, W.F. and Shinnars, L.H. 1999. *Shinnars' and Mahler's illustrated flora of North Central Texas*. Fort Worth, TX: Botanical Research Institute of Texas. 1626 p.
- Diggs, G.M., Lipscomb, B.L., Reed, M.D., and O'Kennon, R.J. 2006. *Illustrated flora of East Texas*. SIDA, Botanical Miscellany, No. 26, Botanical Research Institute of Texas & Austin College. 1594 p.
- Diggs, G.M. and Schulze, P.C. 2003. Soil-dependent fire frequency: a new hypothesis for the distribution of prairie and oak woodland/savannas in north central and East Texas. *SIDA, Contributions to Botany* 2003: 1139-1153.
- Dimitrakopoulos, A.P. and Panov, P.I. 2001. Pyric properties of some dominant Mediterranean vegetation species. *International Journal of Wildland Fire* 10(1): 23-27.
- Dorez, G., Ferry, L., Sonnier, R., Taguet, A. and Lopez-Cuesta, J.M. 2014. Effect of cellulose, hemicellulose and lignin contents on pyrolysis and combustion of natural fibers. *Journal of Analytical and Applied Pyrolysis* 107: 323-331.
- Doyle, C.D. 1962. Estimating isothermal life from thermogravimetric data. *Journal of Applied Polymer Science* 6(24): 639-642.

- Eidson, J.A., and F.E. Smeins. 1999. Texas Blackland Prairies. In terrestrial ecoregions of North America: a conservation assessment (Ricketts, T., Dinerstein, E. and Olson, D. editors). Island Press, Washington, DC.
- Elder, T., Kush, J.S., and Hermann, S.M. 2011. Thermogravimetric analysis of forest understory grasses. *Thermochimica Acta* 512: 170-177.
- Enniful, E.K. and Torvi, D.A. 2005. Effects of moisture and incident heat flux on smoke production and heat release rates of vegetation. Presentation at Combustion Institute Canadian Section Spring Technical Meeting, 15 May 2005, Halifax, NS.
- Faulkner, J.L., Clebsch, E.E., and Sanders, W.L. 1989. Use of prescribed burning for managing natural and historic resources in Chickamauga and Chattanooga National Military Park, U.S.A. *Environmental Management* 13: 603-612.
- Finney, M.A. 1998. FARSITE: fire area simulator-model development and evaluation. USDA Forest Service, Rocky Mountain Research Station Research Paper RMRS-RP-4. Ogden, UT. 47 p.
- Flynn, J.H. and Wall, J.H. 1966. General treatment of the thermogravimetry of polymers. *Journal of Research of the National Bureau of Standards* 70: 487-523.
- Friedman, H.L. 1964. Kinetics of thermal degradation of char-forming plastics from thermogravimetry: application to a phenolic plastic. *Journal of Polymer Science Part C: Polymer Symposia* 6: 183-195.
- Frost, C.C. 1993. Four centuries of changing landscape patterns in the longleaf pine ecosystem. In *Proceedings of the Tall Timbers fire ecology conference* 18: 17-43.
- Frost, C.C., 1998. Presettlement fire frequency regimes of the United States: a first approximation. In *Fire in ecosystem management: shifting the paradigm from suppression to prescription*. Tall Timbers Fire Ecology Conference Proceedings 20: 70-81.

- Frost, C.C. 2006. History and future of the longleaf pine ecosystem. The longleaf pine ecosystem. Springer New York, 2006. pp 9-48.
- Frost, C., 2007. History and future of the longleaf pine ecosystem. In The longleaf pine ecosystem. Springer New York. pp. 9-48.
- Gan, J., Miller, J. H., Wang, H., and Taylor, J. W. 2009. Invasion of tallow tree into southern US forests: influencing factors and implications for mitigation. Canadian Journal of Forest Research 39: 1346-1356.
- Ganteaume, A., 2018. Does plant flammability differ between leaf and litter bed scale? role of fuel characteristics and consequences for flammability assessment. International Journal of Wildland Fire 27(5): 342-352.
- Glitzenstein, J.S., Harcombe, P.A., and Streng, D.R. 1986. Disturbance, succession, and maintenance of species diversity in an East Texas forest. Ecological Monographs 56: 243-258.
- Godfrey, R. K. 1988. Trees, shrubs, and woody vines of northern Florida and adjacent Georgia, and Alabama. The University of Georgia Press, Athens. 734 p.
- Goldman, D.H. 2017. Plant guide for live oak (*Quercus virginiana*). USDA-Natural Resources Conservation Service, National Plant Data Team. Greensboro, NC.
- Gorte, R.W. and Bracmort, K. 2012. Forest fire/wildfire protection. CRS report for Congress, order code RL30755. March 7, 2012.
- Grace J.B. 1998. Can prescribed fire save the endangered coastal prairie ecosystem from Chinese tallow invasion? Endangered Species Update 15: 70-76.

- Grace, J. B., Smith, M. D., Grace, S. L., Collins, S. L., and Stohlgren, T. J. 2001. Interactions between fire and invasive plants in temperate grasslands of North America. In Proceedings of the invasive species workshop: the role of fire in the control and spread of invasive species. Pages 40-65 in K.E.M. and T.P. Wilson (eds.). Galley Fire conference 2000: the First National Congress on Fire Ecology, Prevention, and Management. Miscellaneous Publication No. 11, Tall Timbers Research Station, Tallahassee, FL.
- Greene, B.T. and Blossey, B. 2012. Lost in the weeds: *Ligustrum sinense* reduces native plant growth and survival. *Biological Invasions* 14: 139-150.
- Grootemaat, S., Wright, I.J., van Bodegom, P.M. and Cornelissen, J.H. 2017. Scaling up flammability from individual leaves to fuel beds. *Oikos* 126(10): 1428-1438.
- Guyette, R.P., Spetich, M.A. and Stambaugh, M.C. 2006. Historic fire regime dynamics and forcing factors in the Boston Mountains, Arkansas, USA. *Forest Ecology and Management* 234(1): 293-304.
- Guyette, R.P., Stambaugh, M.C., Dey, D.C. and Muzika, R.M., 2012. Predicting fire frequency with chemistry and climate. *Ecosystems* 15(2): 322-335.
- Halls, L.K. 1977. Southern fruit-producing woody plants used by wildlife. USDA Forest Service General Technical Report, Southern Forest Experiment Station SO-16.
- Han, Y., Chen, H., and Liu, N. 2011. New incremental isoconversional method for kinetic analysis of solid thermal decomposition. *Journal of Thermal Analysis and Calorimetry* 104: 679-683.
- Hanson, H.P., Bradley, M.M., Bossert, J.E., Linn, R.R., and Younker, L.W. 2000. The potential and promise of physics-based wildfire simulation. *Environmental Science and Policy* 3: 161-172.
- Hanula, J.L., Horn, S., and Taylor, J.W. 2009. Chinese privet (*Ligustrum sinense*) removal and its effect on native plant communities of riparian forests. *Invasive Plant Science and Management* 2: 292-300.

- Hasanuzzaman, M., Davies, N.W., Shabala, L., Zhou, M., Brodribb, T.J. and Shabala, S. 2017. Residual transpiration as a component of salinity stress tolerance mechanism: a case study for barley. *BMC Plant Biology* 17(1): 1-12.
- Hatch, S.L., Gandhi, K.N. and Brown, L.E. 1990. Checklist of the vascular plants of Texas. College Station, Texas: Texas Agricultural Experiment Station iv, In Maps Plant Records. *Geography* 3. 158 p.
- Hayward, O.T. and Yelderman, J.C., 1991. A field guide to the Blackland Prairie of Texas: from frontier to heartland in one long century. Program for Regional Studies, Baylor University.
- Heilman, G.E., Strittholt, J.R., Slosser, N.C., and Dellasala, D.A. 2002. Forest fragmentation of conterminous United States: assessing forest intactness through road density and spatial characteristics. *Bioscience* 52: 411-422.
- Heinsch, F.A. and Andrews, P.L. 2010. BehavePlus fire modeling system, Version 5.0: Design and Features. Rocky Mountain Research Station-General Technical Report. Fort Collins, CO: U.S. Department of Agriculture, Forest Service, Rocky Mountain Research Station. 111 p.
- Hough, W.A. 1969. Caloric value of some forest fuels of the southern United States. Res. Note SE-120. Asheville, NC: U.S. Department of Agriculture, Forest Service, Southeastern Forest Experiment Station. 6 p.
- Huggett, C. 1980. Estimation of rate of heat release by means of oxygen consumption measurements. *Fire and Materials*, 4(2): 61-65.
- Iglewicz, B. and Hoaglin, D.C. 1993. How to detect and handle outliers (Vol. 16). Asq Press.
- International Code Council 2015: International wildland-urban interface code. International Code Council, Inc. Country Club Hills, IL.
- Jenkins, J.C., Chojnacky, D.C., Heath, L.S. and Birdsey, R.A. 2003. National-scale biomass estimators for United States tree species. *Forest science* 49(1): 12-35.

- Jubinsky, G. and Anderson, L.C. 1996. The invasive potential of Chinese tallow-tree (*Sapium sebiferum* Roxb.) in the southeast. *Castanea* 1996: 226-231.
- Keane, R.E., Parsons, R.A. and Hessburg, P.F. 2002. Estimating historical range and variation of landscape patch dynamics: limitations of the simulation approach. *Ecological Modelling* 151(1): 29-49.
- Keith, E., 2009. Plant community, fuel model, and rare species assessment for Purtil Creek State Park. Huntsville, TX, USA: Raven Environmental Services.
- Komarek, E.V. 1964. The natural history of lightning. Proceedings of the 3<sup>rd</sup> Tall Timbers Fire Ecology Conference. Tall Timbers Research Station, Tallahassee, Fla. pp 139-183.
- Leoni, E., Tomi, P., Khoumeri, N., Balbi, N., and Bernardini A.F. 2001. Thermal degradation of *Pinus pinaster* needles by DSC. Part 1: dehydration kinetics. *Journal of Fire Sciences* 19: 379-397.
- Leroy, V., Cancellieri, D., and Leoni, E. 2009. Relation between forest fuels composition and energy emitted during their thermal degradation. *Journal of Thermal Analysis and Calorimetry* 96: 293-300.
- Leroy, V., Cancellieri, D., Leoni, E., and Rossi, J.L. 2010. Kinetic study of forest fuels by TGA: model-free kinetic approach for the prediction phenomena. *Thermochimica Acta* 497: 1-6.
- Liebhold. A.M., Macdonald, W.L., Bergdahl, D., and Mastro, V.C. 1995. Invasion by exotic forest pests: a threat to forest ecosystems. *Forest Monographs* 30: 1-49.
- Liodakis, S., Kakardakis, T., Tzortzakou, V., and Tsapara, V. 2008. How to measure the particle ignitability of forest species by TG and LOI. *Thermochimica Acta* 477: 16-20.
- Liodakis, S., Vorisis, D. and Agiovlasis, I.P. 2005. A method for measuring the relative particle fire hazard properties of forest species. *Thermochimica Acta*, 437: 150-157.

- Liu, Z., Murphy, J.P., Maghirang, R. and Devlin, D., 2016. Health and Environmental Impacts of Smoke from Vegetation Fires: A Review. *Journal of Environmental Protection* 7: 1860-1885.
- Long, A. J., Behm, A., Zipperer, W. C., Hermansen, A., Maranghides, A., and Mell, W. 2006. Quantifying and ranking the flammability of ornamental shrubs in the southern United States. In 2006 Fire Ecology and Management Congress Proceedings. pp 13-17.
- Lonsdale, W.M. 1999. Global patterns of plant invasions and the concept of invasibility. *Ecology* 80(5): 1522-1536.
- Mack, R.N., Simberloff, D., Lonsdale, W.M., Evans, H., Clout, M., and Bazzaz, F.A. 2000. Biotic invasions: causes, epidemiology, global consequences, and control. *Ecological Applications* 3: 689-710.
- Mack, M.C. and D'Antonio, C.M. 1998. Impacts of biological invasions on disturbance regimes. *Trends in Ecology & Evolution* 13: 195-198.
- MacRoberts, B.R., MacRoberts, M.H. and Cathey, J.C. 2002. Floristics of xeric sandylands in the post oak savanna region of East Texas. *SIDA, Contributions to Botany 2002*: 373-386.
- Madrigal, J., Hernando, C., Guijarro, M., Díez, C., Marino, E. and De Castro, A.J. 2009. Evaluation of forest fuel flammability and combustion properties with an adapted mass loss calorimeter device. *Journal of Fire Science* 27: 323-341.
- Marshall, D.J., Wimberly, M., Bettinger, P., and Stanturf, J. 2008. Synthesis of knowledge of hazardous fuels management in loblolly pine forests. USDA Forest Service, Southern Research Station General Technical Report SRS-110. 43 pp.
- Martin, R.E., Gordon, D.A., Gutierrez, M.A., Lee, D.S., Molina, D.E., Schroeder, R.A., Sapsis, D.B., Stephens, S.L., and Chambers, M. 1993. Assessing the flammability of domestic and wildland vegetation. Proceedings 12<sup>th</sup> Conference on Fire and Forest Meteorology, Society of American Foresters, Bethesda, Md., Jekyll Island, GA, 26-28 October. pp 130-137.



- Maryandyshev, P., Chernov, A., Lyubov, V., Trouvé, G., Brillard, A., and Brillhac, J.F. 2015. Investigation of thermal degradation of different wood-based biofuels of the northwest region of the Russian Federation. *Journal of Thermal Analysis and Calorimetry* 122: 963-973.
- McKenzie, D., Gedalof, Z., Peterson, D.L., and Mote, P. 2004. Climatic change, wildfire, and conservation. *Conservation Biology* 18: 890-902.
- Mell W.E., Manzello S.L., Maranghides A., Butry D., Rehm R.G. 2010. The wildland–urban interface fire problem—current approaches and research needs. *International Journal of Wildland Fire* 19(2): 238-251.
- Merriam, R.W. and Feil, E. 2002. The potential impact of an introduced shrub on native plant diversity and forest regeneration. *Biological Invasions* 4: 369-373.
- Miranda, M.T., Arranz, J.I., Rojas, S. and Montero, I., 2009. Energetic characterization of densified residues from Pyrenean oak forest. *Fuel*: 88(11): 2106-2112.
- Mitchell, R., Cathey, J.C., Dabbert, B., Prochaska, D.F., Dupree, S., and Sosebee, R. 2005. Managing yaupon with fire and herbicides in the Texas Post Oak Savannah. *Rangelands* 27: 17-19.
- Mitchell, R.J., Hiers, J.K., O'Brien, J.J., Jack, S.B., and Engstrom, R.T. 2006. Silviculture that sustains the nexus between silviculture, frequent prescribed fire, and conservation of biodiversity in longleaf pine forests of the southeastern United States. *Canadian Journal of Forest Research* 37: 2724-2736.
- Monti, A., Di Virgilio, N. and Venturi, G. 2008. Mineral composition and ash content of six major energy crops. *Biomass and Bioenergy* 32(3): 216-223.
- Munir, S., Daood, S.S., Nimmo, W., Cunliffe, A.M., and Gibbs, B.M. 2009. Thermal analysis and devolatilization kinetics of cotton stalk, sugar cane, bagasse, and shea meal under nitrogen and air atmospheres. *Bioresource Technology* 100: 1413-1418.

- National Fire Protection Association 2013. NFPA 1144: Standard for reducing structure ignition hazards from wildland fire. NFPA, International Codes and Standards. Quincy, MA.
- Nhuchhen, D.R. and Salam, P.A. 2012. Estimation of higher heating value of biomass from proximate analysis: A new approach. *Fuel* 99: 55-63.
- NICC, 2016. National Interagency Fire Center, Statistics. Located at: [https://www.predictiveservices.nifc.gov/intelligence/2016\\_Statssumm/annual\\_report\\_2016.pdf](https://www.predictiveservices.nifc.gov/intelligence/2016_Statssumm/annual_report_2016.pdf) Accessed on: 12/29/2017.
- Nijjer, S., Lankau, R. A., Rogers, W.E., and Siemann, E. 2002. Effects of temperature and light on Chinese tallow (*Sapium sebierum*) and Texas sugarberry (*Celtis laevigata*) seed germination. *Texas Journal of Science* 54: 63-68.
- NOAA, 2020. Climate Data Online. Located at: <https://www.ncdc.noaa.gov/cdo-web/>.
- Ortega, A. 2000. The kinetics of solid-state reactions toward consensus. Part 2: fitting kinetics data in dynamic conventional thermal analysis. *International Journal of Chemical Kinetics* 34: 193-208.
- Owens, M.K., Lin, C.D., Taylor, C.A. and Whisenant, S.G. 1998. Seasonal patterns of plant flammability and monoterpenoid content in *Juniperus ashei*. *Journal of Chemical Ecology* 24(12): 2115-2129.
- Özyuğuran, A. and Yaman, S. 2017. Prediction of calorific value of biomass from proximate analysis. *Energy Procedia* 107: 130-136.
- Papari, S. and Hawboldt, K. 2015. A review on the pyrolysis of woody biomass to bio-oil: Focus on kinetic models. *Renewable and Sustainable Energy Reviews* 52: 1580-1595.
- Parr Technotes, 2008. Calibration of oxygen bomb calorimeters: procedures for standardization of Parr oxygen bomb calorimeters. *Technotes Bulletin* No.10, October 31, 2008. pp 1-5.

- PerkinElmer, 2010. PerkinElmer sta 6000 users guide. PerkinElmer Inc., 940 Winter Street, Waltham, MA.
- Picou, L. and Boldor, D. 2012. Thermophysical characterization of the seeds of invasive Chinese tallow tree: importance for biofuel production. *Environmental Science and Technology* 46: 11435-11442.
- Pile, L.S., Wang, G.G., Stovall, J.P., Siemann, E., Wheeler, G.S. and Gabler, C.A. 2017. Mechanisms of Chinese tallow (*Triadica sebifera*) invasion and their management implications—a review. *Forest Ecology and Management* 404: 1-13.
- Philpot, C.W. 1971. The seasonal trends in moisture content, ether extractives, and energy of ponderosa pine and Douglas-fir needles (Vol. 102). Intermountain Forest & Range Experiment Station, Forest Service, US Department of Agriculture.
- Pyne, S.J., 2011. Fire: a brief history. University of Washington Press.
- Ramsey, E. III, Rangoonwala, A., Nelson, G., and Ehrlich, R. 2005. Mapping the invasive species, Chinese tallow, with E01 satellite hyperion hyperspectral image data and relating tallow occurrences to a classified landsat thematic mapper land cover map. *International Journal of Remote Sensing* 26: 1637-1657.
- Reichard, S.H. and White, P. 2001. Horticulture as a pathway of invasive plant introductions in the United States: most invasive plants have been introduced for horticultural use by nurseries, botanical gardens, and individuals. *BioScience* 51(2): 103-113.
- Rejmanek, M., Richardson, D.M., and Pysek, P. 2013. Plant invasions and invasibility of plant communities. *Vegetation Ecology Second Edition* 2013: 332-355.
- Renne, I. J., Gauthreaux Jr, S. A., and Gresham, C. A. 2000. Seed dispersal of the Chinese tallow tree (*Sapium sebiferum* (L.) Roxb.) by birds in coastal South Carolina. *The American Midland Naturalist* 144: 202-215.

- Rivera, J.D., Davies, M.G., and Wolfram, J. 2012. Flammability and heat of combustion of natural fuels: a review. *Combustion Science and Technology* 184: 224-242.
- Rollins, D. and Bryant, F.C. 1986. Floral changes following mechanical brush removal in central Texas. *Journal of Range Management*. 39(3): 237-240.
- Rothermel, R.C. 1972. A mathematical model for predicting fire spread in wildland fuels. Intermountain Forest and Range Experiment Station, USDA Forest Service, Research Paper INT-115.
- Rothermel, R.C. 1983. How to predict the spread and intensity of forest and range fires. Intermountain Forest and Range Experiment Station, USDA Forest Service, General Technical Report INT-143.
- Rothermel, R.C. 1991. Predicting behavior and size of crown fires in the Northern Rocky Mountains. Intermountain Forest and Range Experiment Station, USDA Forest Service, Research Paper INT-438.
- Rudis, V. A., Gray, A., McWilliams, W., O'Brien, R., Olson, C., Oswald, S., and Schulz, B. 2006. Regional monitoring of nonnative plant invasions with the Forest Inventory and Analysis program. Proceedings of the sixth annual FIA symposium, USDA Forest Service General Technical Report WO-70. pp 49-64.
- Rundel, P.W., Dickie, I.A., and Richardson D.M. 2014. Tree invasions into treeless areas: mechanisms and ecosystem processes. *Biological Invasions* 16: 663-675.
- Saddawi, A., Jones, J.M., Williams, A., and Wojtowicz, M.A. 2009. Kinetics of the thermal decomposition of biomass. *Energy & Fuels* 24: 1274-1282.
- Safdari, M.S., Rahmati, M., Amini, E., Howarth, J.E., Berryhill, J.P., Dietsberger, M., Weise, D.R. and Fletcher, T.H. 2018. Characterization of pyrolysis products from fast pyrolysis of live and dead vegetation native to the Southern United States. *Fuel* 229: 151-166.

- Sbirrazzuoli, N., Vincent, L., Mija, A., and Guigo, N. 2009. Integra, differential and advanced isoconversional methods complex mechanisms and isothermal predicted conversion-time curves. *Chemometrics and Intelligent Laboratory Systems* 96: 219-226.
- Sbirrazzuoli, N., Vincent, L., and Vyazovkin S. 2000. Comparison of several computational procedures for evaluating the kinetics of thermally stimulated condensed phase reactions. *Chemometrics and Intelligent Laboratory Systems* 54: 53-60.
- Schade, G.W., Goldstein, A.H. and Lamanna, M.S. 1999. Are monoterpene emissions influenced by humidity? *Geophysical Research Letters*, 26(14): 2187-2190.
- Scheld, H.W. and Cowles, J.R. 1981. Woody biomass potential of the Chinese tallow tree. *Economic Botany* 35(4): 391-397.
- Schemel, C.F., Simeoni, A., Biteau, H., Rivera, J.D., and Torero, J.L. 2008. A calorimetric study of wildland fuels. *Experimental Thermal and Fluid Science* 32: 1381-1389.
- Schulz, M., Kussmann, P., Knop, M., Kriegs, B., Gresens, F., Eichert, T., Ulbrich, A., Marx, F., Fabricius, H., Goldbach, H. and Noga, G. 2007. Allelopathic monoterpenes interfere with *Arabidopsis thaliana* cuticular waxes and enhance transpiration. *Plant Signaling and Behavior* 2(4): 231-239.
- Scifres, C.J. 1980. *Brush management*. Texas A&M University Press, College Station, Texas.
- Scifres, C.J. and Hamilton, W.T. 1993. *Prescribed burning for brushland management: the south Texas example*. College Station, TX.
- Scott, J.H., and Burgan, R.E. 2005. *Standard fire behavior fuel models: a comprehensive set for use with Rothermel's surface fire spread model*. USDA Forest Service, Rocky Mountain Research Station Research Paper RMRS-GTR-153.
- Shafizadeh, F., Chin, P.P.S, and DeGroot, W.F. 1977. Effective heat content of green forest fuels. *Forest Science* 23: 81-89.

- Shadow, R. A. 2011. Plant fact sheet for yaupon, *Ilex vomitoria*. USDA-Natural Resources Conservation Service, East Texas Plant Materials Center, Nacogdoches.
- Shaw, R.B., 2011. Guide to Texas grasses. Texas A&M University Press.
- Short, H.L., 1976. Composition and squirrel use of acorns of black and white oak groups. *The Journal of Wildlife Management* 1976: 479-483.
- Sinha, A., Kopachena, J.G. and Eidson, J. 2010. Plant diversity in an imperiled gamagrass community in Northeastern Texas. *The Southwestern Naturalist* 55(2): 254-262.
- Smeins, F.E. 1972. Influence of fire and mowing on vegetation of the Blackland Prairie of Texas. In *Third Midwest Prairie Conference Proceedings*. Manhattan, KS. pp. 4-7.
- Smeins, F.E., Fuhlendorf, S.D. and Taylor Jr, C.A. 2005. History and use of fire in Texas. Fire as a tool for managing wildlife habitat in Texas. Texas Cooperative Extension, San Angelo, Texas, USA, pp.6-16.
- Stambaugh, M.C., Creacy, G., Sparks, J. and Rooney, M. 2017. Three centuries of fire and forest vegetation transitions preceding Texas' most destructive wildfire: Lost Pines or lost oaks? *Forest Ecology and Management* 396: 91-101.
- Stambaugh, M.C., Guyette, R.P., and Marschall, J.M. 2011. Longleaf pine (*Pinus palustris Mill.*) fire scars reveal new details of a frequent fire regime. *Journal of Vegetation Science* 22: 1094-1104.
- Stambaugh, M.C., Guyette, R.P. and Marschall, J.M. 2013. Fire history in the Cherokee nation of Oklahoma. *Human Ecology* 41(5): 749-758.
- Stambaugh, M.C., Sparks, J.C., and Abadir, E.R. 2014. Historical pyrogeography of Texas, USA. *Fire Ecology* 10(3): 72-89.
- Stambaugh, M.C., Sparks, J., Guyette, R.P. and Willson, G. 2011a. Fire history of a relict oak woodland in northeast Texas. *Rangeland ecology and management* 64(4): 419-423.

- Stambaugh, M.C., Guyette, R.P. and Marschall, J.M. 2011b. Longleaf pine (*Pinus palustris* Mill.) fire scars reveal new details of a frequent fire regime. *Journal of Vegetation Science* 22(6): 1094-1104.
- Starink, M.J. 2003. The determination of activation energy from linear heating rate experiments: a comparison of the accuracy of isoconversion methods. *Thermochimica Acta* 404: 163-176.
- Steelman, T.A., and Burke, C.A. 2007. Is wildfire policy in the United States sustainable? *Journal of Forestry* 105: 67-72.
- Stephens, L., McIver, J.D., Boerner, R., Fettig, C.J., Fontaine, B.R., Hartsough, B.R., Kennedy, P.L., and Schwilk, D.W. 2012. The effects of forest fuel-reduction treatments in the United States. *Bioscience* 62: 549-560.
- Stocker, R. and Hupp, K.V., 2008. Fire and nonnative invasive plants in the southeast bioregion. In: Zouhar, Kristin; Smith, Jane Kapler; Sutherland, Steve; Brooks, Matthew L. *Wildland fire in ecosystems: fire and nonnative invasive plants*. Gen. Tech. Rep. RMRS-GTR-42-vol. 6. Ogden, UT: USDA Forest Service, Rocky Mountain Research Station. p. 91-112.
- Stransky, J.J. and Halls, L.K. 1979. Effect of a winter fire on fruit yields of woody plants. *The Journal of Wildlife Management* 43(4): 1007-1010.
- Stratton, R.D. 2006. Guidance on spatial wildland fire analysis: models, tools, and techniques. USDA Forest Service, General Technical Report RMRS-GTR-183. pp 1-15.
- Sullivan, J. 1994. *Smilax bona-nox*. In: Fire Effects Information System, USDA, Forest Service, RMRS, Fire Sciences Laboratory. Located at: <https://www.fs.fed.us/database/feis/plants/vine/smibon/all.html> Accessed on 12/18/2017.
- Susott, R.A. 1980. Thermal behavior of conifer needle extractives. *Forest Science* 26: 347-360.
- Swetnam, T.W. and Betancourt, J. L. 1990. Fire- southern oscillation relations in the southwestern United States. *Science* 249: 1017-1020.

- Texas A&M Forest Service. 2012. 2011 Texas wildfires: common denominators of home destruction. TAMU Forest Service. pp 1-50.
- Texas A&M Forest Service. 2012. Texas wildfire risk assessment portal (TxWRAP) user manual. TAMU Forest Service. pp 1-69.
- Thomas, E.H. 1980. The New York Botanical Garden illustrated encyclopedia of horticulture. Garland STPM Press, New York, New York.
- Tihay, V. and Gillard, P. 2011. Comparison of several kinetic approaches to evaluate the pyrolysis of three Mediterranean forest fuels. *International Journal of Wildland Fire* 20: 407-417.
- Tiller, M.B., Oswald, B.P., Frantzen, A.S., Conway, W.C., and Hung, I. 2020. Initial investigation of seasonal flammability of three invasive East Texas forest understory fuels using thermogravimetric analysis. *Forest Research* 9:230. doi: 10.35248/2168-9776.20.9.230.
- Toman E., Stidham M., McCaffrey S., and Shindler B. 2013. Social science at the wildland-urban interface: A compendium of research results to create fire-adapted communities. USDA Forest Service, Northern Research Station, General Technical Report NRS-111. Newton Square, PA.
- Turner, B.L., Nichols, H., Denny, G. and Doron, O. 2003. Atlas of the vascular plants of Texas. SIDA, Botanical Miscellany, No. 24: 1-888.
- Twidwell, D., Rogers, W.E., Fuhlendorf, S.D., Wonkka, C.L., Engle, D.M., Weir, J.R., Kreuter, U.P. and Taylor, C.A. 2013. The rising Great Plains fire campaign: citizens' response to woody plant encroachment. *Frontiers in Ecology and the Environment* 11(s1): 64-71.
- Ulyshen, M.D., Horn, S., and Hanula J.L. 2010. Response of beetles (Coleoptera) at three heights to the experimental removal of an invasive shrub, Chinese privet (*Ligustrum sinense*), from floodplain forests. *Biological Invasions* 12: 1573-1579.
- USDA Forest Service. 1981. Fire regimes and ecosystem properties. USDA Forest Service General Technical Report WO-26. pp 112-136.



- USDA Forest Service Forest Resource Report No. 24. 1988. The South's fourth forest: Alternatives for the Future. pp 29-81.
- USDA Natural Resource Conservation Service. Chinese privet (*Ligustrum sinense*). In: USDA NRCS Plant Guide. Located at: [https://plants.usda.gov/DocumentLibrary/plantguide/pdf/pg\\_lisi.pdf](https://plants.usda.gov/DocumentLibrary/plantguide/pdf/pg_lisi.pdf). Accessed on 12/18/2017.
- Uzun, H., Yıldız, Z., Goldfarb, J.L. and Ceylan, S. 2017. Improved prediction of higher heating value of biomass using an artificial neural network model based on proximate analysis. *Bioresource Technology* 234: 122-130.
- Van Wagtendonk, J.W., Sydorik, W.M., and Benedict, J.M. 1998. Heat content variation of Sierra Nevada conifers. *International Journal of Wildland Fire* 8: 147-158.
- Varner, J.M., Gordon, D.R., Putz, F.E. and Hiers, J.K. 2005. Restoring fire to long-unburned *Pinus palustris* ecosystems: novel fire effects and consequences for long-unburned ecosystems. *Restoration Ecology* 13(3): 536-544.
- Veblen, T.T., Kitzberger, T., and Donnegan, J. 2000. Climatic and human influences on fire regimes in ponderosa pine forests in the Colorado Front Range. *Ecological Applications* 10: 1178-1195.
- Vines, R.A. 1960. Trees, shrubs, and woody vines of the Southwest. Austin, TX, University of Texas Press. pp 646-647.
- Vyazovkin, S. and Wright, C.A. 1999. Model-free and model-fitting approaches to kinetic analysis of isothermal and non-isothermal data. *Thermochimica Acta* 340: 53-68.
- Wade, D.D. and Lunsford, J.D. 1989. A guide for prescribed fire in southern forests. USDA Forest Service, Southeastern Forest Experiment Station Technical Publication R8-TP 11. 56 p.
- Wang, H.H., Wonkka, C.L., Grant, W.E., and Rogers, W.E. 2016. Range expansion of invasive shrubs: implication for crown fire risk in forestlands of the southern USA. *AoB Plants* 8: 1-14.

- Webster, C.R., Jenkins, M.A., and Jose, S. 2006. Woody invaders and the challenges they pose to forest ecosystems in the eastern United States. *Journal of Forestry* 104: 366-374.
- Weise, D.R., White, R.H., Frommer, S., Beall, F.C., and Etlinger, M. 2005. Seasonal changes in selected combustion characteristics of ornamental vegetation. *International Journal of Wildland Fire* 14: 321-338.
- Wells, G. 2008. The Rothermel fire-spread model: still running like a champ. *Fire Science Digest, Joint Fire Science Program* 2: 3-10.
- White, R.H., Weise, D.R., Mackes, K., and Dibble, A.C. 2002. Cone calorimeter testing of vegetation: an update. In *Proceedings of 35<sup>th</sup> International Conference on Fire Safety, 22-24 July 2002, Columbus, OH.* pp 1-12.
- White, R.H. and Zipperer, W.C. 2010. Testing and classification of individual plants for fire behavior: plant selection for the wildland-urban-interface. *International Journal of Wildland Fire* 19: 213-227.
- Wildland Fire Leadership Council 2014. The national strategy: the final phase in the development of the National Cohesive Wildland Fire Management Strategy. Washington, DC; available at: <http://www.forestsandrangelands.gov/strategy/documents/strategy/CSPhasellNationalStrategyApr2014.pdf> [Verified 11 December 2015].
- Wimberly, M., Bettinger, P., and Stanturf, J. 2008. Synthesis of knowledge of hazardous fuels management in loblolly pine forests. USDA, Forest Service, Southern Research Station, GTR SRS-110. pp 1-43.
- Williams, G.B. and Black, E.M. 1981. High temperature of forest fires under pines as a selective advantage over oaks. *Nature* 293: 643-644.
- Williamson, N.M., and Agee, J.K. 2002. Heat content variation of interior Pacific Northwest conifer foliage. *International Journal of Wildland Fire* 11: 91-94
- Yang, H., Yan, R., Chen, H., Lee, D.H. and Zheng, C. 2007. Characteristics of hemicellulose, cellulose and lignin pyrolysis. *Fuel*, 86(12-13): 1781-1788.

## VITA

Michael Brian Tiller was born and raised in California. In the summer of 1988 he entered into state service with the California Department of Forestry and Fire Protection (CAL FIRE), where he served 15-years as a firefighter and fire apparatus engineer. He graduated from Butte Community College in June 1996 with an Associate of Science in Fire Science. He was awarded a Bachelor of Science in Wildlife and Fisheries Science in 2008 from Texas A&M University. In May 2015, Michael received a Master of Science in Environmental Science with a minor in Spatial Science from Stephen F. Austin State University (SFASU). He also served as wildland urban interface specialist II for the Texas A&M Forest Service from 2014-2016. In January 2016, Michael reentered graduate school at SFASU to pursue a Ph.D. in Forestry.

Permanent Address: 3706 Rodgers Avenue  
Chico, CA 95928

Style Manual: Forest Science

This dissertation was typed by Michael B. Tiller.